AD NUMBER

ADB021193

LIMITATION CHANGES

TO:

Approved for public release; distribution is unlimited.

FROM:

Distribution authorized to U.S. Gov't. agencies only; Test and Evaluation; AUG 1977. Other requests shall be referred to Rome Air Development Center, Griffiss AFB, NY.

AUTHORITY

RADC ltr 17 Apr 1978

RADC-TR-77-274
Final Technical Report
August 1977

ECCM WAVEFORM INVESTIGATION

General Electric Company

ROME AIR DEVELOPMENT CENTER
Air Force Systems Command
Griffiss Air Force Base, New York 13441

This report has been reviewed and is approved for publication.

APPROVED: Vincent Vannicola

VINCENT VANNICOLA
Project Engineer

APPROVED: Joseph L Ryerson

JOSEPH L. RYERSON
Technical Director
Surveillance Division

FOR THE COMMANDER: John P. Huss

JOHN P. HUSS
Acting Chief, Plans Office

If your address has changed or if you wish to be removed from the RADC mailing list, or if the addressee is no longer employed by your organization, please notify RADC (DAP) Griffiss AFB NY 13441.

Do not return this copy. Retain or destroy.

UNCLASSIFIED

SECURITY CLASSIFICATION OF THIS PAGE *(When Data Entered)*

REPORT DOCUMENTATION PAGE

READ INSTRUCTIONS BEFORE COMPLETING FORM

1. REPORT NUMBER: RADC-TR-77-274	2. GOVT ACCESSION NO.
3. RECIPIENT'S CATALOG NUMBER	
4. TITLE *(and Subtitle)*: ECCM WAVEFORM INVESTIGATION •	5. TYPE OF REPORT & PERIOD COVERED: Final Technical Report, 12 April 1976 — 12 May 1977.
6. PERFORMING ORG. REPORT NUMBER: N/A	
7. AUTHOR(s): Ramon Nitzberg, Richard D. Taylor	8. CONTRACT OR GRANT NUMBER(s): F30602-76-C-0210
9. PERFORMING ORGANIZATION NAME AND ADDRESS: General Electric Company, Court Street Plant, Syracuse NY 13201	10. PROGRAM ELEMENT, PROJECT, TASK AREA & WORK UNIT NUMBERS: 62702F, 45060198
11. CONTROLLING OFFICE NAME AND ADDRESS: Rome Air Development Center (OCTS), Griffiss AFB NY 13441	12. REPORT DATE: August 1977
	13. NUMBER OF PAGES: 104
14. MONITORING AGENCY NAME & ADDRESS *(if different from Controlling Office)*: Same	15. SECURITY CLASS. *(of this report)*: UNCLASSIFIED
	15a. DECLASSIFICATION/DOWNGRADING SCHEDULE: N/A

16. DISTRIBUTION STATEMENT *(of this Report)*

Distribution limited to U.S. Gov't agencies only; test and evaluation; August 1977. Other requests for this document must be referred to RADC (OCTS) Griffiss AFB NY 12441.

17. DISTRIBUTION STATEMENT *(of the abstract entered in Block 20, if different from Report)*

Same

18. SUPPLEMENTARY NOTES

RADC Project Engineer: Vincent Vannicola (OCTS)

19. KEY WORDS *(Continue on reverse side if necessary and identify by block number)*

ECCM
Frequency Diversity Waveforms
Bandwidth
Target Modeling
Range Ambiguous PRF

20. ABSTRACT *(Continue on reverse side if necessary and identify by block number)*

The program's objective was to determine the potential ECCM performance of coded waveforms for a tactical radar scenario. The waveform parameters investigated were phase/frequency coding, bandwidth, repetition period, duration/peak power, and side lobe levels. A recommended waveform library is presented.

One of the program results is that an optimum waveform bandwidth exists for detecting targets in broadband noise. For tactical radar targets this bandwidth is of the order of 40 MHz or less. However, the recommended waveform is a low-

OVER

DD FORM 1 JAN 73 1473 EDITION OF 1 NOV 65 IS OBSOLETE

UNCLASSIFIED

SECURITY CLASSIFICATION OF THIS PAGE *(When Data Entered)*

149 500

LB

bandwidth, 250 kHz, multiple-channel frequency diversity waveform. Its performance is only 0.8 dB less than the wide bandwidth optimum. In addition, this waveform has significant advantages in spot jamming and false target repeater jammer environments. It also has significant cost advantages.

TABLE OF CONTENTS

Section	Title	Page
I	INTRODUCTION AND SUMMARY	1
	1. Objectives	1
	2. Study Areas	1
	a. Coding	2
	b. Pulse Repetition Period	5
	c. Peak Power/Pulse Duration	8
	d. Sidelobes	9
	3. Performance Dependence Upon Bandwidth/Bandspan	9
	a. Thermal Noise	11
	b. ECM Chaff and Weather Clutter	11
	c. Noise Jamming	12
	d. Decoy Jamming	13
	4. Frequency Diversity Waveforms	13
	5. Effect of Target Model	19
	6. Waveform Constraints Due to Radar Components	29
	7. Recommended Waveforms	32
	a. Thermal Noise and Ground Clutter	32
	b. ECM Chaff and Weather Clutter	35
	c. Active Jamming	36
II	EFFECTS OF BANDWIDTH UPON DETECTION OF RADAR TARGETS	37
	1. Thermal Noise	37
	2. ECM Chaff and Natural Clutter	38
	3. Distributed Target Effects in Clutter and Noise	40
	a. Clutter Effects	40
	b. Noise Effects	43
	4. Noise Jammers	44
	a. Intercept Receivers	44
	b. Noise Jammer Properties	46
III	EFFECT OF A FEW DOMINANT SPECULAR REFLECTORS TARGET MODEL UPON TARGET DETECTION	49
IV	LOSSES FOR FREQUENCY DIVERSITY WAVEFORM SYSTEMS	53
	1. Correlated Returns Due to Small Channel-to-Channel Frequency Spacing	53
	2. Unknown Doppler Frequency Loss	60

TABLE OF CONTENTS (Cont)

Section	Title	Page
	3. Effect of Detector Law Upon Diversity Gain	61
	4. Constant False-Alarm Rate Processors for Diversity Waveforms	61
	5. Analysis	71
	a. Channel-to-Channel Frequency Spacing Effects	71
	b. Loss for Unknown Doppler Frequency	77
	c. Effect of Detector Law Upon Diversity Gain	80
	d. Optimality Considerations for CFAR Processing of Diversity Channels	82
V	EFFECT OF PULSE REPETITION FREQUENCY UPON REJECTION OF CHAFF AND WEATHER CLUTTER	87

LIST OF ILLUSTRATIONS

Figure	Title	Page
1	Alternate Diversity Waveforms	3
2	Conceptual Block Diagram of Frequency Diversity System	4
3	Chaff Spectral Spread for Lowest Beam (No. 1)	6
4	Effect of PRF Upon Doppler Performance for Matched Filter	7
5	Diversity Gain vs No. of Channels for Swerling 2 Fluctuation	16
6	Critical Bandwidth Required to Resolve Specular Reflectors	20
7	Target Cross Section Density for 10 Reflector Model	21
8	Cross-Section Density for 5 Reflector Model	22
9	Target Cross-Section Probability Density for 2, 3, 4 Reflector Target Models	23
10	Detection Probability for Several Target Models with "Small" Bandwidth Waveforms	24
11	Diversity Gains for Several Fluctuating Targets	25
12	SIR Required as Function of Bandwidth Occupancy 2 Reflector Target Model	26
13	SIR Required as Function of Bandwidth Occupancy 3 Reflector Target Model	28
14	Phased Array Filtering Effects	30
15	Mainlobe Broadening vs Array Bandwidth Ratio R_A	31
16	Diversity Waveforms for Scanning Elevation and Stacked Beam Antennas	34
17	Radar and Intercept Receiver Detection Range	46
18	Four-Channel Diversity Performance As A Function of Normalized Frequency Displacement For Uniform Cross-Section Density	55
19	Four-Channel Diversity Gain for Distributed Targets	56
20	Two-Channel Diversity Performance As A Function of SNR and Normalized Frequency Displacement for Uniform Cross-Section Target	57
21	Two-Channel Diversity System	58
22	Bandspan Effect Upon Diversity Gain for Triangle Cross-Section Density Target	59
23	Multiple Channel Diversity Waveform Unknown Target Velocity Processor	62

LIST OF ILLUSTRATIONS (Cont)

Figure	Title	Page
24	SIRR for Unknown Target Velocity	63
25	Conceptual Block Diagram of Single-Channel CFAR Processor	64
26	CFAR Loss	66
27	Conceptual Block Diagram of Multichannel Normalizer	68
28	Four-Channel Diversity CFAR Loss, Barrage Jamming	69
29	Four-Channel Normalization Losses, Spot Jamming	71
30	Geometry Effects	88
31	Chaff-Clutter Cross Section	89
32	Required Band Occupancy	90
33	Chaff Average Velocity	92
34	Chaff Velocity Spread	93
35	Chaff Spectral Spread for Lowest Beam (No. 1)	94
36	Effect of Pulse Repetition Frequency Upon Doppler Performance for Matched Filter	95
37	16-Pulse Waveform Normalized Clutter Power	97
38	Equivalent Clutter Cross Section vs Target Doppler 50-km Range, 2-MHz Bandwidth, 40-dB Tchebyscheff Weights	99
39	Equivalent Clutter Cross Section vs Target Doppler (2-MHz Pulse Bandwidth, Range = 155 km)	100
40	Coincidence Detection for Ambiguity Removal	102
41	Tradeoff Between Loss and Probability of Ambiguity	103
42	SIR vs Probability of Ambiguity	103

GLOSSARY

ARM	Antiradiation Missile
CFAR	Constant False-Alarm Rate
ECCM	Electronic Counter Countermeasures
ECM	Electronic Countermeasures
IF	Intermediate Frequency
km	Kilometer
LFM	Linear Frequency Modulation
MTI	Moving Target Indicator
nmi	Nautical Mile
PRF	Pulse Repetition Frequency
PRN	Pseudorandom Noise
RF	Radio Frequency
rms	Root Mean Square
RPV	Remotely Piloted Vehicles
SCR	Signal-to-Clutter Ratio
SIR	Signal-to-Interference Ratio
SIRA	Signal-to-Interference Ratio Attained
SIRR	Signal-to-Interference Ratio Required
SNR	Signal-to-Noise Ratio
STC	Sensitivity Time Control
TOA	Time-of-Arrival

SECTION I

INTRODUCTION AND SUMMARY

1. OBJECTIVES

The primary objective of the radar user is to maintain surveillance in a hostile environment. The significant environment features are:

- Destructive threats including antiradiation missiles (ARM); time-of-arrival systems (TOA); and remotely piloted vehicles (RPV).
- Passive and active jamming such as chaff, noise jamming, and false target jamming.
- Natural passive interference consisting of weather and ground clutter.

The study is directed toward investigating the potential that various radar waveforms have in aiding the meeting of the radar user's objectives. The general scenario of interest is aircraft detection with a desired detection range of 240 nmi. The aircraft speed ranges over 50 knots to Mach 3. The general radar parameters are S-band operation with 10-15% instantaneous bandwidth, a data rate of approximately 10 s, 360° azimuth coverage, and up to 20° elevation coverage. The type of radar antenna is not specified. Continuous rotation for azimuth coverage is assumed. The elevation coverage could be obtained either by a stacked beam approach or via sequential elevation scan.

2. STUDY AREAS

The major thrust of the study has been to determine the effects of waveform parameters upon electronic counter countermeasures (ECCM) performance. The parameters that have been emphasized are phase and frequency coding, bandwidth and band span, repetition period, the tradeoff between peak power and pulse duration, and range and Doppler sidelobe levels. The constraints upon waveforms due to the inability of the radar components to support the waveforms has also been considered. The program results are summarized in Section I and a recommended waveform library is also developed. The detailed results are presented in Section II.

a. Coding

The concepts of coding, both frequency and phase, bandwidth, and bandspan become so intertwined that it is desirable to give a precise definition of the usage through an example.

The single pulse waveform, shown as the upper waveform of Figure 1 is phase coded to a bandwidth, B, that can be significantly greater than the reciprocal of the pulse duration τ. The phase coding can be linear-frequency-modulation (LFM), also called chirp, a phase code such as Barker or pseudorandom noise, nonlinear chirps, etc. The second waveform of Figure 1 is frequency coded. Each subpulse is at a different carrier. The spectrum is disjoint. The waveform bandspan is defined as the difference between the highest and lowest frequencies that have significant energy content. There are two versions of this waveform depending upon whether or not there is phase coherence between the subpulses. When there is phase coherence, the subpulses are individually matched-filtered, delayed to give time coincidence, and added prior to envelope detection. The resultant range resolution is inversely proportional to the waveform bandspan. Because of the unfilled spectrum, the waveform has the property that it has range ambiguities spaced at distances that are inversely proportional to the channel-to-channel frequency spacing. The range ambiguities can be eliminated by causing the spectrum to be filled. This is done by choosing the channel-to-channel frequency spacing equal to the per channel bandwidth. For the filled spectrum waveform, and time contiguous subpulses, the difference between phase and frequency coding becomes one of semantics. A filled spectrum waveform that uses a pulse train and changes frequency from pulse to pulse while maintaining phase coherence is another version of a frequency coded waveform. This version differs substantially from phase coding.

A different form of the waveform, shown in Figure 2, adds the matched filtered and delayed subpulses after envelope detection. The range resolution is inversely proportional to the per channel bandwidth rather than the bandspan. There are no range ambiguities and it does not matter whether the spectrum is filled or disjoint. This waveform is commonly denoted as frequency diversity or multiple channels. A detailed discussion of the bandwidth-bandspan of frequency diversity waveform properties is given in a later section.

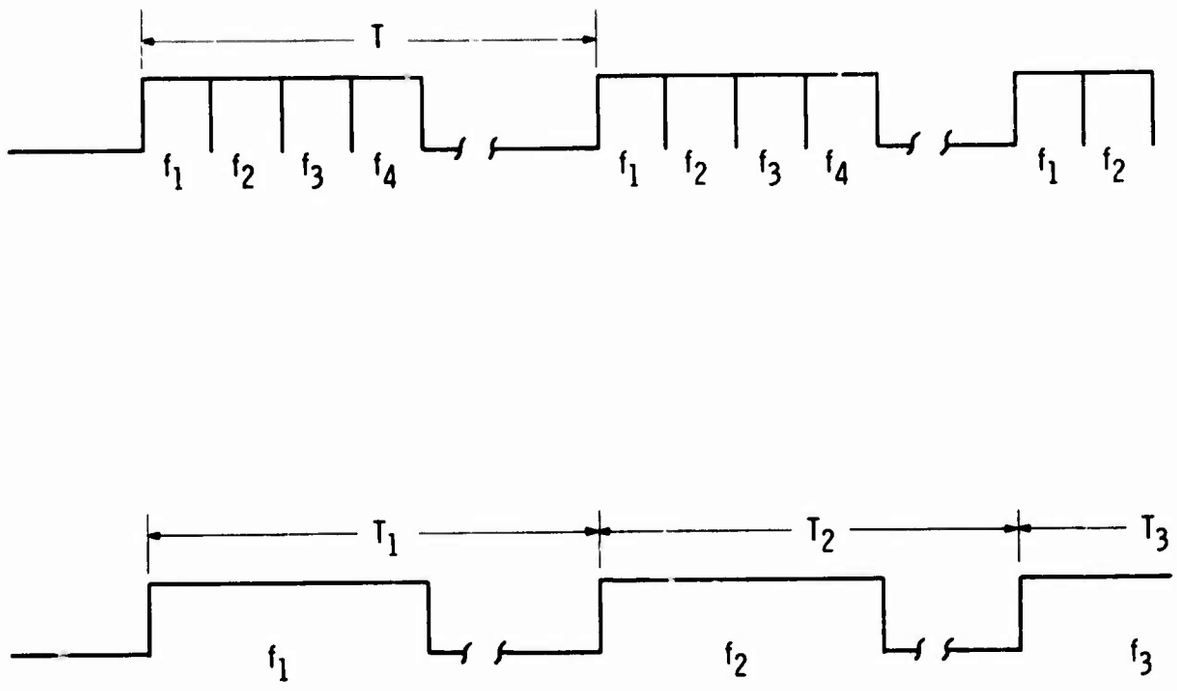

Figure 1. Alternate Diversity Waveforms

It has been found that the choice of which particular phase coding should be used depends primarily upon implementation criteria, and is largely independent of theorectical performance criteria. As an example, for a fixed bandwidth and pulse duration, the target detection performance when using matched filter processing is independent of the phase coding when the interference is thermal noise, barrage noise jamming, and spot noise jamming, since only the total transmit energy is of consequence. There is a third-order sensitivity to detection in homogeneous distributed clutter such as chaff or weather. This occurs because most of the clutter received is at the same range as the target. The clutter received from the range sidelobes is less and, therefore, is a second-order effect. The differential in received clutter due to different sidelobes for different phase codes is a third-order effect.

B5542

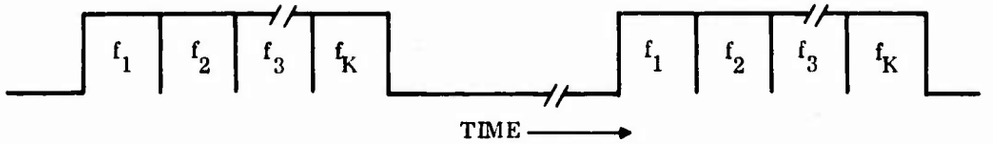

(A) TRANSMIT WAVEFORM ENVELOPE

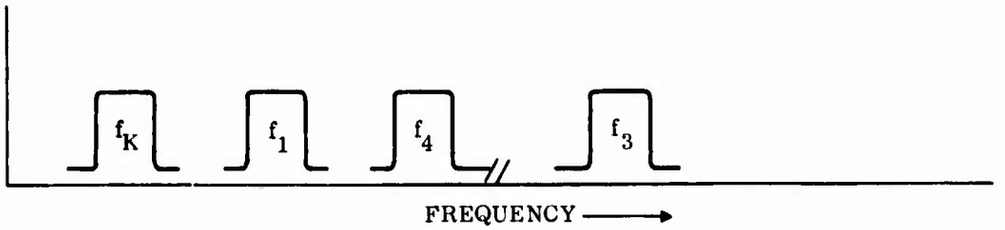

(B) TRANSMIT SPECTRUM

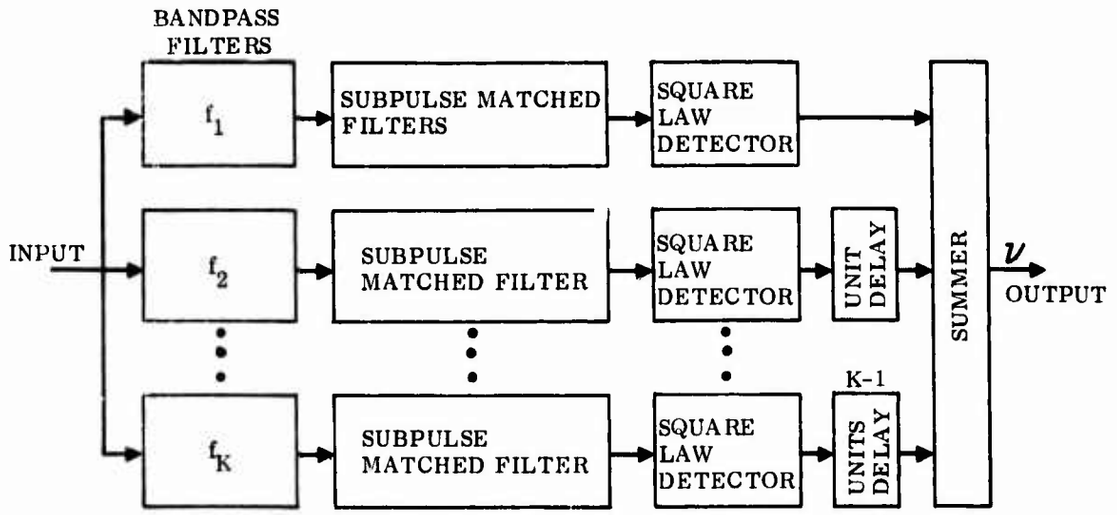

Figure 2. Conceptual Block Diagram of Frequency Diversity System

A difference between different phase codes that is sometimes significant is due to the respective frequency spectra. Phase codes such as LFM have relatively compact spectra. Simple pulses or binary phase codes have spectra with sin x/x forms. There is significantly more energy in the spectral tails for these waveforms than for the LFM. For extremely wideband waveforms this can be important as the degradation in range resolution is much greater for the simple pulse and binary phase code.

Though there is little theoretical reason to prefer one phase code over another, it has been found that there is a significant theoretical advantage for frequency coding. As is discussed in greater detail later, the frequency diversity waveform has many theoretical advantages.

b. Pulse Repetition Period

A constraint upon PRF choice is the relation between the range-time and Doppler ambiguities. The doppler ambiguities are spaced at the pulse repetition frequency; the range-time ambiguities are spaced at the reciprocal of the pulse repetition frequency (PRF). Thus, if a PRF of 300 is chosen to eliminate range ambiguities, the Doppler ambiguities are at 300 Hz. The study of repetition period focused upon the effect of different values of repetition period of pulse trains upon the Doppler rejection of chaff and weather. The chaff and weather have velocity due to being wind blown. The spectrum of the clutter is very broad due to the variation of wind velocity with altitude. Figure 3 is an approximate indication of the spectral content as a function of range for a pencil beam performing horizon search when the wind direction is along the azimuth pointing angle and the chaff extends from zero range to a range of 100 nmi uniformly from the ground to an altitude of 40 kft. The clutter has appreciable energy only at ranges and frequencies within the cross hatched region. As an example, at a range of 100 km, the clutter spectrum extends from 385 Hz to 120 Hz. The spread is 265 Hz so that the chaff and weather cause interference at all Doppler frequencies when the PRF equals 300 Hz. Since this problem is partially due to the closely-spaced Doppler ambiguity, benefits can be obtained by increasing the PRF. However, the improvement is limited due to the range ambiguities at higher PRF values.

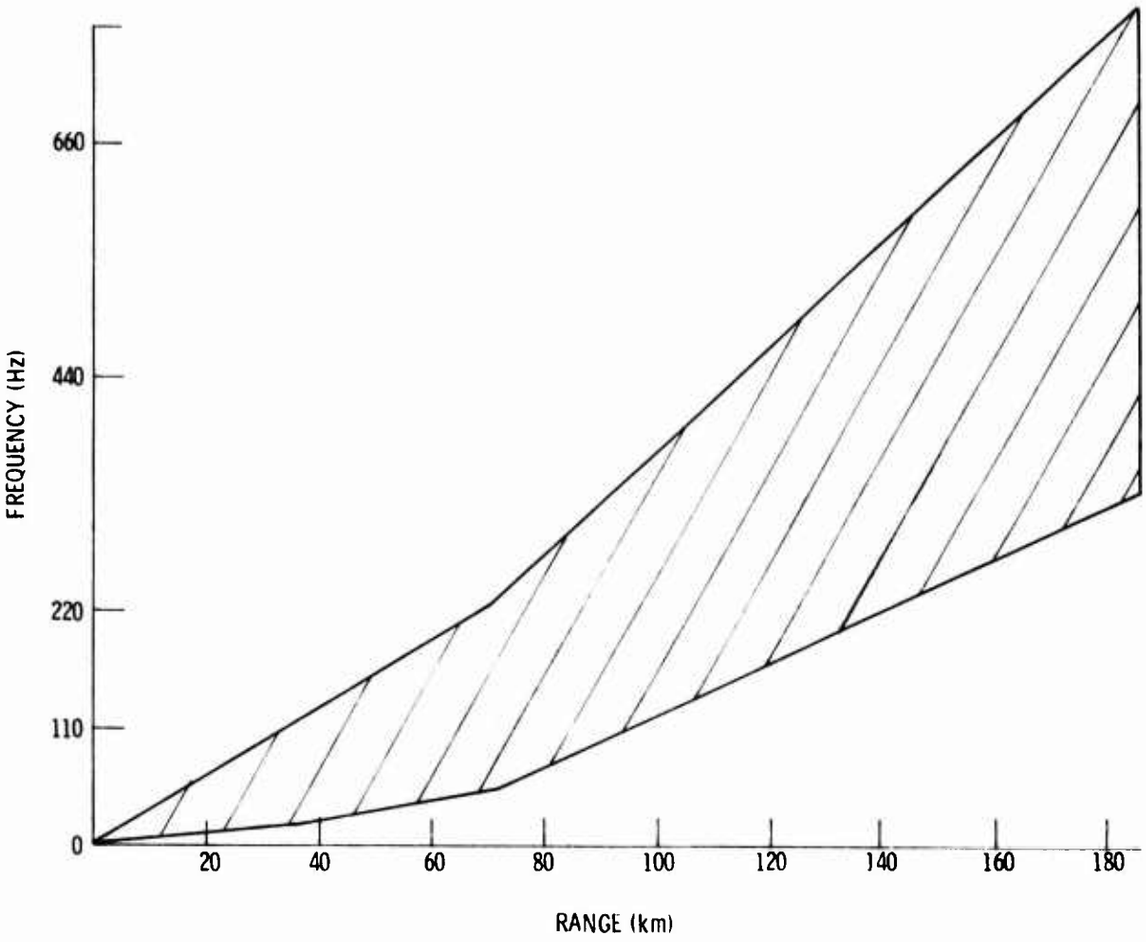

Figure 3. Chaff Spectral Spread for Lowest Beam (No. 1)

Figure 4 shows the effective radar cross section due to the assumed chaff environment at the matched filter output vs the Doppler frequency to which the matched filter is tuned for several different PRF's. The waveform bandwidth is 2 MHz and the range is 100 km. The first case is for the nonrange ambiguous PRF of 300 Hz. The effective radar cross section is approximately 0 dBm^2 at all Dopplers. As the typical target has a radar cross section of about 0 dBm^2 and the signal-to-interference ratio required (SIRR) for detection is approximately 15 dB, it can be seen that targets cannot be detected at this range when using a 2-MHz bandwidth waveform. The next curve is identical except that the PRF has been increased to 1 kHz. The effective clutter cross section is still 0 dBm^2 at and near the clutter's Doppler span

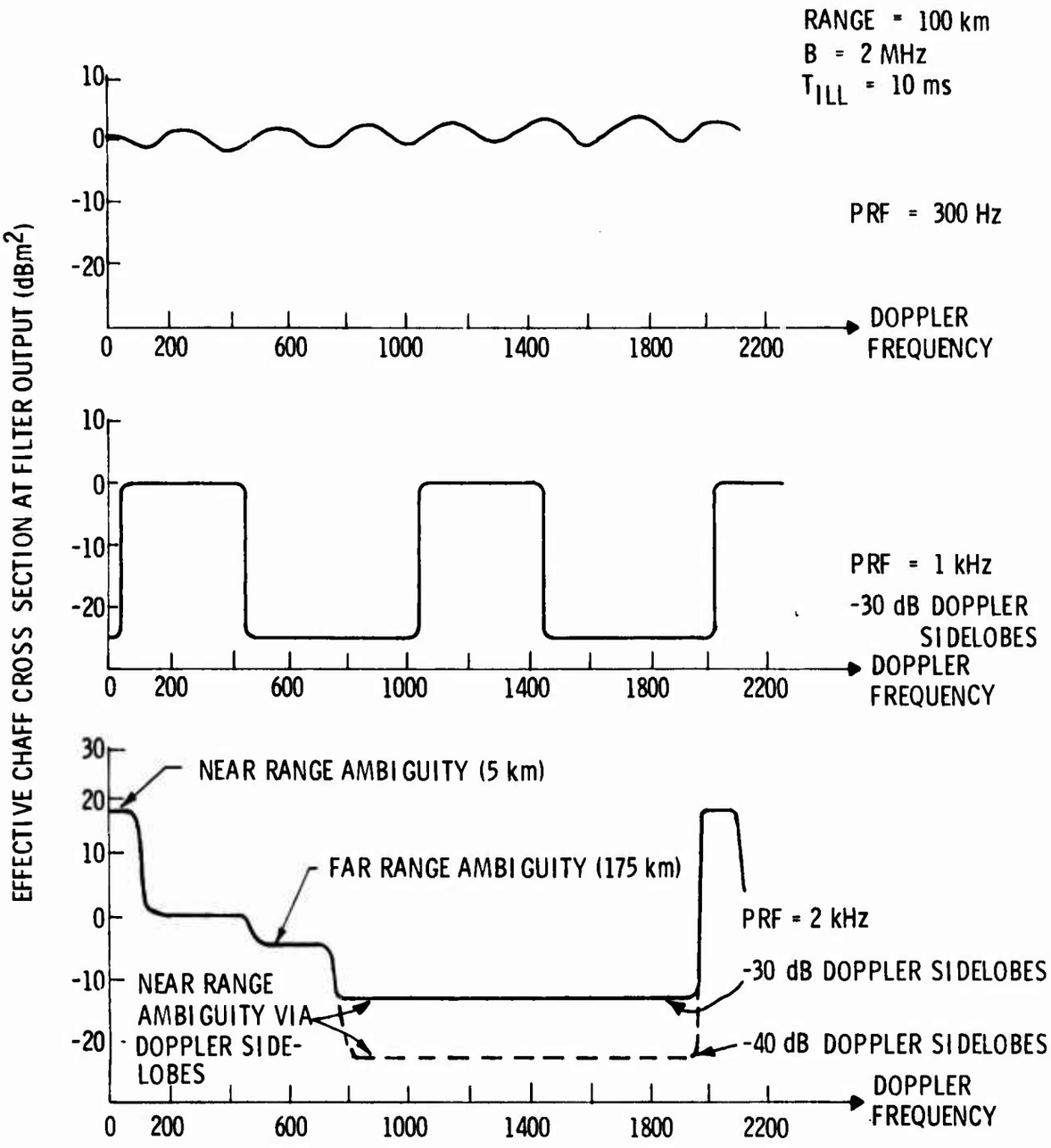

Figure 4. Effect of PRF Upon Doppler Performance for Matched Filter

of 120 Hz to 385 Hz. It is also 0 dBm^2 at higher frequencies due to the Doppler ambiguities. However, there is now a range of Doppler frequency where the effective output clutter cross section is decreased to -25 dBm^2 and targets are easily detectable. This clutter level is due to the clutter picked up via the assumed -30 dB Doppler sidelobes when the matched filter is tuned to Doppler frequencies that are far removed from the clutter's Doppler span. Note that at the 1-kHz PRF, the range ambiguities are separated by 150 km and the near and far range ambiguities are at ranges where there is no chaff. For the next curve, the PRF is increased to 2 kHz so that the unambiguous range is 75 km. Both the near and far range ambiguities are at ranges that contain chaff. It is seen that for some Doppler frequencies, the effective chaff cross section is increased compared to the 1-kHz PRF case whereas for some Doppler frequencies the effective chaff cross section is decreased. In addition, it is seen that though there are no regions where the level is less than -15 dBm^2 when using -30 dB Doppler sidelobes, there is a large clear region if the sidelobes are -40 dB. Note that there are some Doppler ranges where the 1-kHz PRF is superior to the 2-kHz PRF and vice versa. Using both PRF's and combining the target detections by OR logic gives superior performance to that obtained when using either PRF alone. In addition, resolution of range ambiguities requires some form of AND, or coincidence, processing. Thus, transmitting three different high PRF's is recommended.

c. Peak Power/Pulse Duration

The tradeoff between peak power and pulse duration was directed toward decreasing the effectiveness of the destructive threats while avoiding extremely-large minimum ranges caused by the inability to receive while transmitting. The potential for improvement exists because intercept receivers respond to the radar peak power. Decreasing peak power decreases the intercept detection range. However, to maintain the maximum radar range, it is necessary to increase the pulse duration to keep the transmitted energy constant. It was found that while decreasing peak power decreases the maximum intercept range, the decrease is sometimes unimportant in the sense of having small effect upon the destructive threat system performance. This is not always true as the performance depends significantly upon the intercept receiver sensitivity and the range of sensitivities is at least 50 dB. The multiple subpulse diversity waveform is especially well suited for low-peak power long duration waveforms as the minimum range is controlled by the duration of the last subpulse instead of the total pulse duration.

The effect of increasing signal bandwidth, or bandspan, upon intercept range is similarly relatively unimportant. This occurs because some intercept receivers have extremely-broad instantaneous bandpass, covering up to an octave, while some are narrowband with instantaneous bandpass of about 10 MHz. For the former type receiver, the detectability of a radar pulse, subpulse, or frequency diversity waveform pulse is independent of the signal bandspan. For the latter receiver, there is significant difference in the detectability as a function of bandspan and the dependence differs depending upon the waveform.

d. Sidelobes

The sidelobes are of interest primarily to aid in choosing particular "good" codes for the tactical radar scenario. The pertinent sidelobes are the range sidelobes. They depend upon the pulse coding. The Doppler sidelobes depend upon the pulse train parameters and not upon the phase or frequency coding of each pulse. There does not appear to be a requirement for extremely-low range sidelobes for a tactical radar. Sidelobes that are at a -20 dB or -25 dB level appear adequate. These levels are attainable, with sidelobe reduction filtering for some cases, for all of the codes and it is not reasonable to choose any particular coding on the basis of range sidelobe properties.

3. PERFORMANCE DEPENDENCE UPON BANDWIDTH/BANDSPAN

A discussion of the effect of changing bandwidth is complicated. The complications are due to several sources. One is an environment sensitivity. The environments that have been emphasized are:

- Thermal noise
- Electronic countermeasures (ECM) chaff and natural clutter
- Noise jamming
  - Fixed parameter jammers
    - (i) Barrage
    - (ii) Sweeping spot
  - Variable parameter spot
    - (i) Narrowband tunable jammers
    - (ii) Bandwidth and center frequency variable
- Decoy jamming

A second source of complication is that the performance change depends upon whether the increased bandwidth is obtained by increasing the bandwidth of a phase coded pulse or by adding an additional subpulse to a frequency coded (frequency diversity) pulse. As an aid in clarification, and because the performance improvement due solely to the frequency diversity waveform properties are extremely important, only bandwidth changes due to phase coding are considered here. The frequency diversity waveform properties are considered later.

The third source of complication is the target reflection properties. One usual assumption is that the target is a theoretical point of constant radar cross section. This is a nonfluctuating target. Another is that the target is essentially an infinite number of scatterers distributed over range. The instantaneous cross section is caused by the phasor addition of these scatters and the radar cross section is viewed as a random variable. In addition, the theoretical point target can be modelled as a fluctuating target. The waveform properties vs signal bandwidth will be discussed using these assumptions. These assumptions are approximately valid over a broad range of conditions, but tend to be less valid for extremely-wide bandwidths when viewing targets at a nose or tail aspect. These special cases are quite significant for a surveillance radar designed for inherent ECCM capabilities and are considered separately after this subsection.

As is shown in standard textbooks, the optimum processor for detection of point targets in thermal noise is a matched filter processor. The SIRR for detection depends only upon the detection probability and the false alarm probability. It does not depend upon the waveform details such as bandwidth. However, though the SIRR is invariant, the radar system performance does depend upon the signal bandwidth.

A summary of the radar system performance change with bandwidth is that as the pulse bandwidth increases the performance against

- Thermal noise decreases
- Chaff and clutter increases
- Decreases for both types of fixed parameter noise jammers
- Increases for both types of variable parameter jammers
- Increases against decoy jammers

Some details of the performance trends is given below. An expanded discussion is in Section II.

a. Thermal Noise

An aircraft target is reasonably modeled as a point reflector when the waveform range resolution cell length is greater than the target length. Otherwise, a better model can be assumed if the target reflectivity is distributed over several cells. For a Boeing 707, 45-m long, a bandwidth of 3.3 MHz gives a range resolution equal to 45-m long. This bandwidth represents the transition between a point target model and a distributed target model for this aircraft. For either target model and fixed transmit energy, the radar performance decreases as bandwidth increases.

The performance decrease with bandwidth increase is due to two separate causes. One cause is that data processing constraints impose a fixed false alarm rate. As the bandwidth increases, the number of range cells increases, the allowable false alarm probability per range cell decreases, and this increases the required signal-to-noise ratio (SNR). The second cause is appropriate only for targets whose return is distributed over several range cells. For these targets, postdetection integration over the several range cells is required. The loss is due to the noncoherent integration loss incurred when integrating the signal return from several range cells. The losses can be stated in terms of the ratio of the bandwidth used to the bandwidth whose range resolution cell length equals the target length. For the point target, the performance degradation is approximately 0.6 dB when the ratio equals 10 and is approximately 1.2 dB when it equals 100. For a distributed target, the respective losses are 1.7 dB and 5.0 dB. Since the losses increase with bandwidth, the smallest consistent with the required range resolution and range measurement should be used.

b. ECM Chaff and Weather Clutter

The target detection performance for detection in chaff and natural clutter increases monotonically with bandwidth. This is primarily because the signal-to-interference ratio attained (SIRA) increases with bandwidth. For bandwidths much less than the target transition bandwidth, the SIRA increases linearly with bandwidth. For bandwidths much greater than the transition bandwidth, the improvement varies approximately as the square root of bandwidth.

c. Noise Jamming

There are several distinct types of noise jammers. Some are fixed parameter as they do not use any type of receiver, and thus cannot modify their characteristics to match the radars. These are barrage jammers and slow-swept jammers. The latter scan the band (approximately an octave) in a time of the order of seconds. Other noise jammers are somewhat adaptive and use the received radar signal to modify the jammer characteristic. One example is the well-known narrowband tunable jammer; the second is capable of modifying both its center frequency and bandwidth.

The barrage jammer is like thermal noise in that its spectral power density is a constant that does not depend upon the radar's existence. Thus, for the same reasons as for thermal noise, the radar performance decreases with bandwidth increase. Similarly, for the sweeping spot jammer, increasing radar bandwidth decreases radar performance. This occurs because increasing the radar bandwidth increases the instantaneous probability that a portion of the radar spectrum is contained within the jammer spectrum. Thus, for nonadaptive noise jammers, the best performance occurs when the radar bandwidth is minimized.

There are two types of effects to consider for the variable parameter noise jammers. One is the effect of radar bandwidth upon the jamming efficiency; the second is the effect of the bandwidth upon the associated intercept receiver.

Radar performance improvements are possible when the pulse bandwidth is greater than the jammer bandwidth. In addition, even greater improvement can be obtained by using a frequency diversity waveform. For a diversity waveform the subcarrier frequencies are separated by more than the jammer bandwidth. Thus, only one channel can be jammed and the target is detected by the other unjammed channels.

The receivers used to control the jammer parameters use either extremely wideband pre-envelope detector bandwidths (of the order of half or a full octave) or narrow bandwidths (of the order of 1 to 20 MHz). Either receiver type can be used to properly set the center frequency of the fixed bandwidth jammer. Multiple channelized versions of the second are required to control the transmit bandwidth of the second jammer.

The detector output of the wideband receiver is essentially the radar waveform's envelope independent of the radar bandspan. Thus, modifying the radar spectrum has no effect upon this type of receiver. The only way to effect this type of receiver is to decrease the transmit peak power.

The narrowband receiver can be a single channel of a sweeping receiver or it can consist of many parallel channels that cover the overall bandwidth of the wideband receiver. The former can be used to set the center frequency of the fixed bandwidth spot jammers; the latter is required to match the jammer spectrum to the radar spectrum. The intercept receiver output is independent of the radar bandwidth when the radar bandwidth is less than the receiver's bandwidth. For larger bandwidths, the intercept receiver output decreases with increases radar bandwidth.

d. Decoy Jamming

Increasing radar bandwidth tends to degrade the performance of decoy jammers. Quantitative indications of the potential degradation are of limited use as the degradation is due to equipment limitations rather than fundamental limits.

4. FREQUENCY DIVERSITY WAVEFORMS

The frequency diversity waveform has major advantages for an ECM application. One major advantage is that it can produce large bandspan waveforms in an economical manner. This is true because the cost of the waveform/signal processor is primarily determined by the total band occupancy of the waveform. (The band occupancy is defined as the sum of the bandwidths of each subpulse.) The frequency diversity waveform with the nonfilled spectrum maximizes the ratio of bandspan to band occupancy. Another important advantage of frequency diversity waveforms is that their use increases the detectability of fluctuating targets.

It is well known that the SIRR to detect a fluctuating target in noise or clutter (reverberation) depends upon the particular form of the fluctuation characteristic. The fluctuation loss, or increased SIR required for detection as compared to a nonfluctuating target, is discussed in many standard texts. In particular, Nathanson* has a graph of the detection probability vs SIRR for a nonfluctuating target, for Swerling cases 1 through 4, and one of the Weinstock cases. The curves show that for a Swerling 1 or 2 model, the fluctuation loss at a false alarm number 10^6 is 1.5 dB for a detection probability of 0.5 and 8 dB for a detection probability of 0.9.

*Nathanson, F.E., "Radar Design Principles", McGraw-Hill, 1969, p. 84.

The capability of a multiple carrier frequency waveform to reduce the fluctuation loss has been long recognized and the improvement has been experimentally verified.* This class of waveform is denoted by some authors as frequency agility and by others as frequency diversity. A qualitative indication that frequency diversity will decrease the fluctuation loss can be obtained by noting that the total return from a typical target consists of the superposition of the reflections from many individual scattering points. The magnitude of the sum depends upon the relative phasing of these reflections. For some phase conditions, the resultant magnitude is small and the detection probability is small. A change of transmit frequency changes the relative phasing of the reflections. It is improbable that a small target magnitude occurs on all of the different carrier frequencies and the fluctuation loss is decreased.

A quantitative evaluation of the decreased fluctuation loss, or diversity gain, can be obtained by comparing the performance of two systems. The first transmits a single pulse of energy E; the second transmits equal energy by using K-pulses, or subpulses, each of energy E/K at different carrier frequencies. For detection in noise when the SIRA for the single pulse system is γ, the SIRA for each channel of the multiple carrier system is γ/K. The subpulse waveform is the upper plot shown in Figure 1. Each pulse is divided into K-subpulses and each subpulse is at a separate carrier frequency, f_1 through f_K. Another waveform which transmits a single carrier frequency pulse and changes frequency on a pulse-to-pulse basis is shown as the lower plot in Figure 1. The two versions are mathematically equivalent with respect to the target detection properties. The waveforms differ in implementation cost and compatibility with Doppler processing. A conceptual block diagram of the processor for the subpulse waveform is shown in Figure 2.

* Nathanson, F.E., "Radar Design Principles", McGraw-Hill, 1969, pp 183-191.

When the density function for the target cross section is exponential and the carrier frequencies are sufficiently widely spaced so that the returns of the K subpulses are independent, the target fluctuation model is Swerling 2. The diversity gain is given by DiFranco and Rubin*. Related analyses have been discussed by others**. The diversity gain is shown by the curves of Figure 5. It is seen that there is an optimum number of pulses to maximize the diversity gain, but that the optimum value depends upon the detection probability. Note also that for 0.9 detection probability, the diversity gain can recover up to 4.9 dB of the fluctuation loss by using 7 channels. The region of the maximum is relatively broad. For 4 channels, the optimum number when the detection probability equals 0.7, the gain is 4.6 dB. Thus, four or fewer channels seems a reasonable compromise between attained performance and implemention cost. As discussed in detail later, and in Section II, the diversity gain depends upon the target model. It is predicted that the gain is substantially larger than these values when viewing aircraft at nose and tail aspects.

The constraint of equal energy for the two systems was imposed so that the differential performance of detection of targets in noise is due solely to use of multiple frequencies. Similarly, in order to compare the systems for detection of targets in clutter and isolate the multiple frequency effect, it is necessary to compare them so as to isolate the multiple frequency effect. This is done by imposing a constraint of equal total bandwidth. Thus, when the single channel system has a bandwidth of B, each channel of the multiple channel system has a bandwidth of B/K. That the detectability of targets in clutter depends primarily upon the total occupied bandwidth and not upon how it is partitioned between channels can be seen by noting

---

* J.V. DiFranco and W.L. Rubin, "Radar Detection", Prentice-Hall, 1968, p. 405.

** P.F. Guarguaglini, "A Unified Analysis of Diversity Radar Systems", IEEE Trans. on Aerospace and Electronic Systems, March 1968, pp 318-320.

K.L. Horn & N.D. Wallace, "Detection of Slowly Fading Targets With Frequency Agility", Proceedings of the IEEE, May 1969, pp 817-818.

V. Vannicola, "Detection of Slow Fluctuating Targets with Frequency Diversity Channels", IEEE Trans. on Aerospace & Electronic Systems, Vol. AES-10, No. 1, January 1974, pp 43-52.

R.A. Scholtz, J.J. Kappe, N.E. Nahi, "The Detection of Moderately-Fluctuating Rayleigh Targets", IEEE Trans. on Aerospace & Electronic Systems. Vol. AES-12, No. 12, March 1976, pp 117-26.

D.K. Barton, "Comments on the Detection of Moderately Fluctuating Rayleigh Targets", IEEE Trans. on Aerospace & Electronic Systems, Vol. AES-12, p 643.

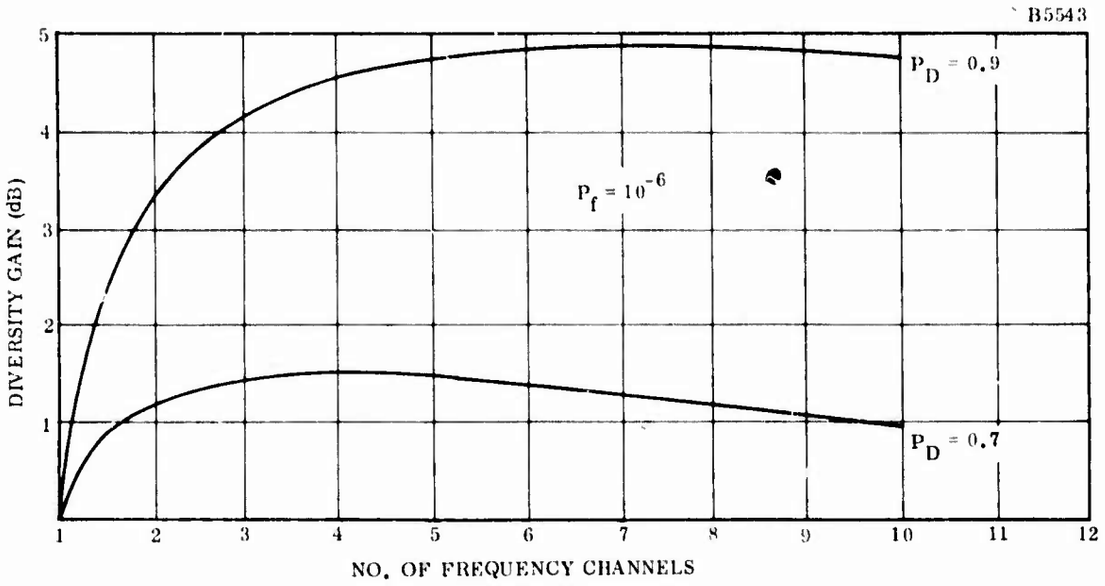

Figure 5. Diversity Gain vs No. of Channels for Swerling 2 Fluctuation

that when the SIRA for the single channel system is γ, the SIRA for each channel of the multiple channel system (assuming the clutter is uniformly distributed in range) is γ/K. As the clutter is statistically independent from channel to channel, noncoherent summing increases the SIRA value by almost a factor of K. Thus, for a nonfluctuating target, the detectability in clutter is almost the same as for the single channel waveform and differs only due to the noncoherent summing loss. Therefore, the significant parameter for detection in clutter is total bandwidth. The total system bandwidth is defined as the band occupancy. Note that the total band spanned is generally larger for the multiple channel system than for the single channel system.

Though detection of nonfluctuating targets is about the same for the two systems, the multiple channel approach gives improved detectability of fluctuating targets in clutter just as it does in a noise environment. Note that the total bandwidth occupancy constraint gives relative SIRA values that are identical to the relative SIRA values attained for a noise environment. Therefore, the diversity gain curves of Figure 5 are also applicable for detection of targets in clutter. This curve gives the diversity gain when the environment is thermal noise, barrage jamming noise, or range distributed clutter.

There are two additional benefits to using a diversity waveform as compared to a single channel waveform of the same band occupancy. First is that, similarly to the comparison made for the thermal and barrage jamming noise environments, the best way to compare the performance of the two waveforms is on the basis of identical false alarm rate rather than false alarm probability per decision. Since the single channel waveform needs to make more target present or absent decisions per unit time than does the multiple channel system, the multiple channel system has an additional gain. Second is that the curves are based upon the assumption that the clutter is continuously distributed in range so that increasing bandwidth always decreases the clutter cross section per range cell and increases the SIRA. Since chaff or weather is actually discretely distributed in range, the assumption is not valid for extremely-large single channel band occupancy. However, increasing band occupancy by increasing the number of channels of a diversity waveform or the bandwidth of a single channel (to resolution values less than the spacing of the discrete scatterers) does increase the SIRA in chaff and weather.

The frequency diversity waveform also has substantially better target detectability for a spot jammer environment. This occurs even though the SIRA increases with bandwidth for a single frequency channel waveform. A numeric example is indicated by Table I.

TABLE I

EFFECT OF SINGLE CHANNEL BANDWIDTH UPON SIRA

1. Thermal Noise Environment

	Signal Bandwidth	
	1 MHz	100 MHz
Peak Target Power at Matched Filter Output	100 μW	10,000 μW
Noise Power	1 μW	100 μW
SIRA	20 dB	20 dB

2. Additive Spot Jammer

	Signal Bandwidth	
	1 MHz	100 MHz
Peak Target Power at Matched Filter Output	100 μW	10,000 μW
Noise Power	1 μW	100 μW
Jammer Power	1,000 μW	1,000 μW
SIRA	-10.0 dB	9.6 dB

The example assumes a case where for thermal noise, the SIRA value is 20 dB. Note that though for white noise the SIRA value does not depend upon the signal bandwidth, the received noise power and peak signal power does change with bandwidth. The second portion of the example assumes a 1-MHz bandwidth spot jammer of power sufficient to decrease the SIRA for the 1-MHz bandwidth waveform to -10 dB. Note that with the same jammer, the SIRA value for the 100 MHz waveform is substantially higher. A 20-dB bandwidth increase improves the SIRA value by almost 20 dB. Though this clearly indicates the improvement attained by increasing the bandwidth of a single channel system, note that even with the improvement the SIRA value is 10.4 dB less than the unjammed value. Contrast this with the performance obtained for a four-frequency diversity system. The spot jammer can only jam one of the four frequencies. The SIRA value is then 0.75 of its unjammed value or 18.75 dB. This is 9.15 dB better than that attained by the wideband single channel waveform. In addition, the noncontiguous-spectra-frequency diversity waveform is better than the single-channel wideband waveform even when the spot jammer bandwidth is capable of matching its bandwidth to the radar signals bandspan.

The preceding was based upon conventional target models. The effects due to more realistic target models are considered in detail in the next section.

A more realistic target model is necessary as it is known that for some aspects, the energy reflected form typical aircrafts is due to four or fewer dominant scattering points. The bandwidth dependent and frequency diversity coding properties of this more realistic target model are significantly different than those obtained for the point or distributed target. For the point target, the SIRR for detection is independent of bandwidth. For the realistic target model, the SIRR depends upon bandwidth. There is an optimum bandwidth that maximizes target detection in a thermal noise or barrage jamming noise environment. The optimum bandwidth depends upon the target's physical structure and for tactical radar targets it is of the order of 35 to 75 MHz.

5. EFFECT OF TARGET MODEL

A common target assumption is that the target is an isolated point and its cross section is a specified constant value. Alternately, the isolated point is assumed to have a fluctuating cross section. The mechanism that causes the fluctuation is the random phasor addition of the scattering from several portions of the target. As this inherently conflicts with the isolated point concept, the target is sometimes viewed as being continuously distributed in space instead of a single point. When the number of scattering point is very large, the fluctuation statistics are consistent with the commonly assumed fluctuation models. However, it is known that for nose and tail aspects, the energy reflected from typical aircraft targets is due to four or fewer dominant scattering points. The fluctuation statistics then differ considerably from the commonly assumed models. The frequency diversity and bandwidth dependent properties of this more realistic target model are significantly different than that obtained for the point target or continuously distributed in range target models. As examples, for the point target models, the SIRR for detection is completely independent of bandwidth. For continuously distributed targets, the SIR required for detection is constant for bandwidths such that the range resolution cell length is greater than the target's radial length. There is a loss associated with large bandwidths since the SIR required for detection increases monotonically with bandwidth when the target encompasses several range resolution cells. This occurs because the optimum processor is to noncoherently sum the square-law detected outputs of the cells encompassing the target. The SIR per cell decreases with bandwidth as the target's cross section is distributed within the cells encompassing the target. The loss incurred is identical to the noncoherent summing loss incurred when summing multiple pulses. For the realistic target model and a single channel phase-coded pulse waveform there is an optimum bandwidth that maximizes target detectability in a thermal noise or barrage jamming environment. The optimum bandwidth depends upon the target's physical structure and is of the order of 35 to 75 MHz. The target model also impacts the diversity channel performance. It is mandatory that the effects due to realistic target models be included when comparing the performance attained by using frequency coding.

The manifestation of the few specular reflectors target model is different depending upon the signal bandwidth. For small bandwidths, the individual reflectors are not resolved. The cross section is due to the random phasor addition and a fluctuating target result. For sufficiently large bandwidths, each individual reflector

is resolved and each is a nonfluctuating target. The signal processor for large bandwidth waveforms is a matched filter with a "small" bandwidth video filter after envelope detection. This filter is used to noncoherently integrate the resolved target returns and its bandwidth is inversely proportional to the target length. A conceptual implementation is a tapped delay line with taps spaced at the reciptocal of the IF bandwidth. The length of the delay line equals the time spanned by the duration of the target return.

The critical bandwidth is defined as that which resolves the reflectors into separate range cells. Below this bandwidth, the target fluctuates and is contained within a single resolution cell. Above this, the target spans several range cells and noncoherent integration of the range cell returns is required. Figure 6 shows the critical bandwidth as a function of reflector spacing. Typical tactical radar targets have spacings of 2 to 4 m. The corresponding critical bandwidth is 75 to 37.5 MHz.

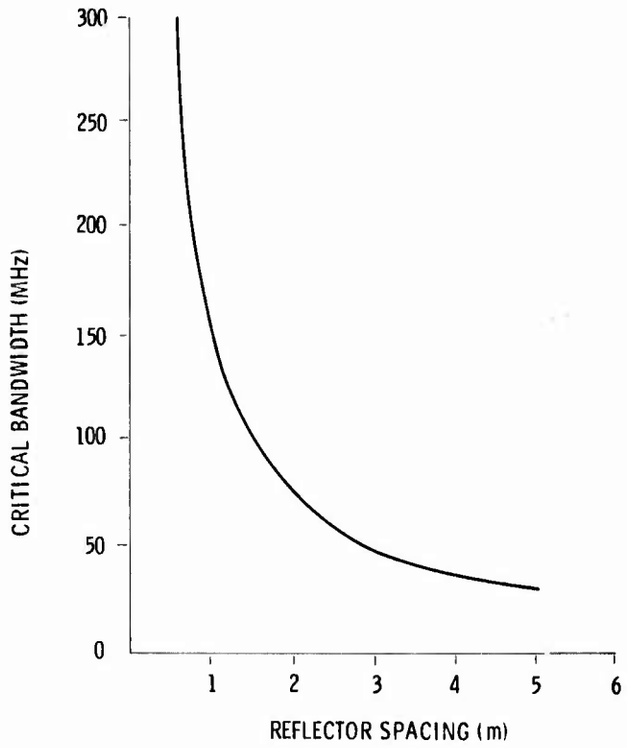

Figure 6. Critical Bandwidth Required to Resolve Specular Reflectors

The cross section fluctuation model for bandwidths less than the critical bandwidth depends upon the number of reflectors. Figures 7 and 8 show the probability density function of the cross section for 10 and 5 equal magnitude specular reflectors. For comparative purposes, the density function for the Swerling exponential model (cases 1 and 2) is also included. It is seen that the agreement is close and it should be expected that analysis based upon the Swerling model is quite satisfactory. However, existing measurements demonstrate that at nose and tail aspects, typical aircraft targets consist of two- or three-large reflections plus several other significantly smaller reflectors. The effect of a target that consists of four or fewer-equal

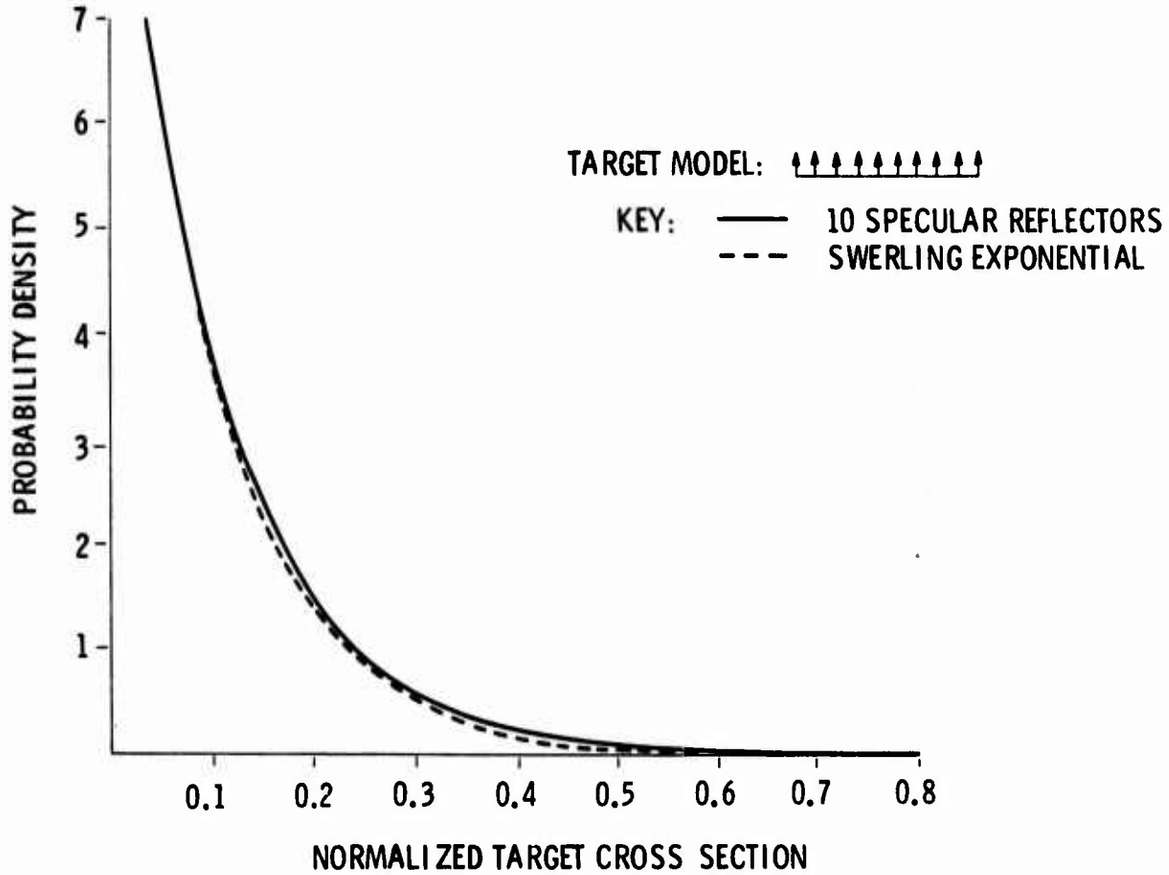

Figure 7. Target Cross-Section Density for 10 Reflector Model

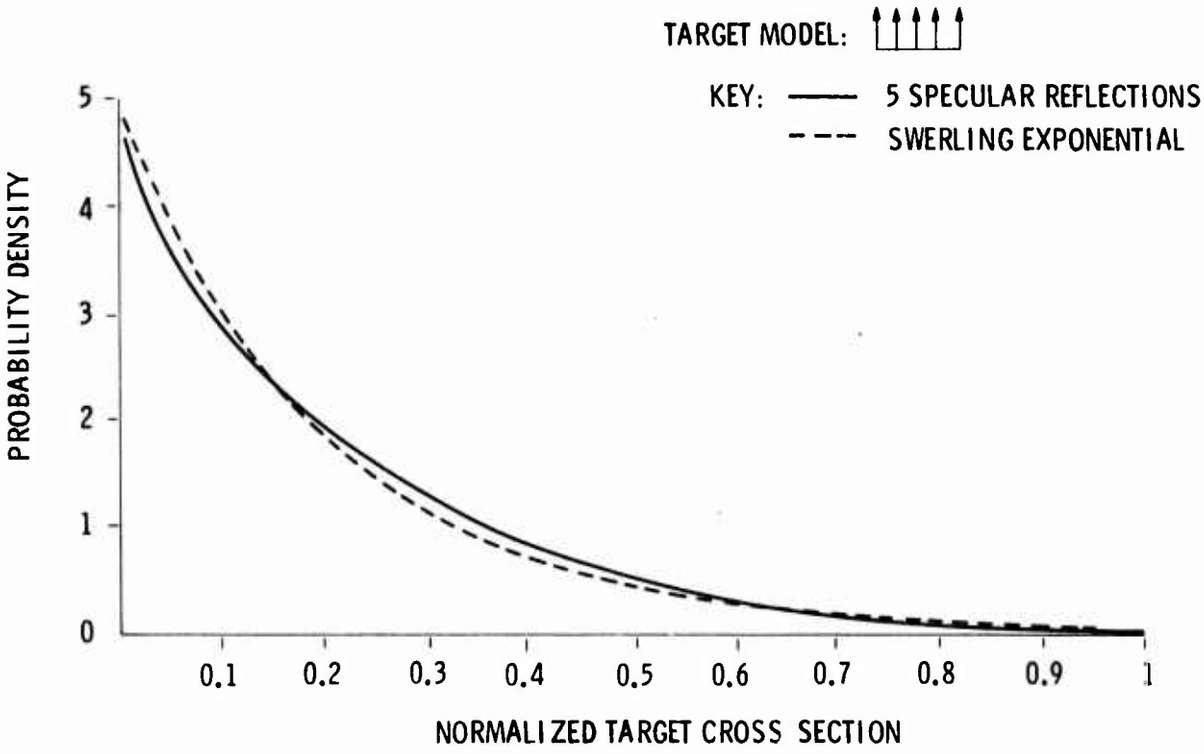

Figure 8. Cross-Section Density for 5 Reflector Model

magnitude reflectors is shown by the curves of Figure 9. It is seen that the density functions are completely different than those considered on the previous curves. The accuracy of results based upon the Swerling fluctuation model is questionable. Figure 10 gives curves of probability of detection vs SIRR for several target models. Note that the fluctuation loss (the additional SIRR for detection probability of 0.9 as compared to the nonfluctuating target) differs considerably from model to model. It is quite large for the two reflector models. This is of major significance for a radar attempting to detect targets at nose or tail aspects.

Frequency diversity waveforms can be used to reduce the fluctuation loss. This reduced loss, or diversity gain, is shown by the curves of Figure 11 for the various target models. It is seen that a reasonable compromise between attained diversity gain and equipment complexity is to use between two and four frequency channels.

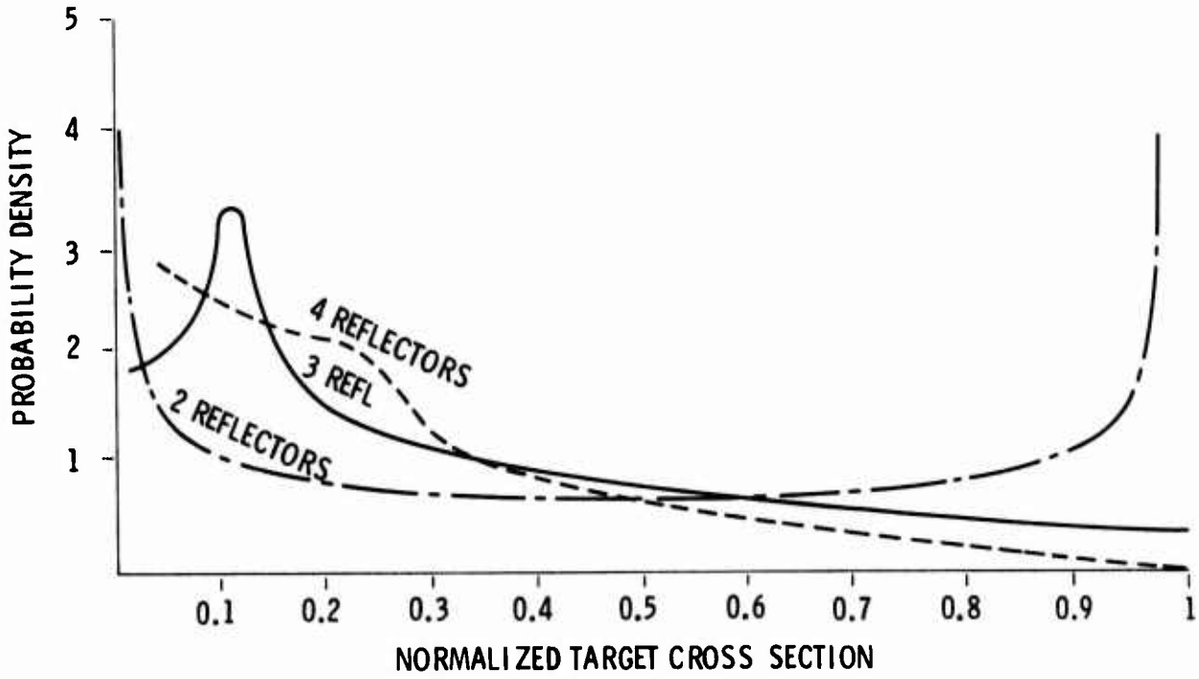

Figure 9. Target Cross-Section Probability Density for 2, 3, 4 Reflector Target Models

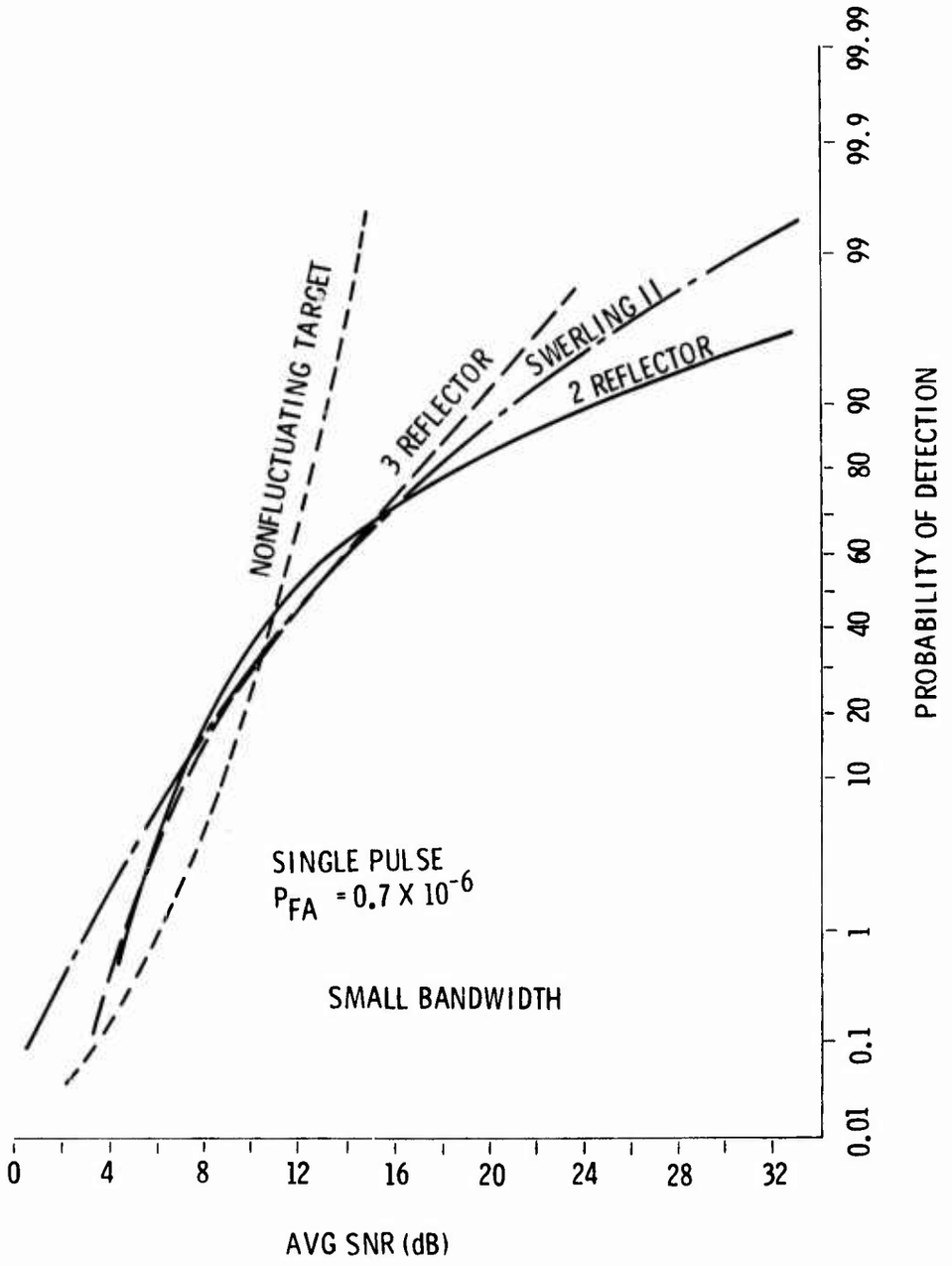

Figure 10. Detection Probability for Several Target Models with "Small" Bandwidth Waveforms

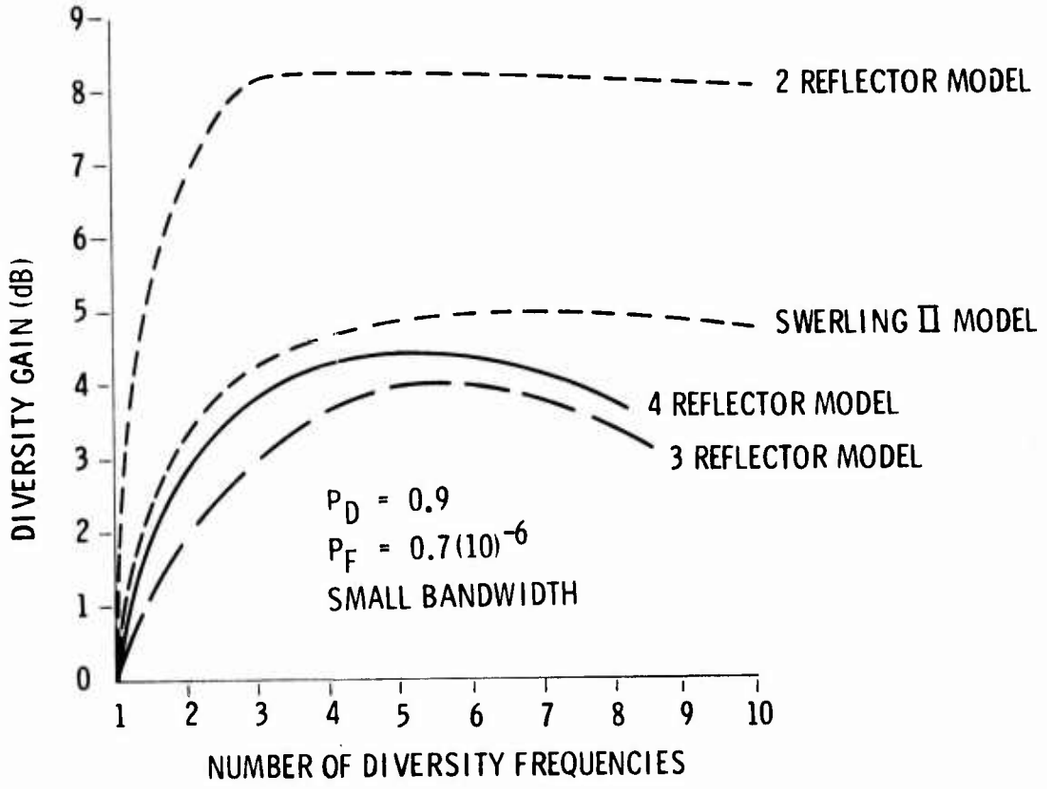

Figure 11. Diversity Gains for Several Fluctuating Targets

The preceding is applicable only when the channel bandwidths are less than the critical bandwidth. Specifically, the diversity gain is accrued due to the fluctuating target characteristics. Diversity gain is defined as the difference in performance between two systems. One is a single channel of transmit energy E and bandwidth B. The other is K-channels with energy E/K per channel and bandwidth B/K per channel. When a channel bandwidth is greater than the critical bandwidth, the individual reflectors are resolved, and there is no longer a fluctuation loss or diversity gain. Thus, when B (the total band occupancy) is slightly greater than the critical bandwidth, the single channel resolves the target reflectors, but each channel of the diversity waveform does not. This modifies the relative performance of the two systems. The curves of Figure 12 shows the SIRR value as a function of normalized band occupancy for the two reflector model. Again it is seen that when the normalized band occupancy is less than unity, the four-channel diversity waveform and processor is better. This is the diversity gain of 8.2 dB. When the normalized band

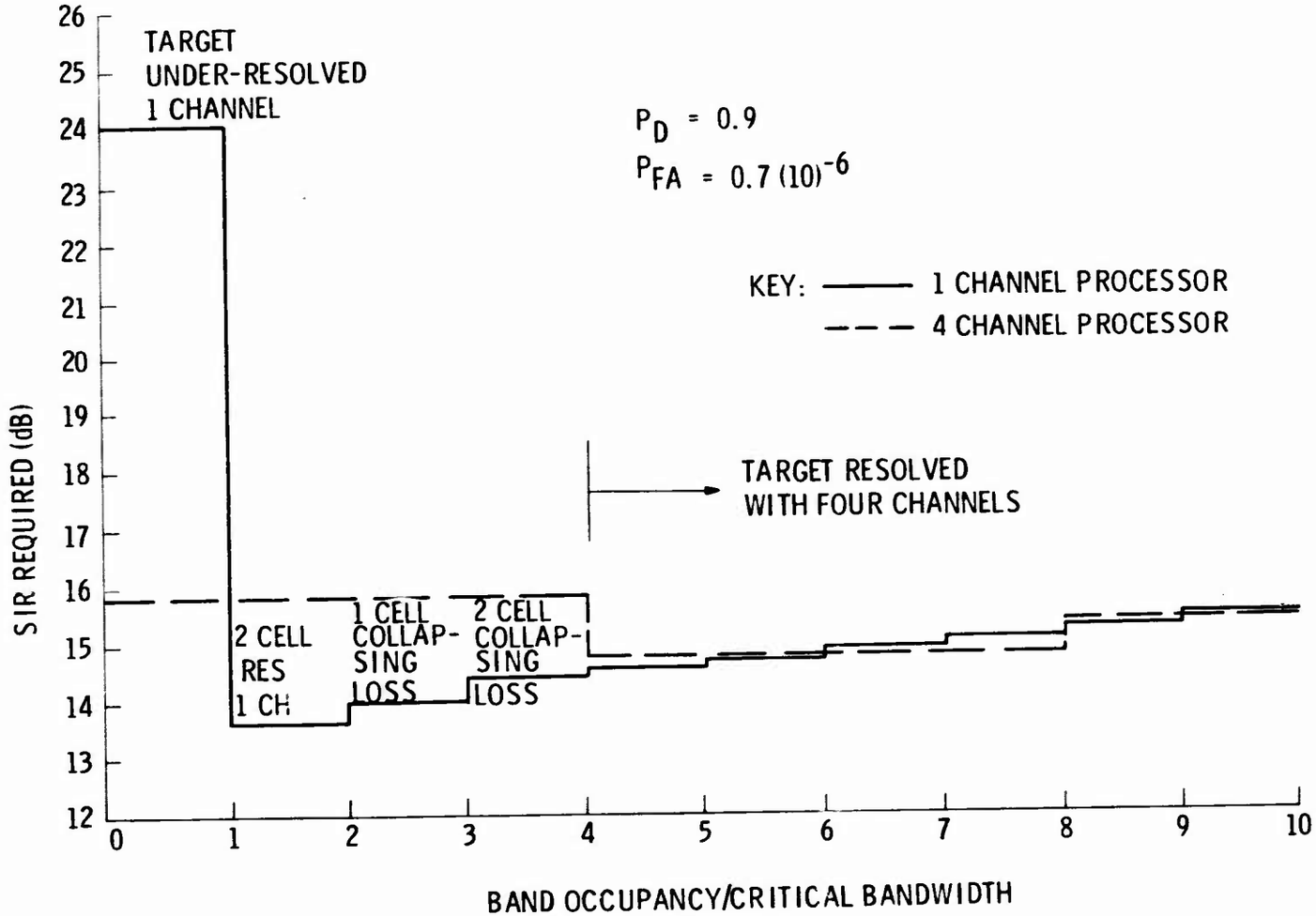

Figure 12. SIR Required as Function of Bandwidth Occupancy
2-Reflector Target Model

occupancy is between one and two, the one channel waveform and processor is superior. Note that as the band occupancy increases, the performance of the single channel degrades. This occurs because it is assumed that the postdetection video filter sums over the full target extent. As the bandwidth increases, the target length encompasses three range cells and there is only target energy in two cells. This causes a collapsing loss. Further increases of band occupancy cause additional SIRR increases due to additional collapsing loss. Note that when the normalized band occupancy exceeds four, each channel of the diversity waveform resolves the target's specular reflectors.

Two significant aspects of these curves are that there is an optimum bandwidth to minimize the SIRR for the single-channel waveform and processor. The SIRR for the small band-occupancy 4 channel waveform is approximately 2.2 dB greater. Note, however, that the four channel waveform can attain this performance with very small values of band occupancy while the single channel waveform requires values between one and two. This large-band occupancy differential is extremely significant as the proper method of comparing waveforms is with a constant false alarm rate constraint whereas the curves of Figure 12 compare them on the basis of the same false alarm probability per decision cell. Comparing on the basis of constant false alarm rate substantially decreases the apparent advantage of the single-channel broad occupancy waveform. As a numeric example, assume the optimum single channel bandwidth is 50 MHz and that the bandwidth of each channel of a diversity waveform is 250 kHz. This latter value is adequate bandwidth for the usual range resolution requirements. The decreased allowable false alarm probability per cell for the single channel waveform causes a 1.4-dB increase in the SIRR. Thus, the advantage of the single-channel wideband occupancy waveform is decreased to 0.8 dB. Since equipment complexity and cost increase with band occupancy, there is an economic trade that must be made. For the tactical radar scenario, it is believed that the small band occupancy frequency diversity waveform is preferable. Figure 13 shows the SIRR values vs band occupancy for a three reflector model. The interpretation of the two graphs is identical to that given for the two reflector model.

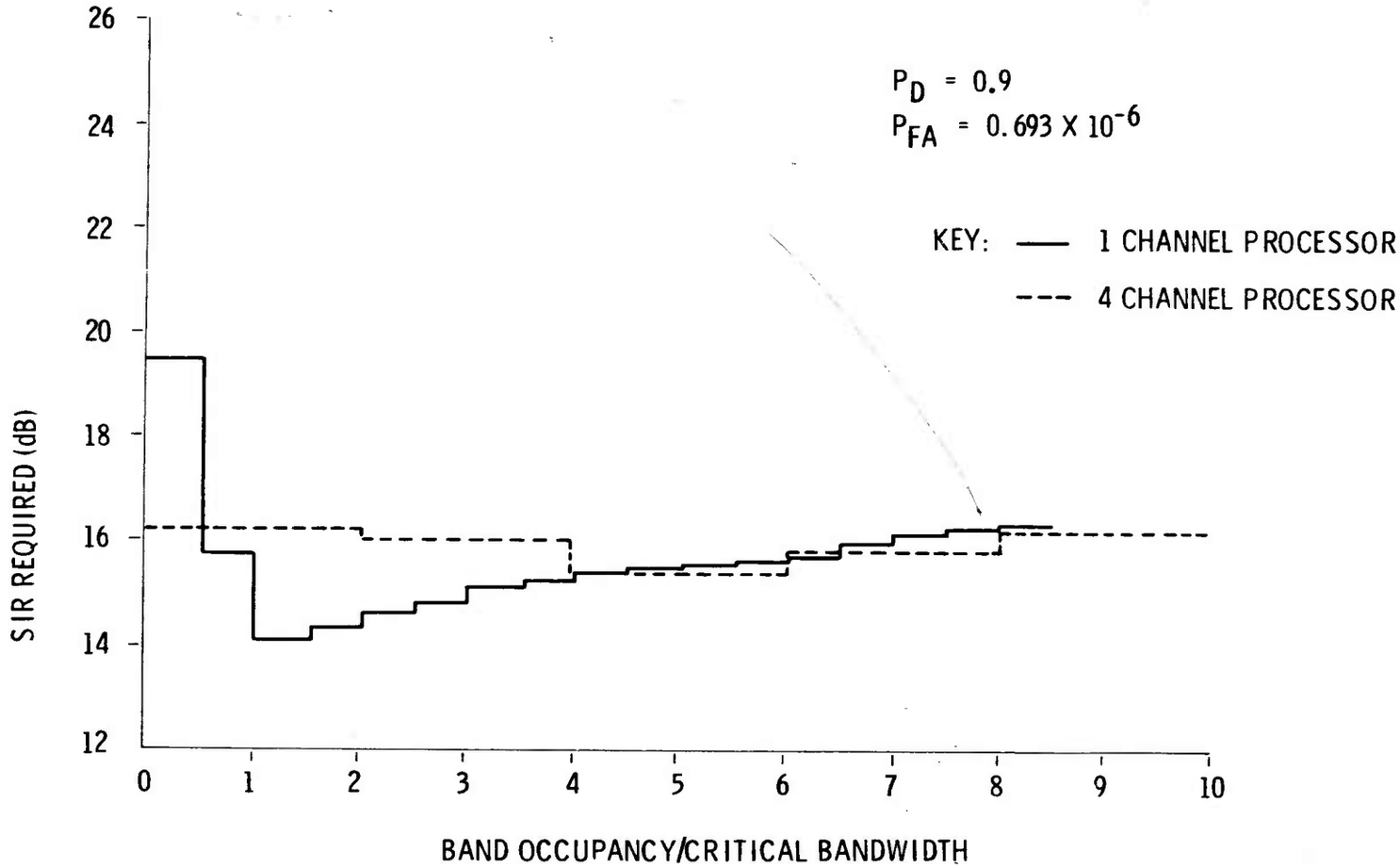

Figure 13. SIR Required As Function of Bandwidth Occupancy 3 Reflector Target Model

C. WAVEFORM CONSTRAINTS DUE TO RADAR COMPONENTS

Several areas have been identified where degraded performance due to processing procedure or due to component deficiencies can occur, and the related effects have been analyzed. The emphasis has been upon fundamental, theoretical limitations, since it appears that the necessary components are available now or are projected to become available. Generation and processing of any bandwith of interest for tactical radars is feasible. Specifically, S-band transmitters with 800-MHz instantaneous 3-dB bandwidths are currently available. Signal processors for extremely wideband waveforms can, in theory, be constructed by employing many, parallel, low-bandwidth channels.

The fundamental limitations that have been considered are:

- Bandwidth limitations of phased arrays
- Sensitivity time control (STC) effect upon long duration waveforms
- Transmitter phase and amplitude ripple vs frequency effects

Array steering by phase shifting rather than the theoretically desired time delay steering effectively creates a filter in the RF line. The filter bandwidth depends upon the array size and the angle steered off broadside. The effective filter bandwidth vs angle for uniformly illuminated square arrays of 33- and 43-dB gain is shown by Figure 14. It is seen that the bandwidth decreases as the antenna gain increases, and as the angle steered off broadside increases.

The effects of the array bandwidth upon a simple pulse, an LFM pulse, and a pseudorandom-noise code (PRN) have been determined. It has been found that the main effect upon the matched filter output is a degradation of the range resolution. There is only a small effect upon the range sidelobes. The range resolution cell broadening factor depends upon the waveform type and upon the ratio of the array bandwidth to the signal bandwidth. The broadening factor is least for the LFM pulse. The simple pulse and PRN waveform broaden identically. The LFM waveform degrades less because almost all of its spectral energy is contained within the -6 dB bandwidths. The other waveforms have spectral tails that decay slowly so that filtering far removed from the carrier frequency has a greater effects. Curves of the broadening factor vs the normalized array bandwidth is given by Figure 15. As an example of the usage of the curves, from Figure 15, the phased array bandwidth when steered ±10° from broadside (20° elevation coverage) for a 43-dB gain antenna is 305 MHz. The data of Table II indicates the broadening factor for 50- and 100-MHz bandwidth LFM and simple pulse or PRN codes.

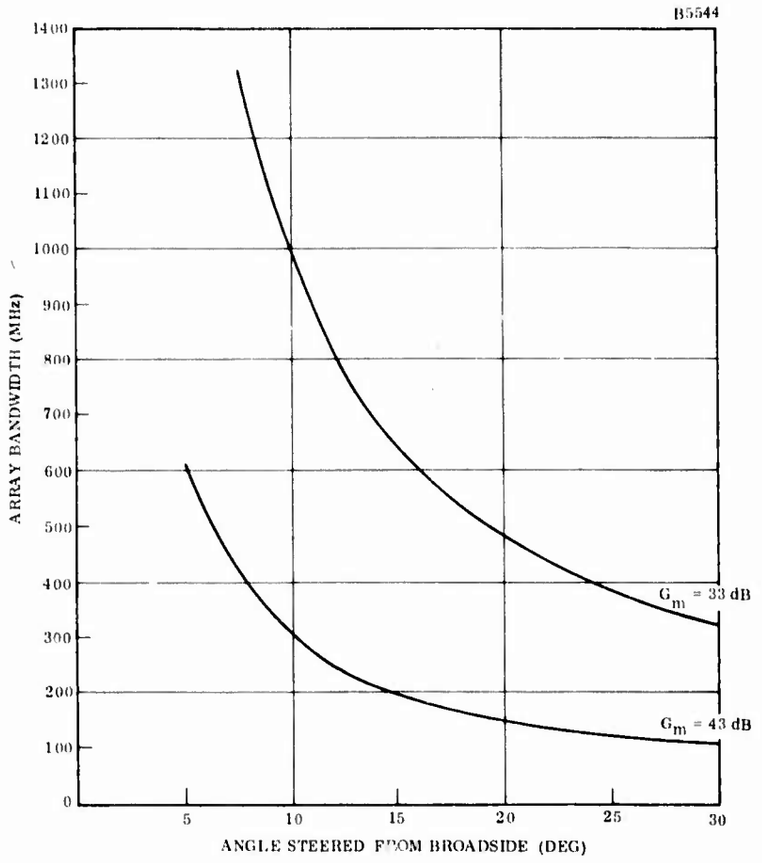

Figure 14. Phased Array Filtering Effects

TABLE II

BROADENING FACTOR

	Bandwidth	
Waveform	50 MHz	100 MHz
LFM	1.0	1.11
Simple Pulse or PRN	1.15	1.33

As discussed later, the preferred maximum bandwidth is approximately 50 MHz. Thus, in general, the problem is not too severe, and using LFM phase coding makes the effect totally negligible.

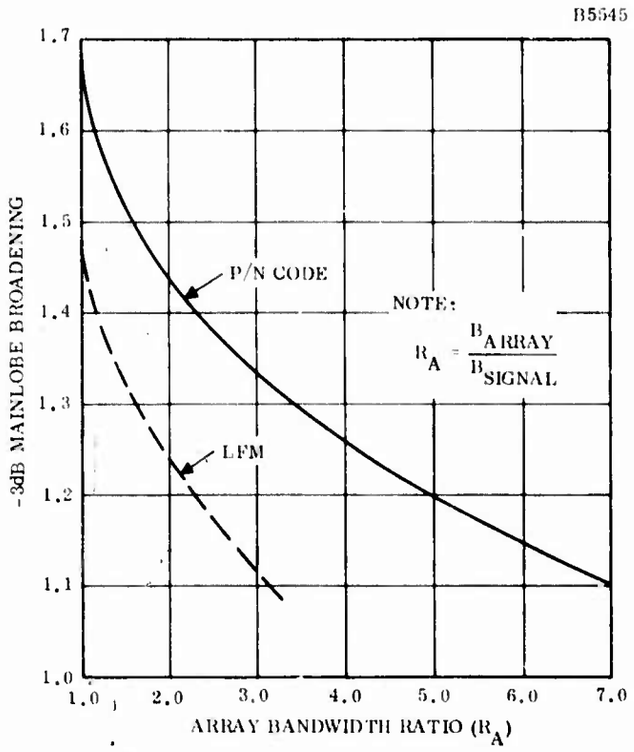

Figure 15. Mainlobe Broadening vs Array Bandwidth Ratio R_A

Another aspect of equipment constraints that has been considered is the effect of sensitivity time control, STC, upon long duration waveforms. STC is necessary because of the limited dynamic range of radar components. Long duration waveforms are of interest because of the applicability when using low-peak power solid-state transmitters and because the use of low peak power and long waveform duration tends to decrease the radar's detectability by enemy intercept receivers.

STC involves increasing receiver gain as a function of range. For a long duration waveform, and short range targets, this can involve a considerable gain increase from the beginning of the pulse to the end of the pulse. There are three areas where this might have significant impact. These are SNR processing losses, range resolution degradation and increased sidelobes. It has been found that the effect is negligible for all these areas.

The effects of transmitter phase and amplitude ripple vs frequency is unimportant if careful attention is given to component choice. The 800-MHz bandwidth transmitter previously mentioned has ripples that cause unequalized range sidelobes that are at least 25 dB below the main response.

7. RECOMMENDED WAVEFORMS

There is no single waveform that is best for all circumstances. The "best" waveform depends upon the condition of the environment. Since the environment state varies with time and over space, it is recommended that a radar have available a library of waveforms. The waveform to be used is determined by checking the instantaneous environment state and choosing the waveform that is best for these conditions. The many benefits that accrue to the frequency diversity waveform dictate that variations of this waveform should always be used.

a. Thermal Noise and Ground Clutter

When chaff, active jamming, or weather is not present, the major considerations are to protect the radar against destructive threats, maximize the detectability of targets at long range, and detect targets in the short-range ground clutter. The radar system will generally not know that destructive threats are in the environment. Therefore, waveforms should always be chosen with regard to their potential to protect the radar. This choice should be tempered by the knowledge that it is practically impossible to prevent the detection of any transmitted pulse. The emphasis should be on choosing waveforms that interfere with the ability to identify and locate the radar. Specifically, a major problem for the destructive threat's intercept receiver is that due to the large numbers of radars, the receiver can usually detect tens or hundreds of thousands of pulses per second in each octave bandwidth. This problem becomes worse as the receiver sensitivity increases. It is relatively easy to identify a fixed parameter radar. That is, if the victim radar's carrier frequency, pulse width, pulse repetition period, phase coding, etc., are rigidly repeated on a pulse-to-pulse basis, it becomes simpler to sort these pulses and, therefore, identify and locate the radar. Parameter agility complicates the sorting task, and it is recommended that as many parameters as possible change on a pulse-to-pulse basis. Frequency agility, change of the carrier frequency on a pulse-to-pulse basis, is mandatory. This prevents the high-sensitivity, high-selectivity, narrowband superhetrodyne receiver from being useful to sort the victim radar from the dense electromagnetic environment. The increased detectability of fluctuating targets due to frequency diversity can be obtained either by partitioning each pulse into subpulses at different carrier frequencies,

or by the noncoherent summing of the nonpartitioned pulses of the frequency agile waveform, or the combination of both techniques. The choice is made by considering the increased implementation cost of multiple receivers for the partitioned subpulse waveform. However, if elevation scanning of a single pencil beam is used, the limited illumination time requires the subpulse technique to implement frequency diversity.

Since, as previously discussed, the radar's detection performance in thermal noise tends to decrease as waveform bandwidth increases, the bandwidth should be chosen to be as small as possible. The range resolution requirements of a tactical radar can usually be satisfied with bandwidths of about 250 kHz.

Narrow bandwidth waveforms with pulse-to-pulse frequency agility do not perform well at detecting targets in ground clutter. It is necessary to augment the long range waveform with a special short range waveform. The short range waveform needs a maximum detection range of approximately 30 nmi. As this is one-eighth the long range waveform's range, its required transmit energy is significantly less than that of the long range waveform. Thus, though this waveform is more vulnerable to the destructive threat's intercept receivers due to lack of frequency agility, it is somewhat less vulnerable because of its decreased energy. In order to improve target detection in clutter, increasing the bandwidth to 2.5 MHz is recommended. The combination of moving target indicator (MTI) processing and this bandwidth is generally adequate to detect targets in ground clutter. Two versions of the recommended waveform are shown in Figure 16. One is for the scanning elevation beam antenna; the other is for the stacked beam antenna. Different waveforms are needed as the available dwell time for the scanning elevation beam technique is less than that of the stacked beam technique. Note that the periods T_1, T_2, T_3 are nonequal. This is both to confuse the signal sorting capability of destructive threat intercept receivers and to achieve elimination of blind speeds by staggered PRF technique. The pulses at carrier frequency f_0 is used for MTI processing. The MTI waveform carrier frequency is agile from beam to beam and is denoted as f_9 in the next beam position. Since the required energy for the short range Doppler-sensitive waveform is quite small, it can be of short duration compared to the other subpulses and a simple, nonphase coded pulse is adequate. The longer range detection is achieved by the subpulse frequency coded diversity waveform. It also uses frequency agility on a beam-to-beam basis.

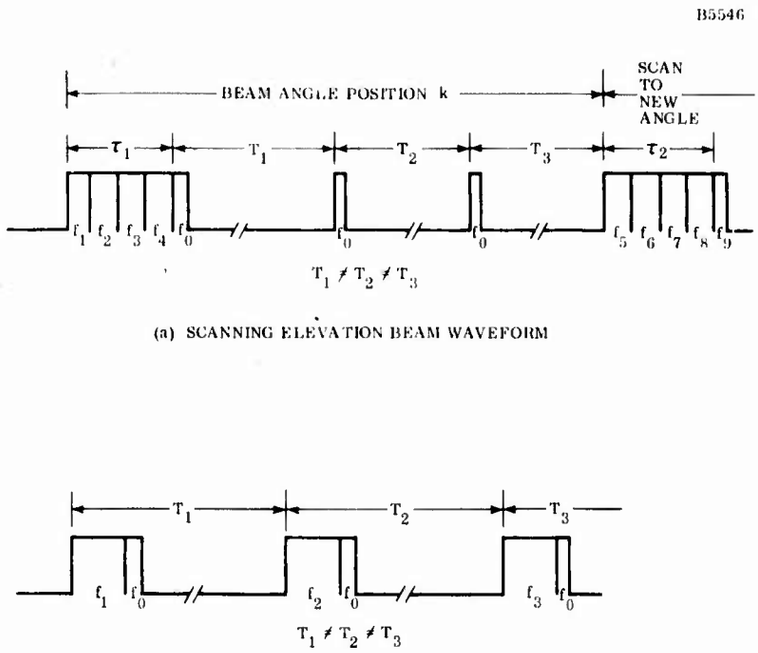

Figure 16. Diversity Waveforms for Scanning Elevation and Stacked Beam Antennas

Phase coding of each subpulse is recommended. One advantage is to decrease the transmitted peak power to aid in reducing the radar's detectability by the intercept receivers of destructive threats. It is also useful when solid-state S-band transmitter modules become available. Since, for a tactical radar application, there is no significant advantage of one phase code over another, the phase coding choice should be made on the basis of equipment simplification. It is, however, recommended that different phase codes be used on a subpulse-to-subpulse basis. This should tend to interfere somewhat with the sorting capability of intercept receivers. Also, this capability is desired in environments containing false target jammers. Since it is available, it should be used even if the advantage is marginal.

The depicted stacked beam waveform achieves frequency diversity on a pulse-to-pulse basis. This procedure decreases cost by eliminating the need for the multiple receivers required for simultaneous multiple channels of a frequency diversity waveform. This nonsimultaneous approach is possible due to the increased

illumination time of stacked beam antennas. Note that there is no true savings in receivers as compared to the scanning elevation beam system since it is necessary to use multiple receivers for the simultaneous multiple elevation channels. The other considerations in choosing this waveform are identical to those used for the elevation scanning approach.

b. ECM Chaff and Weather Clutter

The main attribute of chaff and weather clutter is the large Doppler spread of the wind-blown interference. High PRF waveforms tend to reduce the problem but there is no single choice of PRF that eliminates the problem. The use of several different PRF's is necessary. In addition, the a priori determination of which PRF values are "best" is complicated as the preferred values change drastically with the chaff or weather intensity, range spread, and Doppler spread. Because of this, a large library of PRF values should be available. Different sets can be used on a scan-to-scan basis to improve the target detectability.

The method of achieving elevation coverage has a major impact upon the desired PRF value. The typical target illumination time for the stacked beam antenna is 30 ms. For the scanning elevation beam antenna, this time is allocated to the sequential beam positions. For the low elevation angles, the typical illumination time budget is 5 ms. The impact of this can be seen by noting that the total waveform duration of a 16-pulse train with an average PRF of 4 kHz is 4 ms. Since the propagation time to a range of 240 nmi is 2.93 ms, it is seen that this waveform is not usable for the scanning elevation beam technique, but is usable for the stacked beam antenna. An acceptable waveform for the scanning beam antenna is obtained by either reducing the number of pulses transmitted or the waveform used is changed to the filled burst. For the filled burst, the 16-phase coded pulses are contiguous so that the overall envelope is rectangular. Thus, the total waveform is transmitted in one block. Reception is not interleaved with transmission as with a train, but is done after the complete waveform is transmitted. The total waveform duration must be less than 2 ms in order to meet the time budget and allow for reception time. Sixteen pulses within 2 ms indicates that the minimum PRF is 8 kHz. A small minimum range requirement would require that the waveform duration is less than 2 ms and that the minimum PRF is higher than 8 kHz. It becomes appropriate to consider a PRF of 20 kHz as it gives unambiguous Doppler coverage for the range of target velocities that are of interest. A full investigation of the overall properties of using a Doppler unambiguous PRF has not been performed. It is recommended that additional study work be done in this area.

The waveform bandwidth has a direct impact upon target detection in continuous homogeneous clutter. In theory, performance improves monotonically with waveform bandwidth. Therefore, bandwidths greater than the 0.25 MHz recommended for thermal noise environments should be used. A practical constraint is clearly that radar cost increases with bandwidth. A theoretical constraint is that the clutter particles are discrete, so that the clutter cross section does not truly decrease monotonically with increases waveform bandwidth. Thus, there is a maximum bandwidth value to maximize the SIRA, but this value is unknown and probably changes as the design of chaff dispensers changes. A reasonable engineering compromise is to use a 10- to 20-MHz bandwidth waveform.

c. Active Jamming

From a radar waveform viewpoint, the wideband barrage jamming environment is essentially identical to the thermal noise environment, and the same waveforms should be used. Spot noise jammers are well countered by frequency diversity and frequency agility, thus again the thermal noise environment waveforms should be used.

SECTION II

EFFECTS OF BANDWIDTH UPON DETECTION OF RADAR TARGETS

There is a strong interrelation between bandwidth effects, target reflection characteristics, and the effects due to frequency diversity waveform. In order to partially isolate these effects, this section will emphasize the effects of bandwidth when the radar target is modeled as either an isolated point scatterer or as a continum of scatterers. The dependence of performance upon bandwidth for different types of interference environments will be the primary focus. The performance of single-and multiple-channel frequency diversity waveforms will be considered and compared.

1. THERMAL NOISE

A major constraint for target detection in a thermal noise environment is the need to avoid overloading data processing equipment. The data processing could be a human observing a scope presentation or could be an automatic data processing computer. In both cases, there is a maximum number of false alarms that can be tolerated per unit time. When the false alarm rate exceeds this maximum value, the overload causes a rapid deterioration of performance.

When the target is a theoretical point reflector, the information rate at the output of the signal processor is the signal bandwidth. This rate represents the number of opportunities per unit time to make a target present or absent decision. The average number of false alarms per second, μ_F, is equal to the product of the signal bandwidth, B, and the false alarm probability per decision, P_{FA}.

$$\mu_F = BP_{FA} \tag{1}$$

As the data processor overload constraint is that μ_F is fixed, the required false alarm probability per decision varies inversely with B. Since for a fixed probability of target detection, P_D, the required SIR, increases monotonically as P_{FA} decreases, the required SIR increases as signal bandwidth increases.

The quantitative dependence of SIR upon P_{FA} or signal bandwidth is a function of the number of pulses that are noncoherently summed and the target fluctuation model. Note that one pulse summed corresponds to Doppler processing (coherent summing) any number of pulses. Consider a nominal case of a signal bandwidth of 500 kHz and a data processing constraint of 5 false alarms per scan when using a 1.1° horizontal beamwidth antenna. This nominal case requires a per cell false alarm probability of 10^{-5}. Thus, a 5-MHz bandwidth would require a P_{FA} of 10^{-6}, etc. It is shown that for a matched filter-Doppler processor increasing the signal bandwidth from 500 kHz to 20 MHz entails a penalty of 1.2 dB for a Swerling 1 target and 0.9 dB for a nonfluctuating target. As is discussed later, there are ECCM advantages to using large-bandwidth pulse signals. However, as indicated here, there are also penalties in using these large-bandwidth pulse signals.

2. ECM CHAFF AND NATURAL CLUTTER

Focusing upon the effect of radar bandwidth upon clutter indicates that there are essentially two types of clutter; homogeneous or distributed clutter and point reflectors.

Chaff, weather, and some ground clutter is homogeneous clutter. The effective radar cross section of homogeneous clutter depends linearly upon the collapsed pulse width of a match filter output. Thus, the radar cross section varies inversely with radar bandwidth.

Point clutter is due to reflections from objects whose dimensions are very small compared to the collapsed pulse width. Water towers and specular reflections from terrain are typical examples. Note that the desired target is also point clutter. Distinguishing between point targets and point clutter must be done on the basis of nonzero radial or tangential velocity. The distinction between point targets and point clutter is only one of semantics.

The radar cross section of theoretical point clutter is independent of the radar bandwidth. The dimension of the theoretical point is always less than the radar resolution. For practical objects, the cross section becomes a function of the bandwidth when the collapsed pulse width becomes comparable to the projected length of the object. This effect is quite significant for common tactical radar targets and affects the variation of signal-to-clutter ratio (SCR) variation with bandwidth.

When the bandwidth is small compared to the target dimension, the cross section of distributed clutter varies inversely with signal bandwidth, but the target cross section is constant. Thus, for "small" bandwidths, the SCR increases monotonically with signal bandwidth. For large bandwidths, the target return decomposes into several reflectors and the definition of SCR becomes complex. It is necessary to give a detailed consideration to the target return decomposition and to the processor used to perform target detection for the over-range resolved situation.

One type of large bandwidth waveform is the large bandspan waveform associated with frequency diversity waveforms. Frequency diversity is essentially parallel radar systems operating at different carrier frequencies. One advantage of frequency diversity is the improved detectability of fluctuating targets.

The target cross section fluctuation occurs because a target consists of many scattering elements. The cross section is the phasor sum of the individual scatterers. Changing the transmit frequency changes the relative phasing of the elements and, therefore, the target cross section. The detection probability is increased because if the target cross section is low at one carrier frequency, it is unlikely to be low at a second frequency. The improvement in detectability is theoretically predictable and has been experimentally verified. *

The channel-to-channel carrier frequency spacing necessary to statistically decorrelate the amplitude of the target returns at the cross section different channels depends upon the target length L_T. When the cross section density is uniform across the target, the decorrelation frequency is

$$\Delta f = \frac{C}{2 L_T} \tag{2}$$

where C is the velocity of light. As shown later, the decorrelation frequency is larger when the cross section density is nonuniform.

The fact that a target is a multipoint scatterer also becomes important when the bandwidth of a channel approaches the decorrelation frequency spacing given by the previous equation. The improvement attained for detecting targets in clutter by

* Nathanson, F.E., "Radar Design Principles", McGraw-Hill Co., p. 183-190

increasing the channel bandwidth beyond the decorrelation frequency, Δf, depends upon the target model and the form of processing. For some cases, the same improvement would be obtained if the full bandwidth were used coherently in a single channel, or if the bandwidth was subdivided into several parallel channels with the outputs noncoherently summed as in Figure 2.

3. DISTRIBUTED TARGET EFFECTS IN CLUTTER AND NOISE

a. Clutter Effects

One target model is the Swerling 1-2 type. This model corresponds to a distributed target. This target displays the frequency dependent fluctuation characteristics previously discussed. As stated, the frequency change necessary to decorrelate returns is inversely related to the target length. For a target length of L_T and a total average cross section of σ_T, the target has a constant cross section density of σ_T / L_T. Similarly, clutter has a constant cross section density of σ_{CD} m^2/m of range resolution. When the signal bandwidth is such that:

$$B < \frac{c}{2L_T}$$

the target is encompassed in a single range cell and the target cross section in the cell is the total cross section equal to σ_T. The clutter cross section is the product of the range resolution length, c/2B, and the clutter cross section density. Thus, the clutter cross section, σ_c, is

$$\sigma_c = \frac{c}{2B} \sigma_{CD} \tag{3}$$

The ratio of target cross section-to-clutter cross section is

$$\sigma_T / \sigma_c = 2B \sigma_T / c \sigma_{CD} \tag{4}$$

and the SCR increases as the bandwidth increases.

This equation breaks down when the range resolution length is less than the target length. In order to explore this more completely, it is convenient to define the bandwidth B_T where the target length equals the range cell size. When the waveform bandwidth equals KB_T, where K is an arbitrary integer, and the total

bandwidth is processed coherently, the target occupies K-cells. SCR in each cell is identical and equal to $\sigma_T/L_T\ \sigma_{CD}$.

The optimum processor for the over-resolved Swerling 2 target is to noncoherently sum the square-law detected outputs of the K-cells and make a target present or absent decision based upon the summed value. This sum is identical in form to that obtained when noncoherently summing K-conventional radar pulses. The improvement for summing K-pulses is less than K due to the noncoherent summing loss. Similarly, the SCR improvement is less than K. Since the noncoherent summing loss approaches the square root of K for large K, the rate of increase of SCR for very large bandwidths approaches the square root of the bandwidth increase. As an example, the range resolution for a 10-MHz bandwidth is 15 m. A Boeing 707 is 45-m long and thus occupies 3 range cells. If it is a homogeneous distributed target, the SCR is the same for each cell. Increasing the bandwidth to, say, 100 MHz changes the range resolution to 1.5 m. Thus, the target occupies 30 range cells. Since the range cell length decreases by a factor of 10, the target cross section decreases by a factor of 10. However, the clutter cross section decreases by a factor of 10 so that the per cell SCR is the same for both bandwidths. However, for the 10-MHz bandwidth, three cells are noncoherently summed whereas for the 100 MHz bandwidth, 30 cells are noncoherently summed. Since, to a first approximation, the noncoherent gain varies as the square root of the number of terms in the sum, the target detection gain in clutter varies as the square root of bandwidth.

An alternate approach is to use the bandwidth noncoherently. That is, use the bandwidth of KB_T for K-parallel channels and noncoherently sum the outputs of the K-channels. Of these techniques, slightly better performance is obtained from the procedure using the channelized approach. In order to see this, note that for the channelized noncoherent combining technique, the SCR for each channel in the single range cell containing the target equals $\sigma_T/L_T\ \sigma_{CD}$. This is identical to that for each range cell of the coherent bandwidth technique. Thus, summing over the K-frequency channels gives detection performance that is identical to that obtained by summing over the K-range cells containing the target when the false alarm probability is the same for the two techniques. However, the false alarm probability is not the same for the two configurations. Since the coherent bandwidth technique has a range cell size that is K times smaller than that of the noncoherent bandwidth technique, the same average false alarm rate is maintained only by using a false alarm probability

that is K times smaller than that used by the noncoherent bandwidth technique. This difference of per decision false alarm probability indicates that the noncoherent bandwidth technique is superior. The theoretical performance difference is approximately 0.6 dB per order of magnitude of bandwidth increase.

The performance loss cannot be overcome by summing disjoint batches of K-range cells in order to use the same false alarm probability per decision as does the noncoherent bandwidth technique. This is because the target would then straddle two disjoint K-cell batches, and the loss would simply be manifested in a different manner. However, practical implementation problems with channelized contiguous spectra may negate this theoretical difference.

The above considered the special case where the distributed target was a homogeneous distributed target. These results will now be generalized to show that the performance of each processor is approximately independent of the exact variation of the distributed target cross section over the target extent. Thus, the two processors are essentially equivalent for any distributed target.

First note that when using the bandwidth noncoherently, the bandwidth of each channel has range resolution equal to the target length. The signal for this case is the total scattering cross section; the distribution of scatterers as a function of target extent is not discernible. Thus, the detection performance of the parallel channel processor is independent of the exact distribution over target extent.

For the coherent processor, the signal will vary as a function of range when the distributed target is nonhomogeneous. It is convenient to make a minor change in target model. The continuously distributed target will be replaced by a specular reflector model where the cross section of the specular reflector in each cell equals the average cross section of the distributed target for that cell. The change in target model to many small nonfluctuating targets allows the use of powerful statistical theorems with, it is believed, no appreciable error. This assumption is approximately equivalent to the common assumptions that collapsing loss or noncoherent integration losses are independent of the target fluctuation model. For this target model, when the detector is a square law envelope detector, the statistical distribution for each range cell is independent noncentral chi-squared with two degrees of freedom. The noncentrality parameter for each sample is the SCR in the cell. The postdetection filter sums the individual cell voltages. The distribution function

of the sum of K-independent noncentral chi-squared distribution random variates is a noncentral chi-squared distributed random variable whose number of degrees of freedom is the sum of the degrees of freedom of each variate, and whose noncentrality parameter is the sum of the noncentrality parameter of each variate.* However, the sum of the noncentrality parameters is the total cross section. Neither parameter of the distribution depends upon the cross section distribution. Thus, the detection performance of the single-channel coherent processor is approximately independent of the exact distribution over target extent.

b. Noise Effects

It is now shown that the performance of the two signal processors is also identical in thermal or barrage jamming noise for homogeneous and nonhomogeneous distributed targets. The homogeneous target case will be considered in detail. Generalization to the nonhomogeneous case is done by using the special chi-square statistical distribution properties as was done above for clutter.

First consider the homogeneous target and the multiple channel noncoherent processor. For a total energy transmission of E, each channel has an energy of E/K. Each channel sees the total target return σ_T. Thus, the returned signal energy per channel is proportional to the product σ_T E/K. The two-sided noise power density (or noise energy) for the sum of thermal noise and barrage jamming noise is denoted as $N_o/2$. Thus, the per channel signal-to-noise energy ratio is $2\,\sigma_T E/(N_o K)$. Note that when considering energy ratios, the bandwidth of a channel is not pertinent. The postdetection processor then sums K-samples each with SNR of $2\sigma_T E/(N_o K)$.

The single-channel coherent processor has the total energy E. However, the target decomposes into K-range cells each of cross-section σ_T/K. The returned signal energy per range cell is proportional to σ_T E/K and the signal to noise energy ratio per range cell is $2\sigma_T E/(N_o K)$. Note that this is identical to that of each channel of the channelized system. Since one case sums K-range cells while the other sums K-frequency channels, it follows that both have the same detection performance.

---

* C.R. Rao "Linear Statistical Inference and its Application", John Wiley 1965, p. 147

4. NOISE JAMMERS

a. Intercept Receivers

Intercept receivers are used by jammers to measure characteristics of the victim radar. The information can be used to set the center frequency of a narrowband jammer to that of the radar, can be used to aid in measuring the location of a radar for an ARM or TOA system, or can be used to aid in determining the proper characteristics of decoy jamming signals to be directed against the victim radar. The signal bandwidth of the radar pulse can have substantial effect upon the performance of an intercept receiver.

There are basically two classes of receivers in current use, the superheterodyne narrowband receiver and the wideband video receiver.* The narrowband receiver has an instantaneous bandwidth of the order of the radar bandwidth (typically 1 to 10 MHz). The mode of operation is that the receiver sweeps across the band span of interest. Upon detection of the radar pulse, the sweep is stopped, and pertinent radar parameters such as carrier frequency, pulse width, pulse repetition period, etc., are measured. The major advantage of this type of receiver is its high sensitivity and its good selectivity. The sensitivity is approximately -90 dBm. One disadvantage is that it has low probability of intercepting the radar antenna mainlobe because of the combination of the receiver scanning in frequency and the radar scanning in space. Another disadvantage is that the receiver cannot stay locked to a frequency-agile emitter.

When the radar bandwidth is less than the bandwidth of the intercept receiver, the detectability of the radar signal is independent of the radar bandwidth and depends primarily upon the radar peak power. This is because the output at the envelope detector is essentially the waveform envelope independent of the radar signal bandwidth. When the radar bandwidth is greater than the receiver bandwidth, the detectability depends upon the ratio of the two bandwidths. Radar quieting is theoretically possible since increasing the radar bandwidth to values greater than the intercept receiver bandwidth decreases the radar energy within the receiver pass band.

---

* F. Rappolt and N. Stone, "Receivers for Signal Acquisition" Microwave Journal, Jan. 1977, pp. 29-33

The second type of intercept receiver has instantaneous bandwidths of the order of the band span of interest. Thus, the bandwidth is approximately 0.5 to 1.5 GHz when monitoring S-band. If RF amplifiers are not used, the receivers detect immediately and the sensitivity is approximately -50 dBm. Receivers using low-noise solid-state RF amplifiers before detection increase the sensitivity by approximately 20 dB. The advantage of this receiver is that it has unity probability of detecting the mainlobe of the radar antenna. The disadvantage is the poorer sensitivity. For this type of receiver, the radar bandwidth is always less than the receiver bandwidth. The detectability of the radar signal depends primarily upon the radar peak power. Radar quieting by bandwidth expansion techniques is not feasible.

Thus, to reduce the effectiveness of intercept receivers, the radar bandwidth should at least equal the superheterodyne receiver bandwidth and have low peak power.

The detection range of radars and intercept receivers is shown by the parametric curves of Figure 17. The curves assume operation at S-band. The radar curves take the detectability criterion as the range where the SNR is 13 dB. The radar parameter is the product of the target cross section in square meters, σ, transmitter pulse duration, τ, in seconds, the number of pulses, M, of duration τ, and the square of the radar antenna gain, G. The intercept receiver is assumed to have an antenna gain of 0 dB, and is assumed to be receiving the radar pulses from the radar antenna sidelobes. The radar sidelobes are assumed to average 0 dB relative to an isotropic antenna. As a typical example, 10-pulses each of 10 μs, a 30-dB radar antenna gain, and a 1 m^2 target yields a radar parameter equal to 100. The radar's target detection range for a 1-MW peak power pulse (60 dBW) is 125 nmi. When the target has an intercept receiver with -70 dB sensitivity, the target detects the radar antenna sidelobes at the enormous range of 420 nmi. The radar detection range is maintained at 125 nmi if the pulse width is increased to 100 μs, the antenna gain increased to 35 dB and the peak power reduced to 10 kW. However, the intercept receiver detection range is reduced to 42 nmi. Thus, low peak power, high antenna gain and long duration waveforms help protect the radar. Note, however, that the superhetrodyne receiver detection range is still enormous and that detection of the radar mainlobe by either receiver is essentially impossible to prevent.

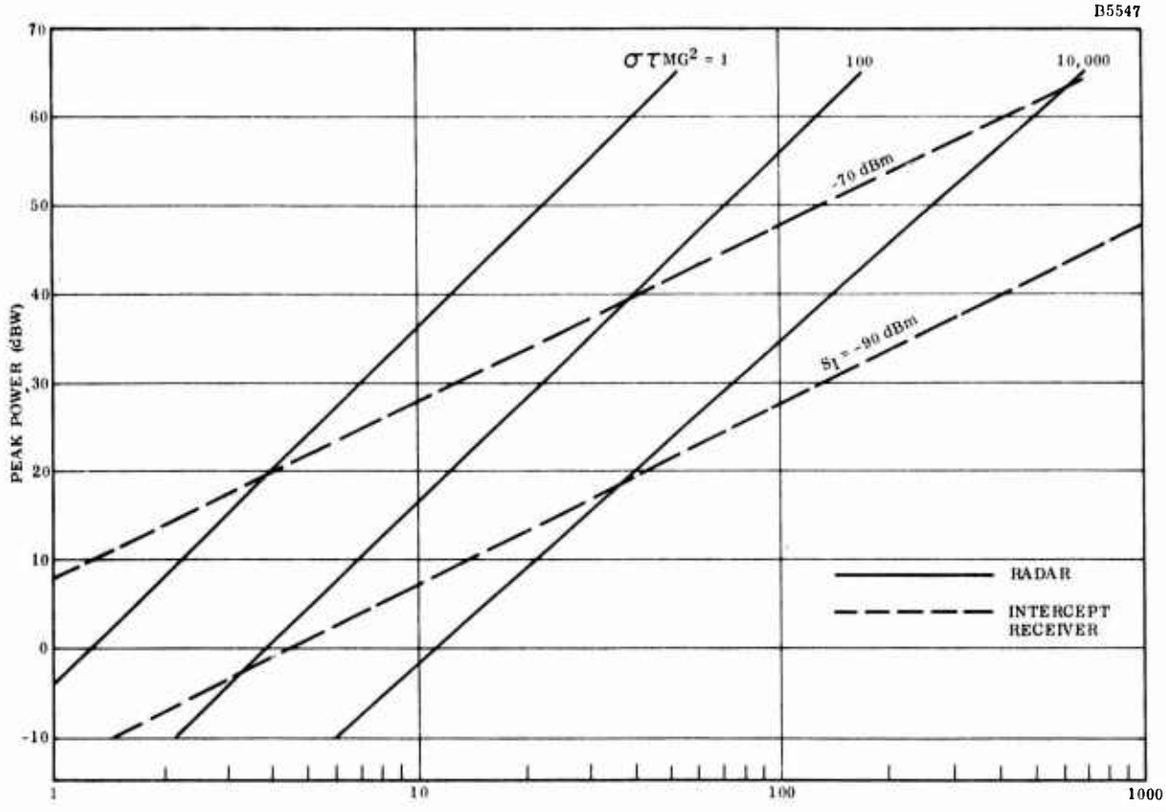

Figure 17. Radar and Intercept Receiver Detection Range

For conventional constant carrier frequency pulses, increasing the pulse width decreases the pulse bandwidth. Since, as regards performance against intercept receivers, it is desirable to keep the bandwidth at least equal to that of a superhetrodyne receiver, phase coded waveforms are required to aid in countering intercept receivers.

b. Noise Jammer Properties

The jamming effectiveness of a noise jammer is determined by the spectral density of the radiated interference. For a fixed output power, a spot jammer covering, say, 10 MHz has a spectral density, and potential effectiveness; that is, 20-dB greater than that of a barrage jammer covering 1000 MHz. Thus, it is to the radar's advantage to have the jammer radiate over broader bandwidths. However, for almost all current jammers, the jammer bandwidth is independent of the radar bandwidth.

In order for the radar waveform's bandwidth to affect existing jammer's effectiveness, the jammer design must be capable of adapting its spectral characteristics to match that of the radar. For the usual spot or barrage jammer, the noise bandwidth is not changeable. The barrage jammer response can be completely independent of the radar. The conventional spot jammer requires the aid of an intercept receiver to correctly tune the center frequency, but does not otherwise modify its jammer spectrum.

The radar's bandwidth can affect future jamming effectiveness since the design of the next generation of noise jammers will be influenced by the trends for the next generation of radar waveforms.

One type of noise jammer that can adopt its output spectrum to match that of the radar's is implemented by measuring the received energy at several closely-spaced frequencies. Noise jamming is only radiated at those frequencies where significant radar energy is detected.

A quantitative measure of the improvement achievable by wideband techniques is obtained by considering the case where the interference consists of only white noise. Then, target detectability is dependent only upon the ratio of the reflected target energy, E, and the two-sided spectral energy density of the noise $N_o/2$. That is, detection depends only upon the peak SNR:

$$\Gamma_o = \frac{2E}{N_o} \tag{5}$$

When the noise interference is due to both white noise and jammer noise, it is necessary to use the combined spectral energy density of the white noise plus jamming. Thus, when the received jammer noise power, P_{JR}, is contained within the jammer bandwidth, B_J, the two-sided spectral energy density for the jammer is $P_{JR}/2B_J$. The energy density of the noise and jamming is:

$$N_1 = \frac{1}{2} \left(N_o + \frac{P_{JR}}{B_J} \right) \tag{6}$$

The peak SNR is now:

$$\Gamma_1 = \frac{2E/N_o}{1 + \frac{P_{JR}}{N_o B_J}} \tag{7}$$

Combining Equations (6) and (7) gives the normalized SNR:

$$\frac{\Gamma_1}{\Gamma_o} = \frac{1}{1 + \frac{P_{JR}}{N_o B_J}} \tag{8}$$

The ratio represents the loss caused by the jammer. Note that, when the total jammer power is fixed, the loss approaches 0 dB as the bandwidth becomes large.

SECTION III

EFFECT OF A FEW DOMINANT SPECULAR REFLECTORS TARGET MODEL UPON TARGET DETECTION

The analysis of the detectability of targets by radar or sonar is conventionally based upon mathematical models of the target cross section characteristics. The targets are modeled as either having a constant (nonfluctuating) cross section or as having a nonconstant cross section. For most real targets, the cross section is nonconstant and depends significantly upon the viewing angle. Since the cross section can vary by orders of magnitude with small angle changes, the cross section is often modeled as a random variable. The commonly assumed density functions for the random variables lead to the well-known Swerling models and other models.

The detectability of a fluctuating target in noise or clutter (reverberation) depends upon the attained SIR and the particular form of the fluctuation characteristic. The fluctuation loss, or increased SIR required for detection as compared to a nonfluctuating target, is discussed in many standard texts. In particular, Nathanson* has a graph of the detection probability vs SIR for a nonfluctuating target, for Swerling cases 1 through 4, and one of the Weinstock cases. The curves show that for a Swerling 1 or 2 model, the fluctuation loss at a false alarm number 10^6 is 1.5 dB for a detection probability of 0.5 and 8 dB for a detection probability of 0.9.

The use of a multiple-carrier frequency waveform to reduce the fluctuation loss has been suggested, and the improvement has been experimentally verified.** This class of waveform is denoted by some authors as frequency agility and by others as frequency diversity. A qualitative indication that frequency diversity will decrease the fluctuation loss can be obtained by noting that the total return from a typical target consists of the superposition of the reflections from many individual scattering points. The magnitude of the sum depends upon the relative phasing of these reflections. For some phase conditions, the resultant magnitude is small and the detection probability is small. A change of transmit frequency changes the relative phasing of the reflections. Thus, it is less probable that a small target magnitude would occur on all of several different carrier frequencies and the fluctuation loss might be decreased.

---

* Nathanson, F.E., "Radar Design Principles", McGraw-Hill, 1969, p. 84.
** op cit., p. 183-191.

A quantitative evaluation of the decreased fluctuation loss, or diversity gain, can be obtained by comparing the performance of two systems. The first transmits a single pulse of energy E; the second transmits equal energy by using K-pulses each of energy E/K at different carrier frequencies. A conceptual block diagram of a particular diversity waveform and processor implementation is shown in Figure 2. Each pulse is divided into K-subpulses, and each subpulse is at a separate carrier frequency, f_1 through f_K. Other implementations which transmit a single carrier frequency waveform for each pulse and change frequency on a pulse-to-pulse basis are mathematically equivalent. For detection in noise when the SIR for the single pulse system is γ, the SIR for each channel of the multiple carrier system is γ/K.

Assume that the carrier frequencies are sufficiently widely spaced so that the returns of the K-pulses are independent random variables. This corresponds to a pulse-to-pulse fluctuation model. For a Swerling 2 model, the diversity gain is given by DiFranco and Rubin.* The curves of Figure 5 are similar but are for modified detection and false alarm probabilities. It is seen that there is an optimum number of channels to maximize the diversity gain, but that the optimum value depends upon the detection probability. Note also that for 0.9 detection probability, the diversity gain can recover up to 4.9 dB of the fluctuation loss by using 7 channels. The region of the maximum is relatively broad. For 4 channels, the optimum number when the detection probability equals 0.7; the gain is 4.6 dB. Thus, four or fewer channels seems a reasonable compromise between attained performance and implementation cost.

The physical basis for the Swerling and Weinstock models is a target consisting of a very large number of scattering points. Some measurements indicate that when viewed from tail and nose aspects, the radar properties of typical aircraft are well modeled as being due primarily to reflection from a few isolated points. These typically are from wing edges, engines, cockpits, etc. For low bandwidth signals, these specular reflectors are not resolved and the random phase addition of these reflected waveforms causes cross section fluctuation. However, for large bandwidth waveforms, these reflectors are resolved. Due to this, the detectability of a target modeled as a few dominant specular reflectors depends upon the signal bandwidth. A detailed analysis of the fluctuation loss and diversity gain as a function of signal bandwidth for this target model has been performed.

* J.V. DiFranco and W.L. Rubin, "Radar Detection", Prentice-Hall, 1968, p. 405.

The target has been modeled as n equispaced equal amplitude reflectors. Each reflector is a nonfluctuating target. For low bandwidth waveforms, the reflectors are unresolved and the return is due to the random angle phasor addition of the individual reflectors. The distribution function for the magnitude of the sum is given by Bennett as*

$$F(r) = 1 - 2 \sum_{m=1}^{\infty} \frac{J_1(j_m/n)\, J_o^{n-1}(j_m/n)}{j_m\, J_1^2(j_m)}\, J_o(rj_m/n) \qquad (9)$$

$$0 \leq r \leq n$$

where $J_o(\ )$ and $J_1(\ )$ are Bessel functions of the first kind and zeroth and first order respectively and j_m are the ordered roots of $J_o(\ )$. The density function for the cross section, the square of the magnitude, is then easily obtained.

Closed form equation for the probability of detection vs SIR for these targets have not been found. An approximate analysis was performed by using the distribution function to derive a discrete density that approximates the continuous case. Convolving the discrete density function with the curve of detection probability vs SIR for a nonfluctuating target then gives the curves for the fluctuating target model.

The analysis for the wideband waveforms that resolve the target into the individual nonfluctuating reflectors is identical to the classical analysis performed by Marcum.

* W.R. Bennett, "Distribution of the Sum of Randomly Phased Components", Quarterly of Applied Mathematics, Vol. 5, No. 4, January 1948.

SECTION IV

LOSSES FOR FREQUENCY DIVERSITY WAVEFORM SYSTEMS

It has been established that the frequency diversity waveform is the preferred waveform for an ECCM oriented radar. In order to properly assess its capability an investigation of some implementation losses has been performed. The losses considered are primarily due to system limitations rather than circuitry implementation limitations. Specifically, the diversity gain is decreased when the frequency spacing between pulses is insufficient to completely decorrelate the returns. Small frequency spacings might be used due to restricted bandwidths of the antenna, or transmitter. Small frequency spacings might be used to avoid the requirement of readjusting the phase shifters for a phased array. The available gain is also reduced due to the target's unknown Doppler frequency and the need for constant false-alarm rate (CFAR) circuitry. In addition, though the optimum processor requires square-law envelope detection, processors using linear envelope detectors are often configured. These aspects of diversity gain reductions are discussed in detail in the following sections. The losses are evaluated for the case where the first-order density function of the target cross section is exponential. This is a generalization of the Swerling 1 and 2 cases.

1. CORRELATED RETURNS DUE TO SMALL CHANNEL-TO-CHANNEL FREQUENCY SPACING

An evaluation of the diversity gain as a function of the frequency separation between channels has been performed. Define f_R as the bandwidth that causes a range resolution equal to the target length L. The parameter that gives the effect of channel-to-channel frequency separation, f_s, is the normalized channel spacing equal to the ratio of f_s to f_R. In addition, the diversity gain depends upon the target's cross section density (the cross section per unit length of target). General equations are obtained and two cases are considered in detail. The first is where the target cross section density is uniform; the second is for a triangular cross section density. That is, the cross section density is zero at the target end points, maximum at the target center, and decreases linearly from the center to either end point.

Figure 18 shows the detection probability of a four frequency waveform as a function of SIR with the normalized frequency spacing of each channel as a parameter for a uniform-density cross section target. A curve of the single channel performance is also included as a reference. For the single channel case, the target fluctuation model is Swerling 1. When f_s/f_R equals unity, the returns from the subpulses are independent and the corresponding target fluctuation model is Swerling 2. It is seen that for f_s/f_R equal to 0.05, the performance is worse than that of the single channel. This is caused by the fact that the returns are very highly correlated. Thus, essentially no benefit due to frequency diversity and target fluctuation modification are accrued. However, there is a loss due to noncoherent combining of four returns. As the value of the normalized frequency displacement increases, it is seen that there is a performance improvement for the higher detection probabilities.

Figure 19 gives the diversity gain vs normalized frequency displacement of the channels for the two cross section density profiles. The normalized frequency displacement required to attain within 0.5 dB of the maximum attainable is 1.0 for the triangle density target and 0.72 for the uniform density target. This differential behavior is due to the broader mainlobe of the correlation function for a triangle density target compared to a uniform density target when both targets are the same total length.

Figures 20 and 21 give similar results for the two-channel diversity system. It is seen that the normalized frequency displacement required to attain within 0.5 dB of the maximum attainable is 0.87 for the triangle density target and 0.55 for the uniform density target.

Note that for narrowband signals and equal channel-to-channel frequency displacement, the two channel system requires one-third the bandspan of the four channel system. Since the subpulse waveform requires a large instantaneous bandspan, a comparison of the relative performance vs number of channels for this waveform should include the total instantaneous bandspan effect. This is achieved on Figure 22. It is seen that two channels have more diversity gain than four channels unless the normalized instantaneous bandspan exceeds 2.16. As a numeric example, for a target whose length is 10 m, f_R equals 15 MHz. Thus, a four channel system has more diversity gain than the two channel system only when the instantaneous bandspan exceeds 32.4 MHz.

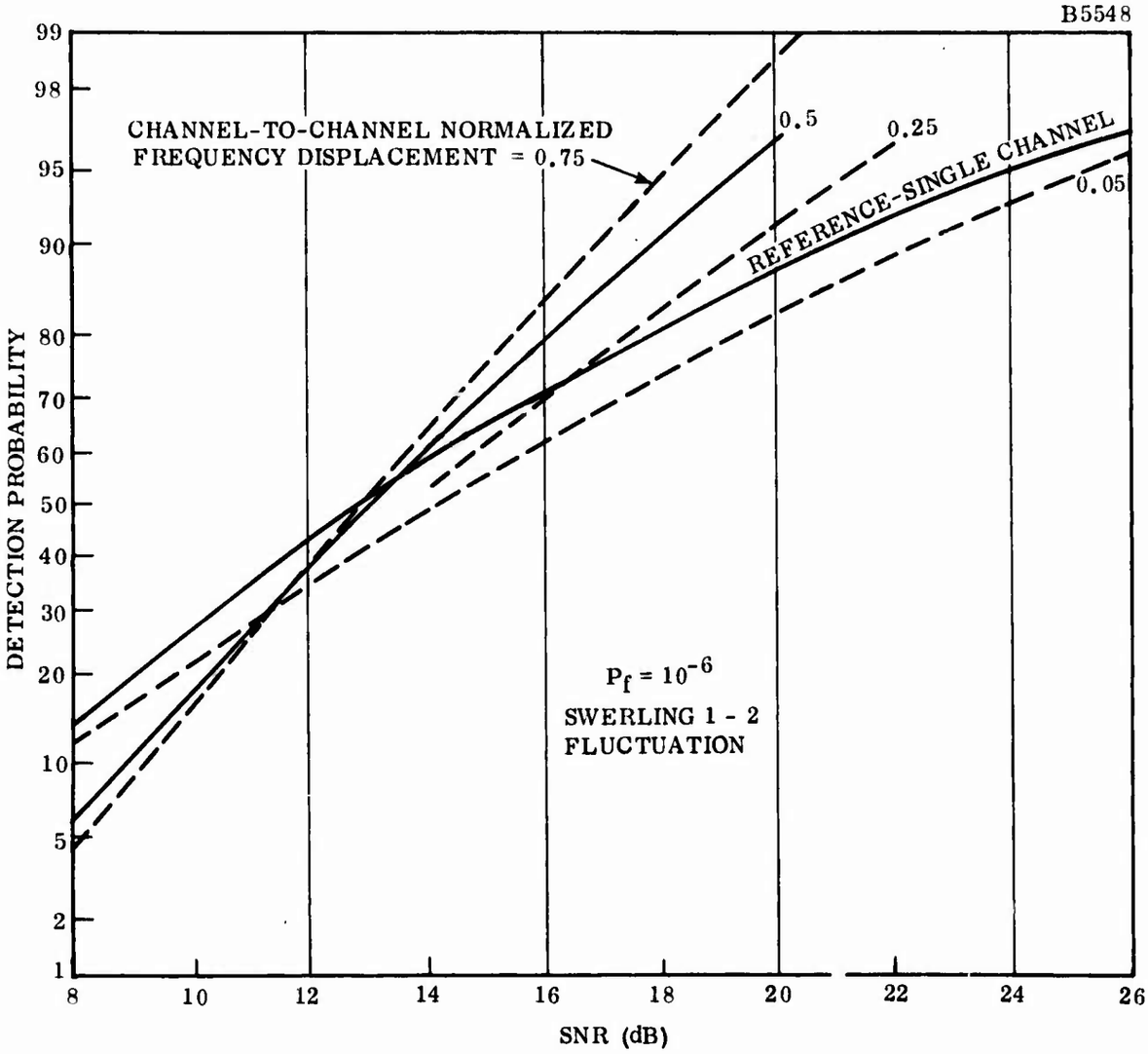

Figure 18. Four-Channel Diversity Performance As A Function of Normalized Frequency Displacement For Uniform Cross Section Density

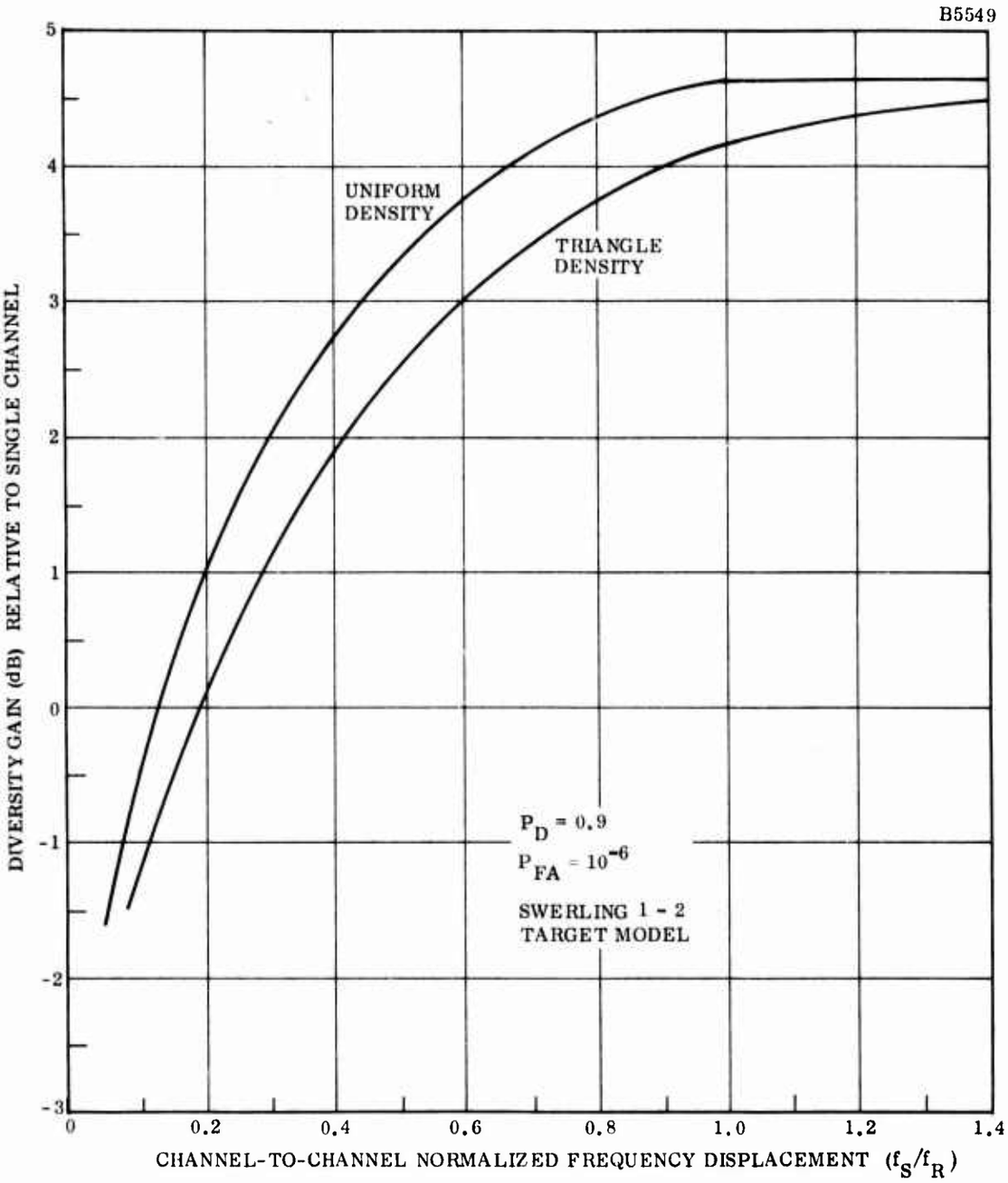

Figure 19. Four-Channel Diversity Gain for Distributed Targets

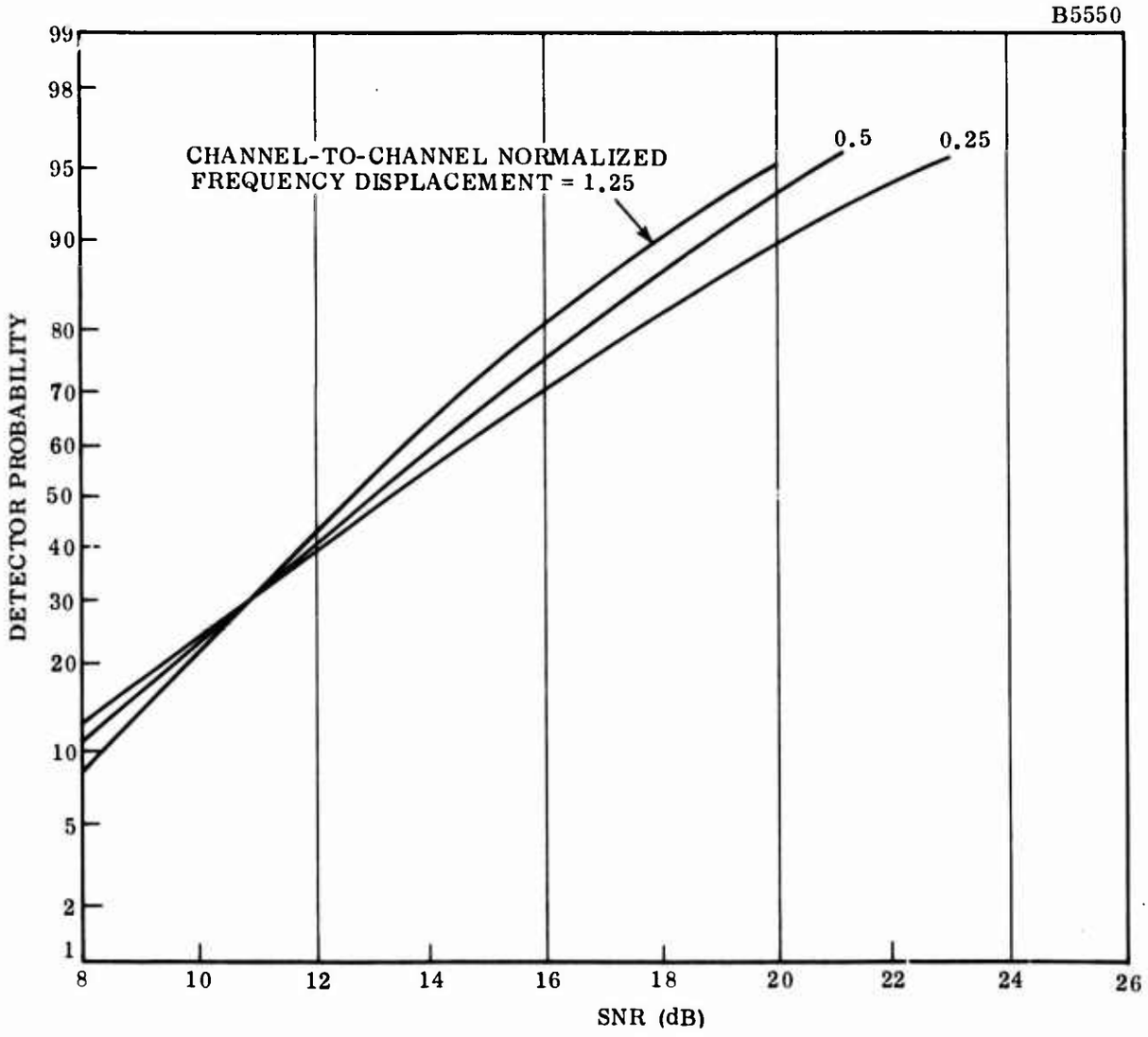

Figure 20. Two-Channel Diversity Performance As A Function of SNR and Normalized Frequency Displacement for Uniform Cross Section Target

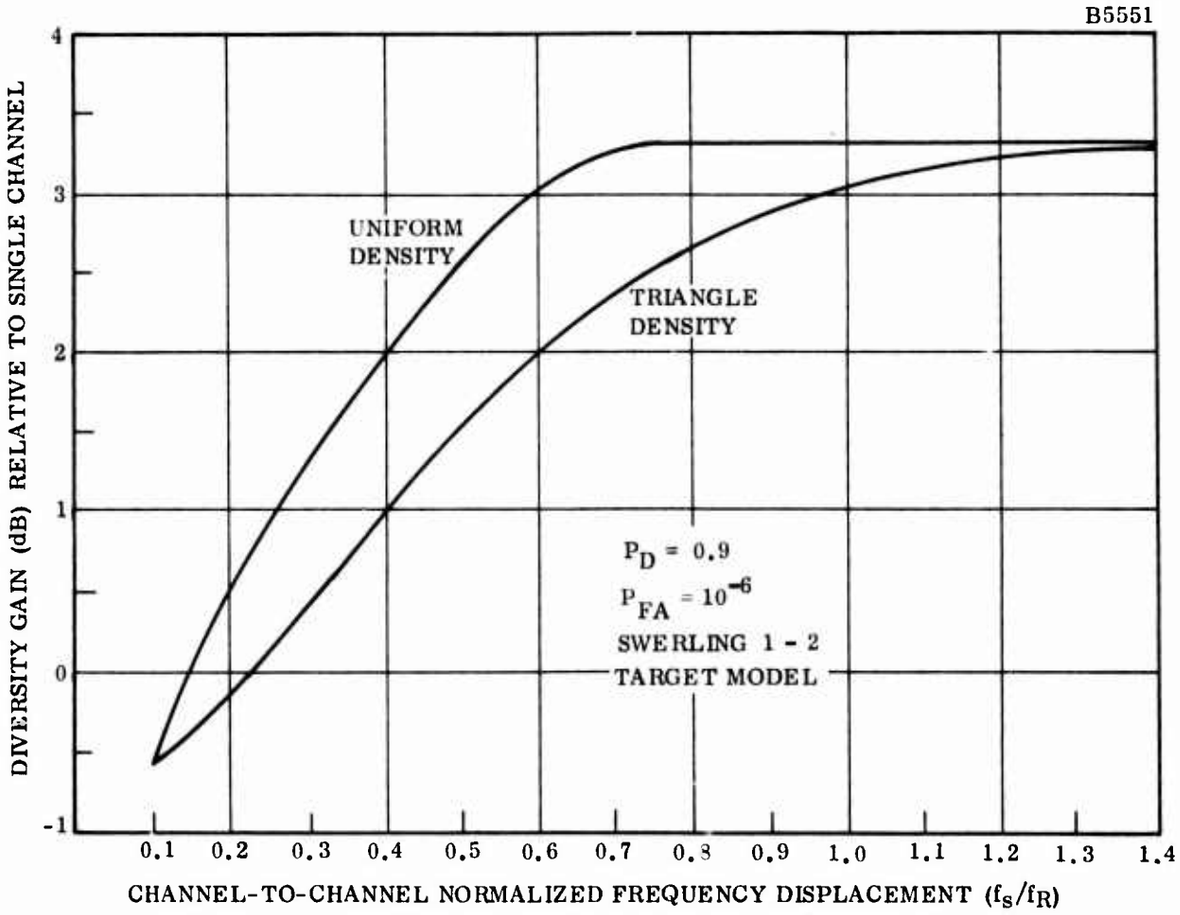

Figure 21. Two-Channel Diversity System

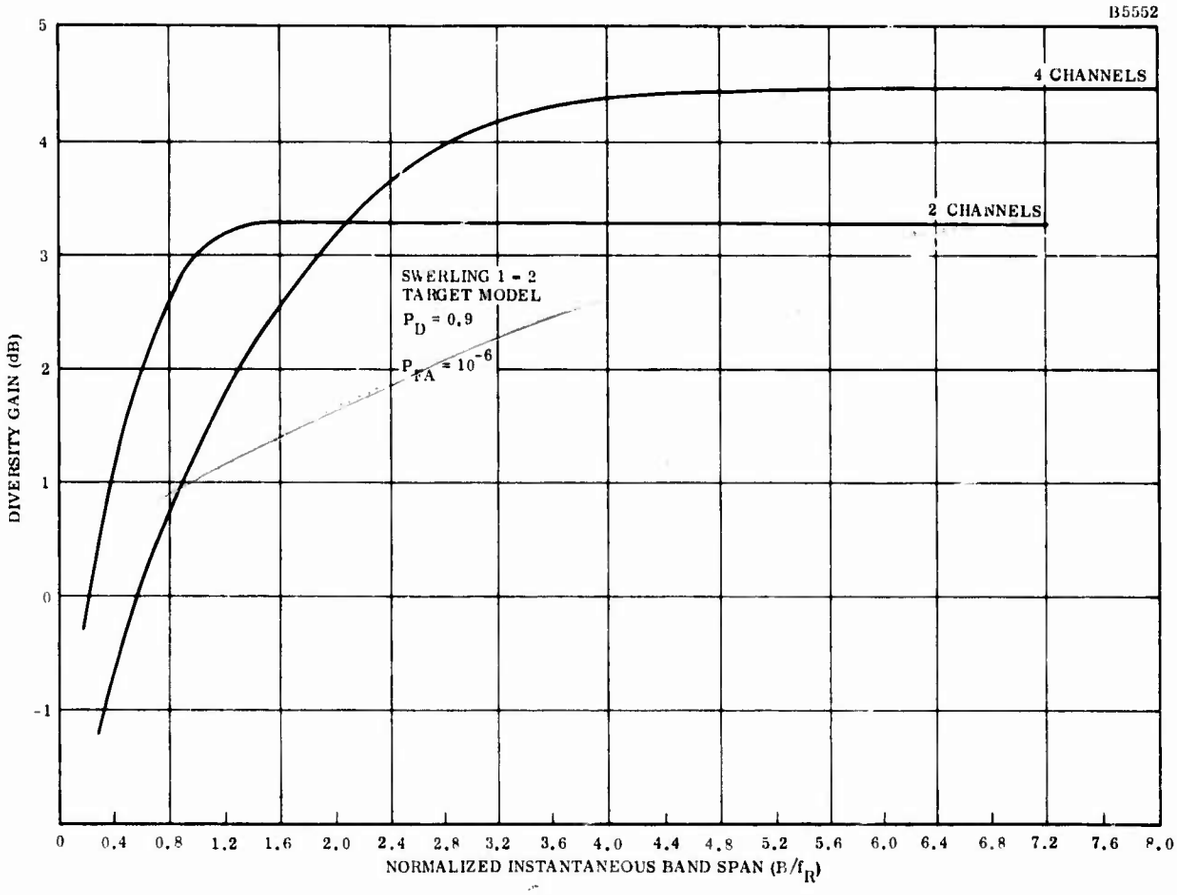

Figure 22. Bandspan Effect Upon Diversity Gain for Triangle Cross Section Density Target

2. UNKNOWN DOPPLER FREQUENCY LOSS

The analysis of the diversity gain improvement achieved when using a diversity waveform was based upon matched filter theory and, therefore, made the implicit assumption that the Doppler frequency is known exactly. In practice, for a search radar, the target Doppler is unknown and a bank of filters covering the range of Doppler frequency might be used. This causes a loss as compared to the matched filter theory. The loss occurs for either a single channel waveform or for a multiple-channel diversity waveform.

For a single channel waveform, a target present decision is made whenever the output of any Doppler filter exceeds the threshold value. For a fixed threshold value, the probability of false alarm increases as the number of Doppler filters increases. Since a specified false alarm probability per range cell is desired, the required threshold value increases monotonically with the number of Doppler filters. The increased threshold value causes a loss in target detectability. As a numeric example, the loss equals 0.6 dB for an 8 filter bank for a detection probability of 0.9 and a false alarm probability of 10^{-6}. The loss for an N-filter bank is approximately the SIRR increase required to maintain the detection probability when the false alarm probability decreases from P_{FA} to P_{FA}/N. The loss is denoted as the greatest-of loss as a common circuitry implementation is to determine the maximum output among all the filters and make a target present or absent decision by comparing this maximum to the threshold value.

The greatest-of loss differs for the multiple channel waveform. This is primarily because of the complicating factor that the Doppler shift value is different for each carrier frequency. When detecting a known velocity target this effect can be accounted for by identifying which filter of the bank for each diversity channel will contain the target return and then noncoherently summing the appropriate outputs. However, for a M3 target at a nominal S-band carrier frequency, the Doppler shift is 20 kHz. As this is large compared to the usual PRF, there is considerable potential Doppler ambiguity. For the unknown target velocity case and an N-filter Doppler bank, the target Doppler can be in any of the N-filters. At a different carrier frequency it would generally be in a different filter. For a two-channel waveform, direct noncoherent summing would require summing each filter output of the first frequency channel with every filter output of the second frequency channel. Thus, a total of N^2 sums would be required. For a four-channel diversity waveform, N^4 sums are required. This implementation is costly.

The SIRR loss is approximately that caused by decreasing the false alarm probability by a factor of N^4. As shown in the analytic section, for an 8 Doppler filter bank, the loss is 2.05 dB. A simpler processor, shown in Figure 23, is to take the greatest-of the Doppler filters for each diversity channel and noncoherently sum these. In addition to being simpler to implement, its loss is only 1.82 dB. Since the loss for a single channel waveform is 0.6 dB, the differential greatest-of loss for a four-channel diversity waveform when using a bank of 8 Doppler filters is 1.22 dB. Thus, the four-channel diversity gain for a Swerling 2 target is 4.6 dB for the known velocity case and 3.38 dB for the unknown velocity case and 8 Doppler filters in the bank.

Figure 24 shows the SIRR for a single channel and for a four-channel diversity waveform vs the number of Doppler filters. The unknown velocity loss for each is the difference between the SIRR value for N-filters and for one filter. For each N value, the unknown velocity loss is greatest for the diversity waveform. The difference of the differences represents a decrease in the achievable diversity gain.

3. EFFECT OF DETECTOR LAW UPON DIVERSITY GAIN

The statistically optimum detector law for combining the outputs of a multichannel diversity waveform is square law when the target has a Swerling 2 fluctuation. For some applications, equipment constraints cause a linear envelope detector to be used instead of a square law detector. The decrease in diversity gain due to the use of a linear detector instead of a square law detector has been evaluated for a two channel and four channel waveform. The decrease is 0.35 dB for two channels and is 0.45 dB for four channels.

4. CONSTANT FALSE-ALARM RATE PROCESSORS FOR DIVERSITY WAVEFORMS

Conventional signal processing compares the envelope of the matched filter output to a threshold value in order to make target present or absent decisions. The required threshold voltage is proportional to the root-mean-square (rms) value of the interference at the matched filter output. When the environment is exclusively thermal noise, the required threshold value may be specified a priori. When the environment contains noise jammers, chaff, or natural clutter, the rms value of the interference level at the output of the matched filter is unknown and the required threshold value cannot be specified a priori. If the fixed threshold used for thermal noise is used for the nonthermal noise environment, the false alarm rate increases monotonically with the interference power. CFAR processors, whose false alarm probability is independent of the power level of the interference environment, are desired.

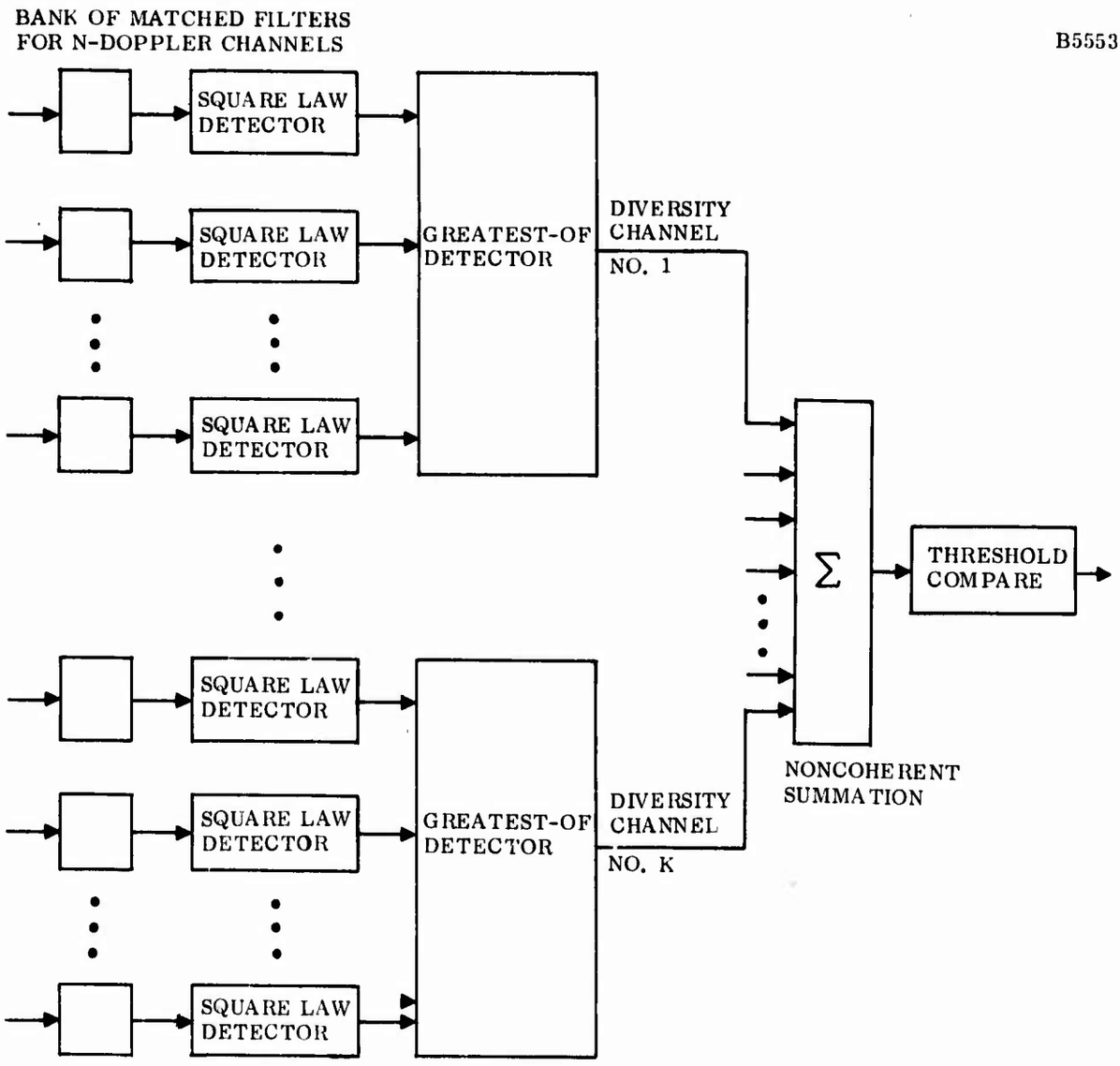

Figure 23. Multiple Channel Diversity Waveform Unknown Target Velocity Processor

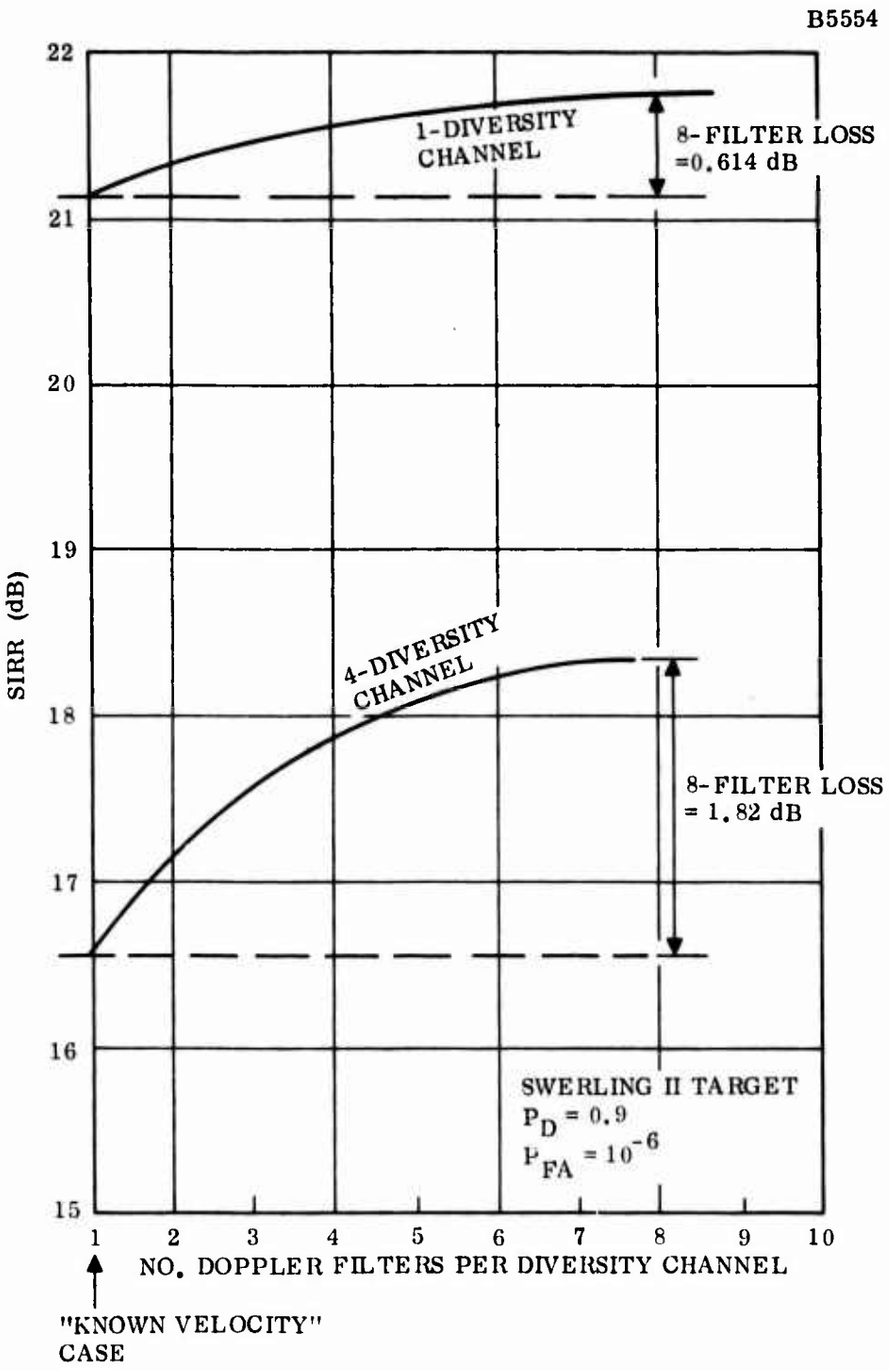

Figure 24. SIRR for Unknown Target Velocity

There are several CFAR schemes. The appropriate technique is chosen to fit the environment properties. As an example, the statistics for an environment that is the sum of thermal noise, jamming noise, and returns from chaff or weather clutter is complex Gaussian independent of the respective levels of the components. This is due to the fact that each component has a complex Gaussian distribution and therefore the sum has a complex Gaussian distribution. The only parameter of the distribution that changes is the total power. This constancy of distribution form does not always occur. When the environment also contains log normally distributed clutter, such as ground or sea clutter, the distribution of the sum is no longer complex Gaussian. A technique that attains a constant false rate independent of the power when the total interference has a complex Gaussian distribution will, in general, not maintain the constant false rate when arbitrary levels of ground or sea clutter are also added. There are CFAR techniques that can cope with the latter, more complicated case, but these, in general, have not found much application in radar signal processing. The basic CFAR technique that is considered is the normalizing technique shown in Figure 25. The threshold value that is used for detection is adaptive. Its value is derived by averaging the voltages in the cells bracketing the target cell.

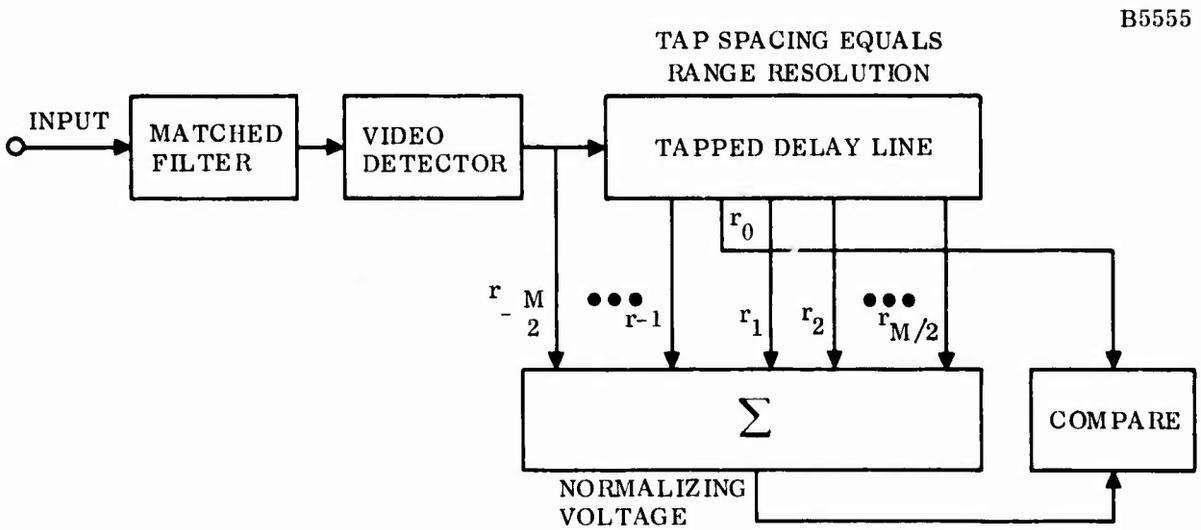

Figure 25. Conceptual Block Diagram of Single-Channel CFAR Processor

The average voltage gives an estimate of the rms value of the interference. The term "normalizer" is based upon one particular conceptualization of the technique. Specifically, for the case when the interference is thermal noise alone, the target present or absent decision is made by comparing the envelope of the matched filter in the target test cell, r_o, to a threshold T. The threshold is $T = k\, v_n$ where v_n is the rms value of the noise and k is chosen to give the desired false alarm probability. Thus, the test is

$$r_o \gtrless k\, v_n$$

where a target present decision is made when r_o exceeds the threshold and a target absent decision is made when r_o is less than the threshold. Equivalently,

$$\frac{r_o}{v_n} \gtrless k$$

The rms value of the interference "normalizes" the voltage in the test cell. The normalizing CFAR technique obtains an estimate of v_n, denoted as $\hat{v}_n$, by averaging the voltages in the cells adjacent to the test cell. For an M-cell normalizer that uses a normalization window centered on the test cell,

$$\hat{v}_n = \frac{1}{M} \sum_{i=1}^{M/2} (r_i + r_{-i}) \qquad (10)$$

The normalizing CFAR processor then performs the comparison

$$\frac{r_o}{\hat{v}_n} \gtrless k_1$$

where k_1 is a new constant chosen to give the desired false alarm probability. Because the estimate, $\hat{v}_n$, has a statistical error, the SIR required for target detection increases over the SIR value required for the known level, thermal noise background. This increase is termed the CFAR loss. Since the statistical error decreases as the number of normalization cells increases, the CFAR loss monotonically decreases to zero with M. In addition to the loss being a function of M, it is also a function of the detector law. It is known that the loss is smallest for a square law detector.* Thus,

* R. Nitzberg, "Application of Invariant Hypothesis Testing Techniques to Signal Processing", Ph.D Dissertation, Syracuse University, June 1970, GE TIS Series R70ELS53.

the best normalizing CFAR processor, for any target fluctuation model, implements the equation

$$\frac{r_o^2}{\frac{1}{M}\sum_{i=1}^{M/2}(r_i^2 + r_{-1}^2)} \gtrless k_2$$

A graph of this loss versus M is shown in Figure 26 for a Swerling 1 fluctuating target.

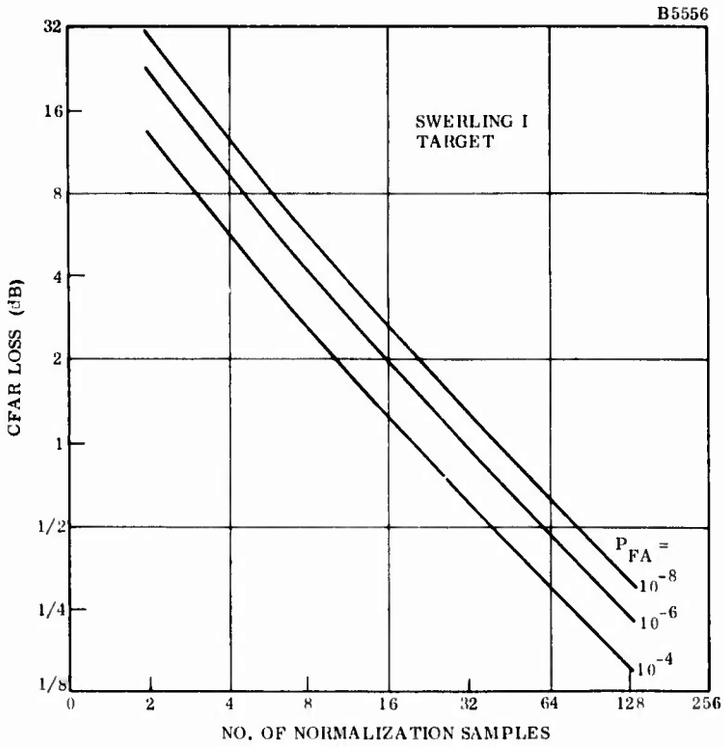

Figure 26. CFAR Loss

This loss is applicable for the single-frequency channel waveform and processor. Modification is required for the multiple frequency waveform. The first modification is that the form of the normalizing CFAR processor that should be used depends upon the environment conditions. Specifically, note that the prior defined normalization voltage is an estimate of the rms voltage of the interference (interference power when square law detectors are used). If the interference power is the same in each channel, then an overall normalization voltage can be formed by combining the normalization voltages from each channel. The voltage from the test cell of each channel can be added and the normalization voltage is applied to this sum. If the interference power is different in each channel, as would be true when narrowband spot jammers are present, then the normalization voltages should not be added. It is necessary to normalize the test cell of each channel and then add the normalized outputs. These two configurations are shown in Figure 27. As discussed in detail later, the normalization algorithm must also be modified.

The specific normalization algorithm for the upper normalizer of Figure 27 is as follows. Denote the square-law detected voltage from the test cell of the jth diversity channel as y_{oj}. Denote the square-law detected voltages from the ith range cell of the jth diversity channel as y_{ij}. The subnormalization for the jth channel is

$$e_j = \sum_{i=1}^{M/2} (y_{i,j} + y_{-i,j}) \tag{11}$$

The signal processing consists of summing the test cell voltages and normalizing this sum by the sum of the subnormalization voltages. Thus, the derived output, t, for N diversity channels, is

$$t = \frac{y_{01} + y_{02} + \cdots y_{0N}}{e_1 + e_2 + \cdots e_N} \tag{12}$$

This output is compared to a constant threshold voltage for target present or absent decisions to be made.

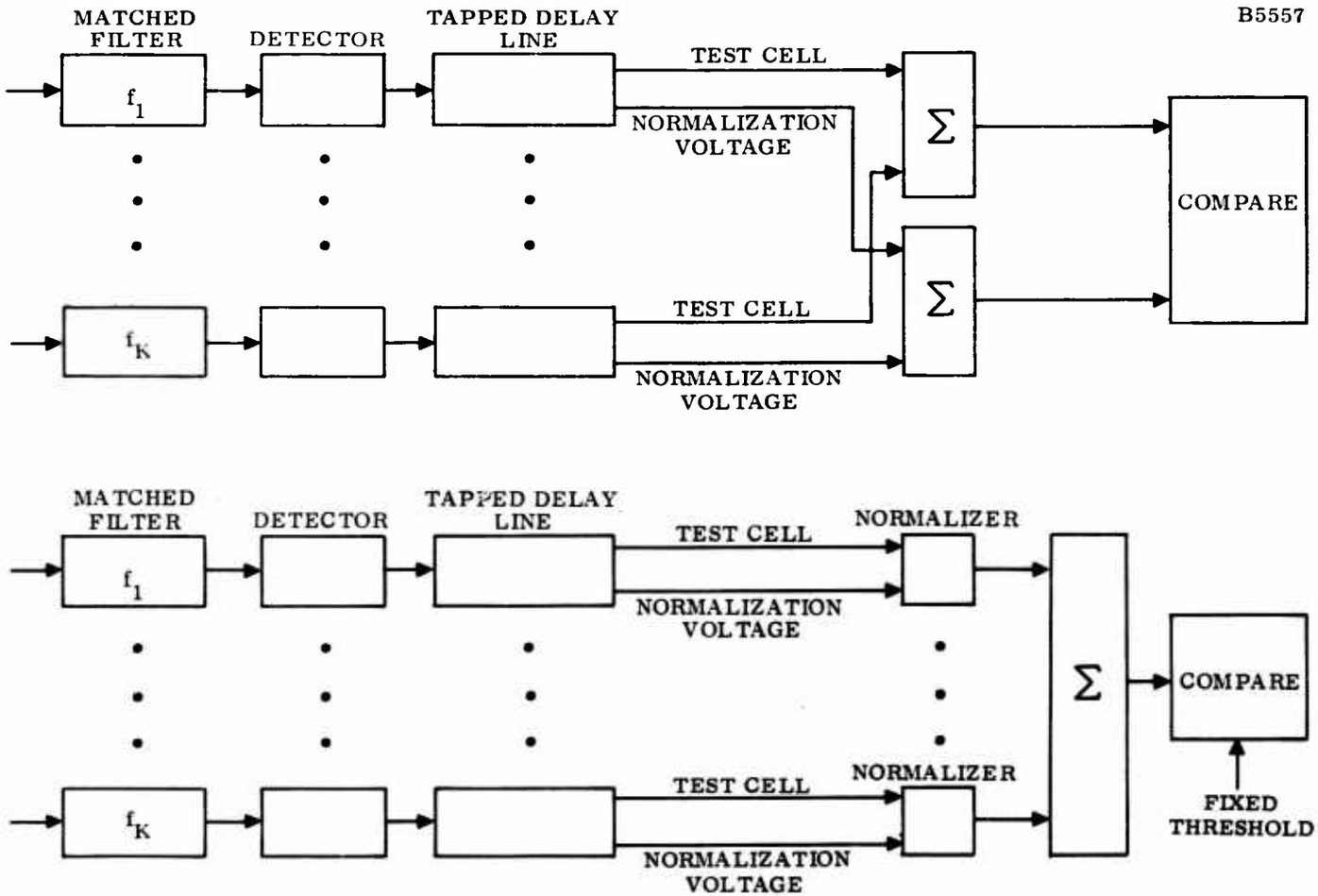

Figure 27. Conceptual Block Diagram of Multichannel Normalizer

The density function of the random variable t is well known. It has the central f distribution for target absent conditions and the noncentral f distribution for target present conditions when the target is nonfluctuating. For a Swerling 2 target fluctuation, the density is proportional to central f for both target present and absent. Thus, curves for the probability of detection vs SNR can be computed by using the properties of the well known density. Figure 28 summarizes these curves into a CFAR loss curve for a four-channel diversity system.

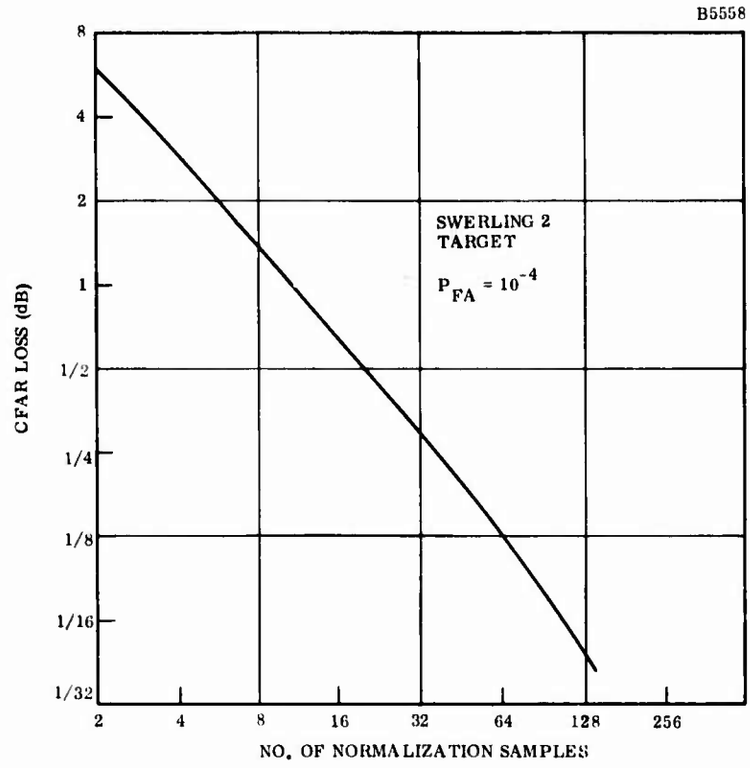

Figure 28. Four-Channel Diversity CFAR Loss, Barrage Jamming

Though this CFAR processor works well for a barrage noise jamming environment, alternate configurations are desired for a spot noise jammer environment. If only one of (say) four channels is being jammed, the normalization voltage for the three unjammed channels should be derived from thermal noise alone. However, the combining of the normalized channels is not straightforward, and needs to be considered with care. Consider a diversity channel with normalization voltage derived only from range cells of that channel. The normalized output is

$$t = \frac{y_{01}}{e_1} \tag{13}$$

and this is compared to a threshold. Alternately, any monotonic function of t can be used for the signal processor and identical target detection performance is obtained. As an example, if the test cell voltage is added to the normalization voltage, an alternate, but equivalent in terms of performance, processor is

$$b = \frac{y_{01}}{e_1 + y_{01}} \tag{14}$$

When combining the normalized outputs of the several channels, it is not proper to simply sum the t values obtained for each channel. It might be that summing monotonic functions of the t values for each channel, such as the b value, is better. In fact, there is no reason to believe that simple summing is sufficient. More complex combining may be superior.

It is shown in Section IV, par. 5a that combining the normalized channels, in general, requires complicated functions of the b variates. An asymptotic approximation shows that simple summing is satisfactory and the recommended combining procedure is

$$t_1 = \sum_j \frac{y_{0j}}{e_j + y_{0j}} \tag{15}$$

The normalization loss for a four-channel diversity system has been evaluated. In addition, the normalization loss obtained when using

$$t_2 = \sum_j \frac{y_{0j}}{e_j} \tag{16}$$

for a four-channel diversity system has been obtained. These two results are shown in Figure 29. It is seen that the differential normalization loss is large only when the number of normalization cells is small.

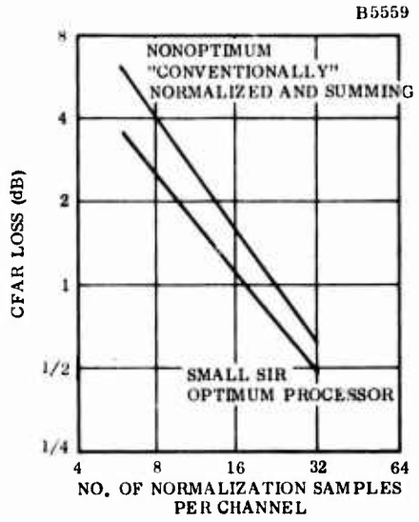

Figure 29. Four-Channel Normalization Losses, Spot Jamming

5. ANALYSIS

a. Channel-to-Channel Frequency Spacing Effects

The received signal from a target is due to reflections from the multiple scatterers of the target. The random phasing of the multiple reflections cause the value of the envelope of the return signal to be a random variable.

The density function of the match-filtered square-law detected output, q, for Swerling 1 fluctuation is

$$p(q) = \exp\left[-q/(1+\gamma)\right]/(1+\gamma) \tag{17}$$

and γ is the average SNR of the single channel waveform. For an K-channel waveform of equal energy, the SNR for each channel is γ/K and the density function of the kth matched-filtered square-law detected output is

$$p_k(q_k) = \exp\left[-q_k/(1+\frac{\gamma}{K})\right]/(1+\frac{\gamma}{K}) \tag{18}$$

For a multireflector target, as shown in the following par. 5a(1), the correlation of the signal amplitude at carrier frequency f_1 and carrier frequency f_2 is obtained from the Fourier transform of the target cross section profile. Specifically, denote the cross section of a scatterer located at a distance ℓ from the beginning of the target as $\sigma(\ell)$. Then the correlation coefficient depends only upon the difference between f_2 and f_1. When the carrier frequencies are equally spaced, the correlation between the ith and the kth return is

$$\rho(f_i - f_k) = \rho[(i - k) f_s] = \int_{-\infty}^{\infty} e^{-j2\pi(i - k) f_s \chi} \sigma(\chi)\, d\chi \Big/ \int_{-\infty}^{\infty} \sigma(\chi)\, d\chi \qquad (19)$$

where f_s is the carrier frequency spacing. Two cases are considered in detail. The first is when the target cross section density is uniform over the target length. Then

$$\rho[(i - k) f_s] = \frac{\sin \pi (i - k) \frac{f_s}{f_R}}{\pi (i - k) \frac{f_s}{f_R}} \qquad (20)$$

where f_R depends upon the target length, L, and equals

$$f_R = \frac{c}{2L} \qquad (21)$$

The frequency variable f_R is essentially the signal bandwidth that produces a range resolution size equal to the target length. Thus, the correlation coefficient depends upon the ratio of the channel displacement, f_s, and target resolution bandwidth f_R. This ratio is denoted as the normalized channel displacement. The second case considered is when the target cross section density is a triangle over the target length so that

$$\rho[(i - k) f_s] = \left[\frac{\sin 2\pi (i - k) \frac{f_s}{f_R}}{2\pi (i - k) \frac{f_s}{f_R}} \right]^2 \qquad (22)$$

As discussed in par. 5a(2), the covariance matrix of the returns for the K-channels is given by the product of the scalar $1 + \frac{\gamma}{K}$ and the K by K-correlation coefficient matrix V_ρ. The i, k entry of V_ρ equals $\rho(f_i - f_k)$. Thus,

$$V = \frac{1}{2}\left(1 + \frac{\gamma}{K}\right) V_\rho \tag{23}$$

It is also shown in par. 5a(2) that the density function of the output voltage, v, for the target present case is given by

$$p(v/\text{target}) = \sum_{i=1}^{K} \frac{\exp\left[-\dfrac{v}{d_i\left(1 + \frac{\gamma}{K}\right)}\right] / \left(d_i\left(1 + \frac{\gamma}{K}\right)\right)}{\displaystyle\sum_{j=1,\, \neq i}^{K} \left(1 - \frac{d_j}{d_i}\right)} \tag{24}$$

where d_i are the (assumed distinct) eigenvalues of the matrix V_ρ. For the target absent condition, the density function of the output voltage is proportional to a chi-square with 2K degrees of freedom. Thus, for each target cross section profile, the detection performance can be obtained.

(1) Correlation of Returned Signal at Different Carrier Frequencies

It is assumed that the target can be satisfactorily modeled as a continum of independent reflectors. Thus, the impulse response of a target of length L is

$$\begin{aligned} h(t) &= a(t) && 0 \leq t \leq 2L/C \\ &= 0 && \text{elsewhere} \end{aligned} \tag{25}$$

where C is the velocity of propagation. The return for a cissoid transmitted waveform is given as the convolution of h(t) and exp (jωt). Thus,

$$g(t) = \int e^{j\omega(t - \tau)} a(\tau)\, d\tau = e^{j\omega t} a(\omega) \tag{26}$$

where $a(\omega)$ is the complex amplitude of the return. The correlation between the complex amplitudes at radian frequency ω_1 and ω_2 is then

$$R(\omega_1, \omega_2) = E \int\int_{-\infty}^{\infty} e^{-j\omega_1 x} a(x)\, e^{j\omega_2 y} a^*(y)\, dx\, dy \tag{27}$$

where E is the expectation operator. Assuming the target return from a scattering point is uncorrelated with the returns from other scattering points.

$$E[a(x)\, a^*(y)] = \sigma(x)\, \delta(x - y) \tag{28}$$

where $\sigma(x)$ is the target cross section vs length profile and $\delta(x)$ is the Dirac impulse function. Then,

$$R(\omega_1, \omega_2) = \int_{-\infty}^{\infty} e^{-j(\omega_1 - \omega_2) x}\, \sigma(x)\, dx \tag{29}$$

so that the correlation depends only upon the frequency difference and equals the Fourier transform of the cross section profile of the target. The correlation coefficient is then obtained by dividing $R(\omega_1, \omega_2)$ by $R(0, 0)$. In addition, since the return is due to the superposition of many individual returns, it is reasonable to assume that the joint density of the two returns is a complex bivariate Gaussian.

(2) Density Function for Diversity Channels Output For Correlated Signal Returns*

The sampled complex envelope of the matched filter output of the ith diversity channel is denoted as z_i. The square-law detected output for this channel is $q_i = |z_i|^2$. When the target cross section fluctuation is Swerling 1, the density function for q_i is

$$p_i = \exp\left[-q_i/(1 + \frac{\gamma}{K})\right] / (1 + \frac{\gamma}{K}) \tag{30}$$

* The analysis is similar to that in Appendix B of M. Schwartz, W.R. Bennett, and S. Stein, "Communication Systems and Techniques", McGraw-Hill, 1966.

The Swerling 1 target cross section fluctuation assumption is equivalent to the assumption that the density function for z_i is a zero mean complex Gaussian. The variance of z_i is

$$\text{Var}(z_i) = \frac{1}{2}\left(1 + \frac{\gamma}{K}\right) \tag{31}$$

Define the vector whose ith component is z_i as Z. The density function for Z is a multivariate complex Gaussian with zero mean. The covariance matrix of Z, is

$$V = \frac{1}{2}\left(1 + \frac{\gamma}{K}\right) V_\rho \tag{32}$$

where the entries of V_ρ are the appropriate correlation coefficients.

The summation of the square-law detected outputs is

$$v = \sum_{i=1}^{K} q_i = Z^H Z \tag{33}$$

where superscript H denotes complex conjugate. Note that when R is a unitary matrix and

$$Y = R^H Z \tag{34}$$

then

$$v = Z^H Z = Y^H Y = \Sigma\, |y_i|^2 \tag{35}$$

The covariance matrix of Y is

$$E(R^H Z Z^H R) = \frac{1}{2}\left(1 + \frac{\gamma}{K}\right) R^H V_\rho R \tag{36}$$

where E( ) denotes the expectation operator.

Since V_ρ is an Hermitian matrix, there is a unitary matrix, U, such that

$$U^H V_\rho U = D \tag{37}$$

where D is a diagonal matrix whose main diagonal entries, d_i, are the eigenvalues of V_ρ. When R equals U, the random variates y_i are independent. The variance of y_i is

$$V(y_i) = \frac{1}{2} \left(1 + \frac{\gamma}{K}\right) d_i \tag{38}$$

Denote $|y_i|^2$ as t_i. Then, the density function for t_i is exponential and is

$$p_i = \exp\left[-t_i/d_i \left(1 + \frac{\gamma}{K}\right)\right] / d_i \left(1 + \frac{\gamma}{K}\right) \tag{39}$$

The characteristic function is thus given as

$$\phi(\mu) = \left[1 - j\mu d_i \left(1 + \frac{\gamma}{K}\right)\right]^{-1} \tag{40}$$

Since the set of t_i are independent, the characteristic function for the output v is the product of the K-characteristic functions for t_1 through t_K. When all the eigenvalues are distinct, partial fraction expansion can be used to obtain the density function for v as

$$p(v) = \sum_{i=1}^{K} b_i \exp\left[-\frac{v}{d_i \left(1 + \frac{\gamma}{K}\right)}\right] \Big/ d_i \left(1 + \frac{\gamma}{K}\right) \tag{41}$$

$$b_i = \sum_{j=1,\, \neq 1}^{K} \left(1 - \frac{d_j}{d_i}\right)^{-1} \tag{42}$$

The probability of exceeding a threshold T is then given by

$$p_d = \sum_{i=1}^{K} b_i \exp\left[-\frac{T}{d_i \left(1 + \frac{\gamma}{K}\right)}\right] \tag{43}$$

b. Loss for Unknown Doppler Frequency

(1) Single Channel

For an exponential density function and comparison threshold of T_1, the false alarm probability is

$$p_{f_1} = e^{-T_1} \tag{44}$$

The increase in threshold value required for decreased false alarm probability can be determined by noting that

$$p_{f_2} = e^{-T_2} = e^{-kT_1} = p_{f_1}^{k} \tag{45}$$

Thus,

$$k = \frac{\ell n\, p_{f_2}}{\ell n\, p_{f_1}} \tag{46}$$

When N-parallel filters are used for Doppler processing, the required false alarm probability p_{f_1} per range cell is attained if the false alarm probability for each threshold comparison is

$$p_{f_2} = \frac{p_{f_1}}{N} \tag{47}$$

The ratio of thresholds is

$$k = 1 - \frac{\ell n\, N}{\ell n\, p_{f_1}} \tag{48}$$

For the target present condition, a target detection is made if the cell containing the target exceeds the threshold value, or if any of the cells containing only interference exceeds the threshold. For high detection probability, the probability of the latter events is negligible. Thus, the increase of SIRR for fixed detection probability is given by

$$p_d = \exp\left(-\frac{T_1}{1+\gamma_1}\right) = \exp\left(-\frac{T_2}{1+\gamma_2}\right) \tag{49}$$

where γ_1 and γ_2 are the SIRR values for the different false alarm probabilities. Then

$$\frac{\gamma_2}{\gamma_1} = \frac{1+\gamma_1}{\gamma_1} \; k - \frac{1}{\gamma_1} \tag{50}$$

For large values of γ_1 the increase in SNR is approximated as

$$\frac{\gamma_2}{\gamma_1} = 1 - \frac{\ell n\, N}{\ell n\, p_{f_1}} \tag{51}$$

When N = 8 and the false alarm probability is 10^{-6}, the SNR increase is 0.61 dB. Similarly when N equals 8^4 for this false alarm probability the SNR increase is 2.05 dB.

(2) Multiple Channel Diversity Waveform

As shown in previous Figure 23, the processor takes the greatest detected output of the Doppler filters for each diversity channel. These greatest-of values are summed and compared to a fixed threshold. Denote the ith Doppler filter output of the jth diversity channel as X_{ij} and the output of the greatest-of circuit for the jth diversity channel as Z_j. It is assumed that each X_{ij} is identically distributed and that the filter spacings are such that they are independent. For interference alone, they are distributed with a chi-square density function of two degrees of freedom. The target present condition corresponds to a Swerling 2 model so that more generally the X_{ij} are independently distributed with density function

$$f_{ij}(\chi) = \exp\left[-\frac{\chi}{2(1+\gamma_{ij})}\right] / 2(1+\gamma_{ij}) \tag{52}$$

where γ_{ij} is the SIRA value. For interference alone, each γ_{ij} equals zero. For target present, γ_{ij} is nonzero for each j value at the particular i value corresponding to the target Doppler. As Z_j less than z occurs when each X_{ij} is less than z, the distribution function of Z_j for target absent equals the Nth power of the distribution function of any X_{ij}. Thus

$$F_{Z_j}(z) = [F_x(z)]^N \tag{53}$$

Define Y as:

$$Y = \sum_{j=1}^{K} Z_j \tag{54}$$

The characteristic function for Y equals the kth power of the characteristic function for any Z_j. Then the density function for Y is obtained from the Fourier transform of the characteristic function for Y. The density function for Z_j for target absent can be determined as

$$f_{Z_j}(z) = \frac{N}{2} \sum_{k=1}^{N} a_k \, e^{-\frac{zk}{2}} \tag{55}$$

$$a_k = (-1)^{k-1} \frac{(N-1)!}{(k-1)!\,(N-k)!} \tag{56}$$

The characteristic function for Y can then be obtained as

$$M_Y(\mu) = \left[\frac{N}{2} \sum_{k=1}^{N} \frac{a_k}{\frac{k}{2} - j\mu} \right]^K \tag{57}$$

In general, the Fourier transform of this expression can be found by applying the theory of residues. When K is 4 or less, a reasonable alternative is a tedious and multiterm partial function expansion. The latter was used and a relationship between false alarm probability and threshold value was obtained.

The target present case was analyzed by assuming that the Doppler cell containing the target is always the greatest. This assumption reduces the problem to the standard K-pulse Swerling 2 case. This assumption is conservative in the sense that if a "wrong" Doppler cell produces the greatest value, the total sum is increased, and the probability of detection increases. Thus, the values given for the greatest-of loss are actually an upper bound but the error should be minute.

c. Effect of Detector Law Upon Diversity Gain

(1) Optimum Processor

For a Swerling 1 or 2 target fluctuation model, the density function of the envelope, r_i, of the matched filtered output for the ith channel is

$$f_i(r_i, \bar{x}_i) = r_i \exp\left[-r_i^2/2\,(1+\bar{x}_i)\right]/(1+\bar{x}_i) \tag{58}$$

where $\bar{x}_i$ is the SIR of each channel. When $\bar{x}_i$ equals zero, the equation gives the density function for the interference only case. The optimum processor for a K-channel diversity waveform is obtained by applying the Neyman-Pearson lemma. Thus, for observed envelope values $r_1, r_2, \ldots, r_K$, the statistically optimum function of the observed values that maximizes the probability of detection for a specified false alarm probability, denoted as $d(x_1, x_2, \ldots, x_K)$ is obtained as

$$d(x_1, x_2, \ldots, x_K) = \prod_{i=1}^{K} \frac{f_i(r_i, \bar{x}_i)}{f_i(r_i, 0)}$$

$$= \exp\left[\frac{\bar{x}_i}{1+\bar{x}_i} \sum_{i=1}^{K} r_i^2\right] \Bigg/ \prod_{i=1}^{K} (1+x_i) \tag{59}$$

Any monotonic function of d is equally satisfactory so that another version of the statistically optimum processor is

$$d_1(x_1, x_2, \ldots, x_K) = \sum_{i=1}^{K} r_i^2 \tag{60}$$

Thus, the optimum processor for K-diversity channels and a Swerling 2 target fluctuation model is to sum the squared envelope values.

(2) Evaluation of Diversity Gain

(a) Square-Law Envelope Detector

The density function of the square-law detected match filtered output, v_i, for the ith channel is

$$f_i(v_i, \bar{x}_i) = \exp[-v_i/2(1+\bar{x}_i)]/2(1+\bar{x}_i) \tag{61}$$

For a single channel system the SIR value is denoted as $\bar{x}_0$. The multiple channel system is defined to have equal energy per channel and the total energy equals $\bar{x}_0$. Thus, each $\bar{x}_i$ equals x_0/K. For a single channel system it is shown that the probability of detection, P_D, and the false alarm probability, P_{FA}, are related to the SIR value as

$$P_D = P_{FA}^{\frac{1}{1+\bar{x}_0}} \tag{62}$$

When the desired false alarm probability is 10^{-6}, and the desired detection probability is 0.9, the required value of $\bar{x}_0$ is 21.14 dB.

For a multiple channel system, and Swerling 2 target, the density function for the optimum processor output is the gamma density. The computation of the required SIR values are obtained by using the well known properties of this density function. It is shown that the diversity gain for 2 or 4 channels is 3.3 dB and 4.6 dB, respectively.

(b) Linear Envelope Detector

The nonoptimum processor noncoherently sums the envelope detected outputs. The density function of the envelope of each channel is Rayleigh. In general, the density function of the sum of Rayleigh distributed variates is unknown. The two channel case is known. The density and distribution functions of the sum, s, of two Rayleigh variates are given by Marcum as*

$$f_2(s) = \frac{s}{2} e^{-\frac{s^2}{2}} + \frac{\sqrt{\pi}}{2} \left(\frac{s^2}{2} - 1\right) \operatorname{erf}\left(\frac{s}{2}\right) e^{-\frac{s^2}{4}} \tag{63}$$

* J. I. Marcum, "A Statistical Theory of Target Detection by Pulsed Radar: Mathematical Appendix", RM753, July 1948, p. 30.

for the density function and the distribution function is given by

$$F_2(s) = e^{-\frac{s^2}{2}} + \frac{\sqrt{\pi}}{2}\, s\, \mathrm{erf}\left(\frac{s}{2}\right) e^{-\frac{s^2}{4}} \tag{64}$$

where erf ( ) is the error function. These equations are directly applicable for the interference only condition. For the Swerling 2 target, replacing s by $s/\sqrt{1 + \bar{x}_0/2}$ in the last equation gives the distribution function for the target present case.

The density function for the sum of four envelope detected outputs is given by the convolution of $f_2(s)$ with itself. This cannot be obtained in closed form. An approximation to the desired result was obtained by using $F_2(s)$ to develop a discrete density function. This was convolved with itself on the digital computer using double precision arithmetic.

d. Optimality Considerations for CFAR Processing of Diversity Channels

Denote the square-law detected output of the test cell of the jth diversity channel as y_{o_j} and the voltage formed by summing the outputs from adjacent cells as e_j. Then the normalized output for the jth diversity channel is $t_j = y_{o_j}/e_j$. For a nonfluctuating target, the density function of y_{o_j} is noncentral chi-square with two degrees of freedom. The density function for target absent is central chi-square with two degrees of freedom. It is assumed that the normalization voltage is formed from interference only. The density function for the normalization voltage is therefore always central chi-square with the number of degrees of freedom equal to 2M. The density function for t_j is either the noncentral or central f distribution with 2 and 2M degrees of freedom given by*

$$p(t_j, \bar{x}) = M\, e^{-\bar{x}}\, \frac{{}_1F_1\left(1 + M,\ 1,\ \bar{x}\ \frac{t_j}{1 + t_j}\right)}{(1 + t_j)^{1+M}} \tag{65}$$

* C.R. Rao, "Linear Statistical Inference and Its Applications", John Wiley, 1965, p. 176.

where ${}_1F_1(\ )$ denotes the confluent hypergeometric function and $\bar{x}$ is the SIR of the test cell for each channel. The Neyman-Pearson lemma may be applied to find the optimum method of combining the per channel normalized voltages. Thus for N-diversity channels, the optimum processor is found as

$$t = \prod_{j=1}^{N} \frac{p(t_j, \bar{x})}{p(t_j, 0)} \gtrless T \tag{66}$$

where T is the appropriate threshold value for the desired false alarm probability. This gives the optimum processor as

$$t = \prod_{j=1}^{N} {}_1F_1\left(1 + M, 1, \bar{x}\ \frac{t_j}{1 + t_j}\right) \gtrless T \tag{67}$$

Note that the processor depends upon the value of $\bar{x}$ so that there is no single processor that is optimum for all SIR values. Note further that the optimum processor does not depend directly upon the variables t_j but upon $t_j/(1 + t_j)$. In terms of the test cell voltage and normalizing voltage, this is

$$\frac{t_j}{1 + t_j} = \frac{y_{o_j}}{e_j + y_{o_j}} \tag{68}$$

Thus, the "natural" normalized variable when combining diversity channels, includes the test cell voltage in the normalization voltage. The density function of the "natural" normalized variable is the noncentral beta.

The processor that is approximately optimum for small SIR values can be obtained by a series expansion of Equation (67). This results in

$$t = \sum_{j=1}^{N} \frac{y_{o_j}}{e_j + y_{o_j}} \gtrless T' \tag{69}$$

where the modified threshold T' is obtained from T by including the various additive and multiplicative constants associated with the series expansion.

A similar result can be obtained for fluctuating targets. When the target fluctuation model is Swerling 2, the density function of y_{o_j} is exponential. Thus

$$p(y_{o_j}) = \frac{1}{2(1+\bar{x})} \, e^{-\frac{y_{o_j}}{2(1+\bar{x})}} \tag{70}$$

It reduces to the central chi-square distribution with two degrees of freedom when $\bar{x}$, the SIR value, equals zero. When $\bar{x}$ equals zero, the density function of t_j is an f distribution. For nonzero $\bar{x}$, the variate $t_j/(1+\bar{x})$ has an f density function. Manipulating Equation (65) gives that t_j has the density function

$$p(t_j) = \frac{1}{1+\bar{x}} \, \frac{M}{\left(1 + \frac{t_j}{1+\bar{x}}\right)^{1+M}} \tag{71}$$

Applying the Neyman-Pearson lemma for this case gives the optimum test as

$$t' = \prod_{j=1}^{N} \left[\frac{1+t_j}{1+\frac{t_j}{1+\bar{x}}} \right]^{1+M} \gtrless T \tag{72}$$

Again, the optimum test depends upon the specific value of $\bar{x}$ so that there is no uniformly most powerful test. The approximately optimum test for small SIR values is obtained by noting that t' may be rewritten as

$$t' = \prod_{j=1}^{N} \left(\frac{1}{1+\frac{\bar{x}}{1+t_j}} \right)^{1+M} \gtrless T' \tag{73}$$

Taking logarithms and series expansion results in

$$t' = \sum_{j=1}^{N} -\frac{1}{1+t_j} \gtrless T'' \tag{74}$$

By adding constants to both sides, this becomes

$$t' = \sum_{j=1}^{N} 1 - \frac{1}{1+t_j} = \sum_{j=1}^{N} \frac{t_j}{1+t_j} \gtrless T'' \qquad (75)$$

Comparing Equations (68), (69), and (75), it is seen that the small SIR approximate optimum test is the same for the nonfluctuating target and for the Swerling 2 target.

SECTION V

EFFECT OF PULSE REPETITION FREQUENCY UPON REJECTION OF CHAFF AND WEATHER CLUTTER

Since the radar cross section of the interference is large compared to typical target radar cross sections, the presence of chaff or weather clutter severely limits the capability of tactical radars to detect targets at intermediate and long ranges. In addition, the Doppler spread of the interference is large at S-band. When the pulse repetition frequency is chosen to given unambiguous range information over the entire surveillance range, this relatively low PRF causes the use of Doppler processing for clutter rejection to be only marginally useful.

Figure 30 indicates the geometry effects upon the interference cross section and Doppler spread. The resolved volume increases with the square of range so that the interference cross section increases with the square of range. The wind velocity varies as a function of altitude so that the interference particles are moving at different velocities over the elevation extent of the beam. This velocity spread causes a Doppler frequency spread within each range cell. A quantitative indication of the magnitude of the chaff-clutter cross section for a typical pencil beam performing horizon search is shown in Figure 31. The typical tactical aircraft target has a cross section of 1 m^2. The dashed horizontal line indicates that an SCR of 15 dB, approximately that required for reliable target detection, is obtained when the interference cross section is -15 dB. The difference between the solid line and the dashed line gives the required improvement factor to obtain target detection. The improvement factor can be obtained either by decreasing the resolution volume or by making use of Doppler processing techniques.

Figure 32 indicates the required waveform band occupancy to give the indicated SCR's ratios as a function of detection range. The graph is predicated upon the assumption that the interference is continuously distributed in range so that increasing the waveform bandwidth always decreases the clutter cross section. It is seen that the use of extremely-large band occupancy waveforms can theoretically give the desired detection range. However, the indicated band occupancy values are so large that it becomes extremely difficult to generate and process the waveforms and it also becomes questionable whether or not the interference particles are truly continuously distributed in range.

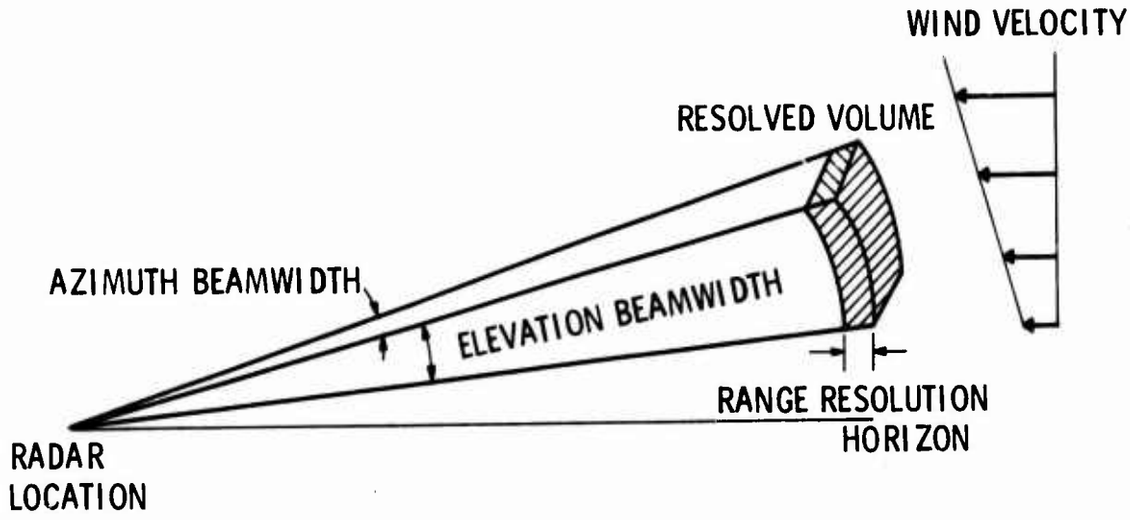

1. RESOLVED VOLUME INCREASES WITH RANGE
2. WIND VELOCITY INCREASES WITH ALTITUDE
3. CLUTTER CROSS SECTION AND DOPPLER SPREAD INCREASES WITH RANGE

Figure 30. Geometry Effects

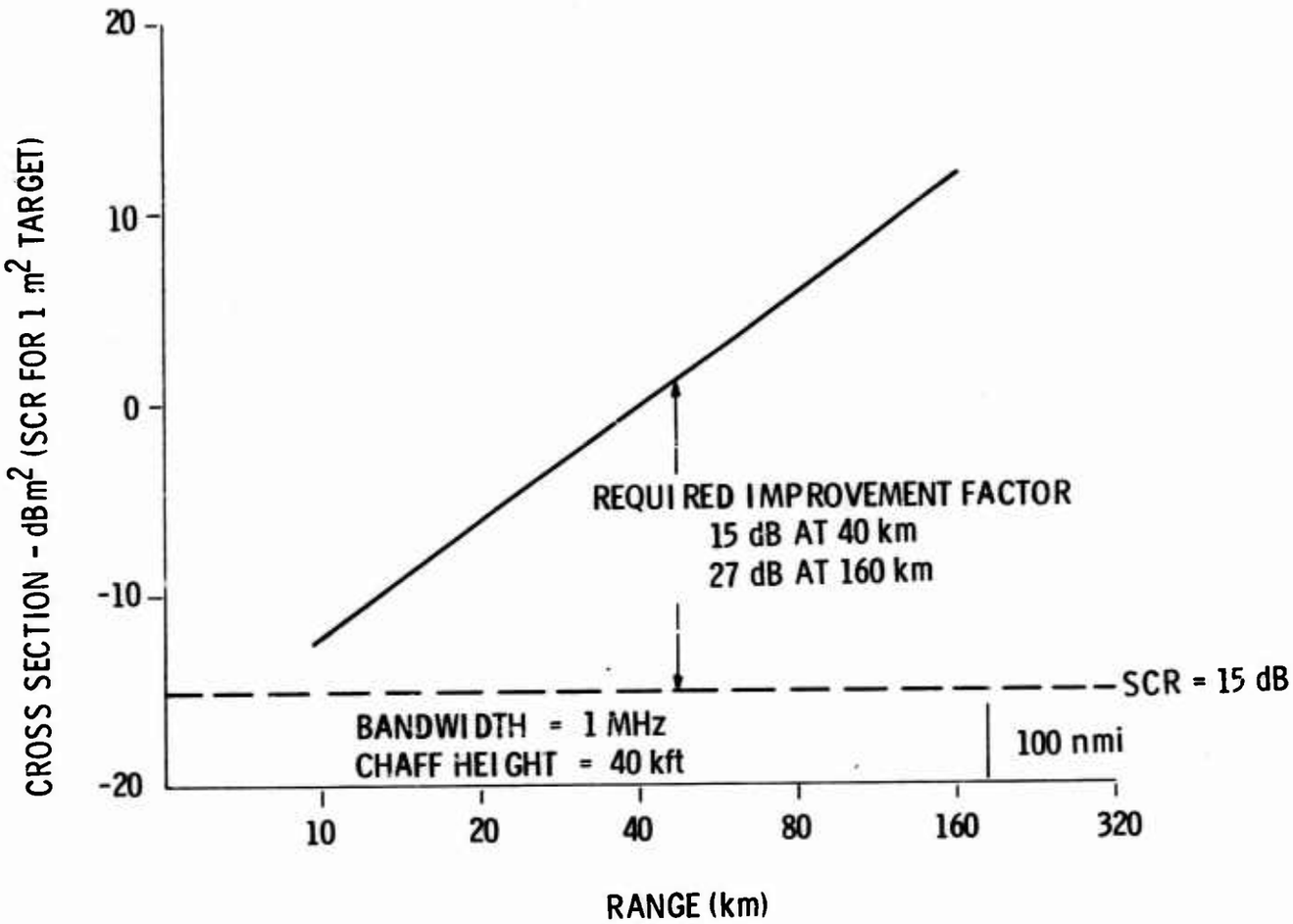

Figure 31. Chaff-Clutter Cross Section

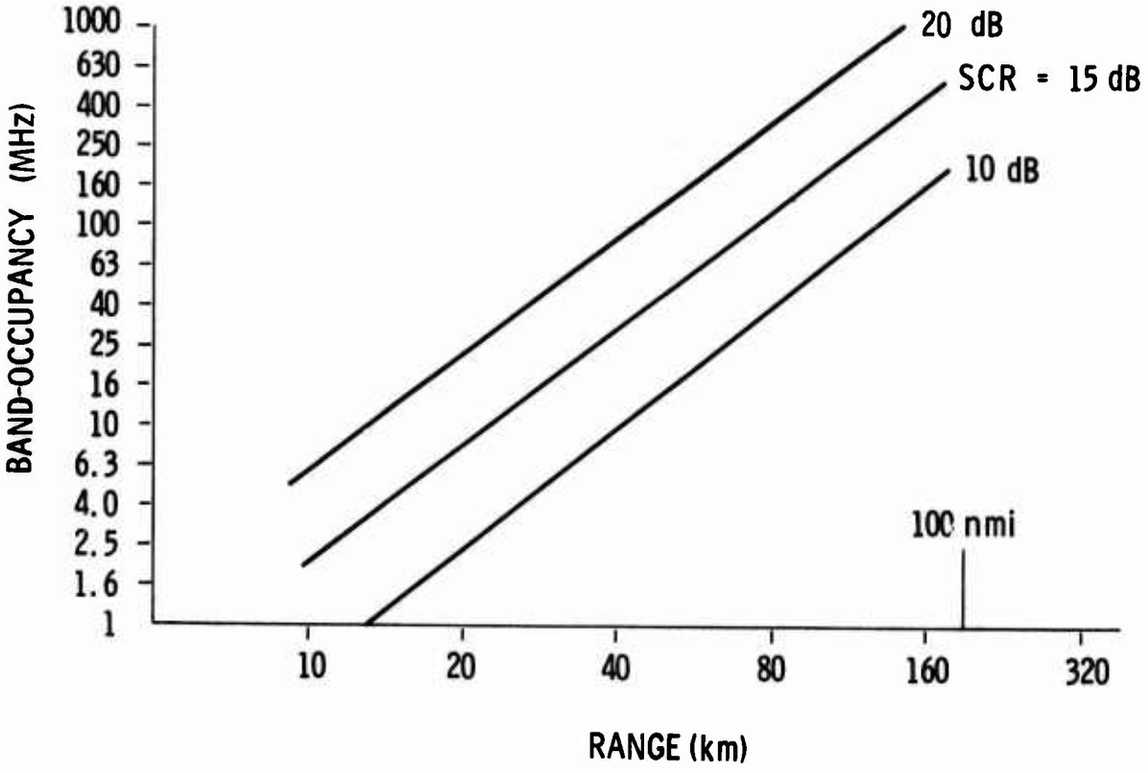

Figure 32. Required Band Occupancy

The effect of the varying wind velocity upon the chaff velocity in the various radar beams are indicated in Figures 33 and 34. The wind velocity model used is that given by Nathanson.* The clutter is assumed to be uniformly distributed over range and altitude. The range extent is from the radar location to a range of 186 km (100 nmi). It is distributed over a spherical earth from the ground to an altitude of 40 kft. The assumed antenna pattern has a total elevation coverage of 0 to 20°. The azimuth beamwidth is 1.1° and the unspoiled vertical beamwidth is 1.55°. The detailed beam characteristics assumed are indicated in Table III below:

TABLE III

ANTENNA ELEVATION COVERAGE

Beam No.	Tilt (Deg)	Vertical Beamwidth (Deg)
1	0.80	1.55
2	1.95	1.70
3	3.60	2.20
4	6.15	4.60
5	9.70	5.20
6	16.05	7.80

Detailed investigation of the Doppler velocity indicates that at any particular range the interference cross section is approximately uniformly spread over the Doppler region given by the average Doppler frequency plus or minus one and a half times the standard deviation of the Doppler frequency. This relationship is indicated by previous Figure 35. It gives an approximate indication of the spectral content as a function of range for a pencil beam-forming horizon search (beam no. 1) when the wind direction is along the azimuth pointing angle. The clutter has appreciable energy only at ranges in frequencies within the cross hatched region. As an example, at a range of 100 km, the clutter spectrum extends from 120 Hz to 385 Hz.

The effect of different pulse repetition frequencies is shown by the curves of Figure 36. This gives the effective chaff cross section at the output of a matched filter as a function of the Doppler frequency to which the matched filter is tuned. The first curve is for the unambiguous range PRF of 300 Hz. Since the Doppler

*Nathanson, F. E., "Radar Design Principles," Mc-Graw-Hill, 1969, p. 207.

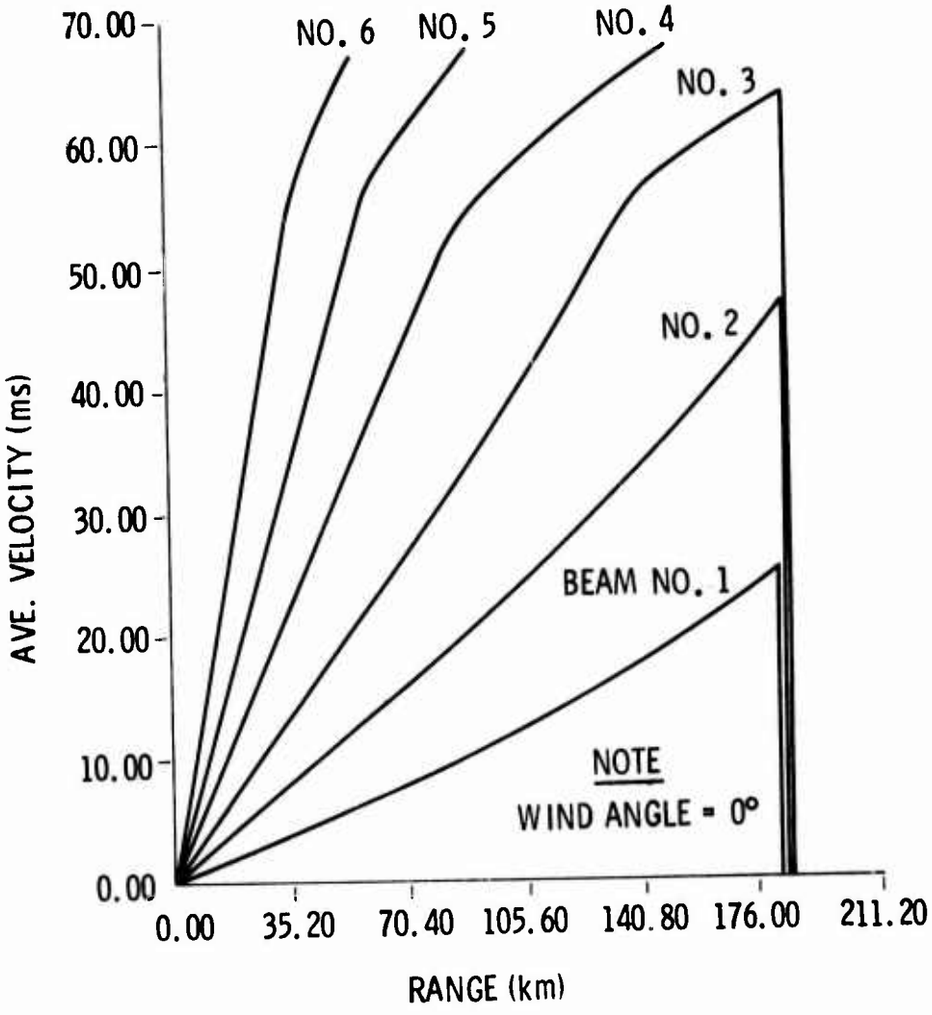

Figure 33. Chaff Average Velocity

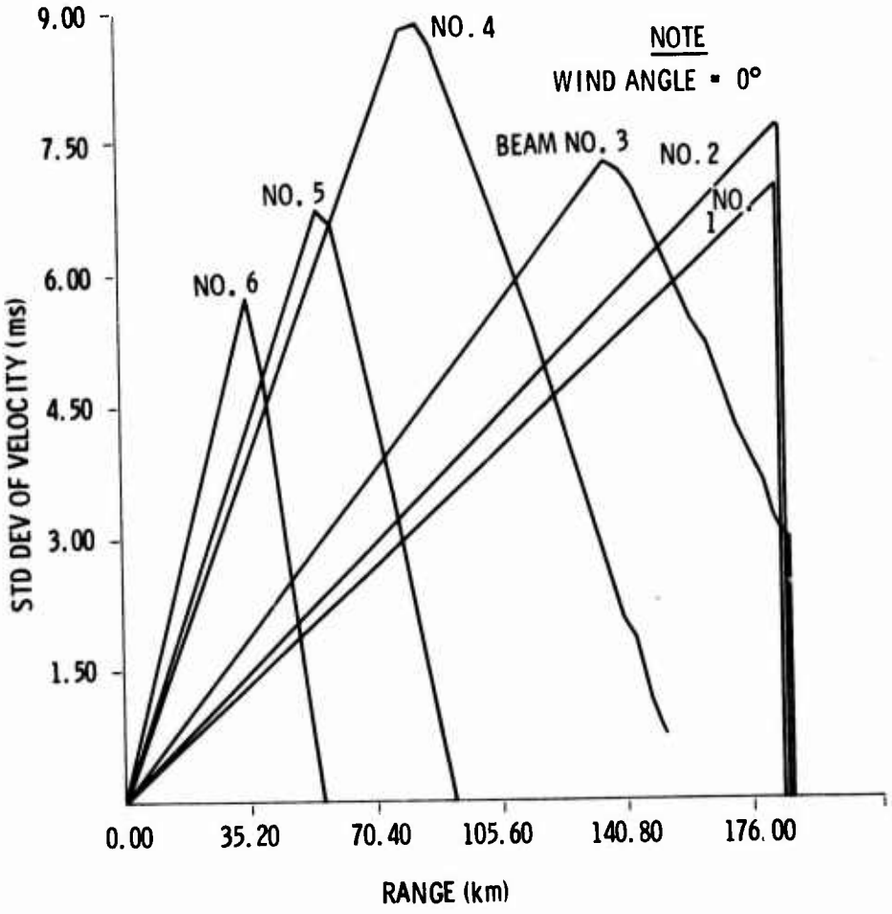

Figure 34. Chaff Velocity Spread

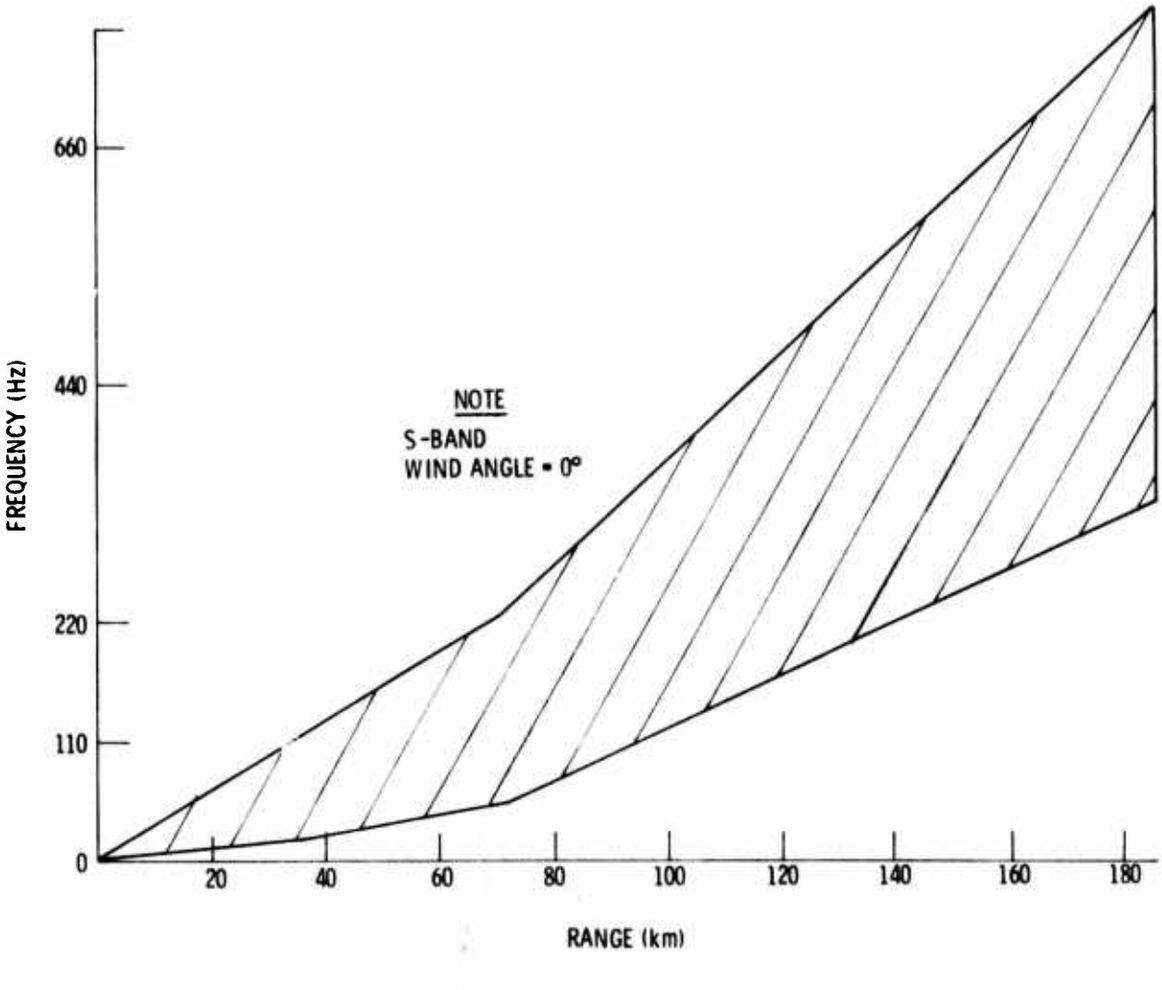

Figure 35. Chaff Spectral Spread for Lowest Beam (No. 1)

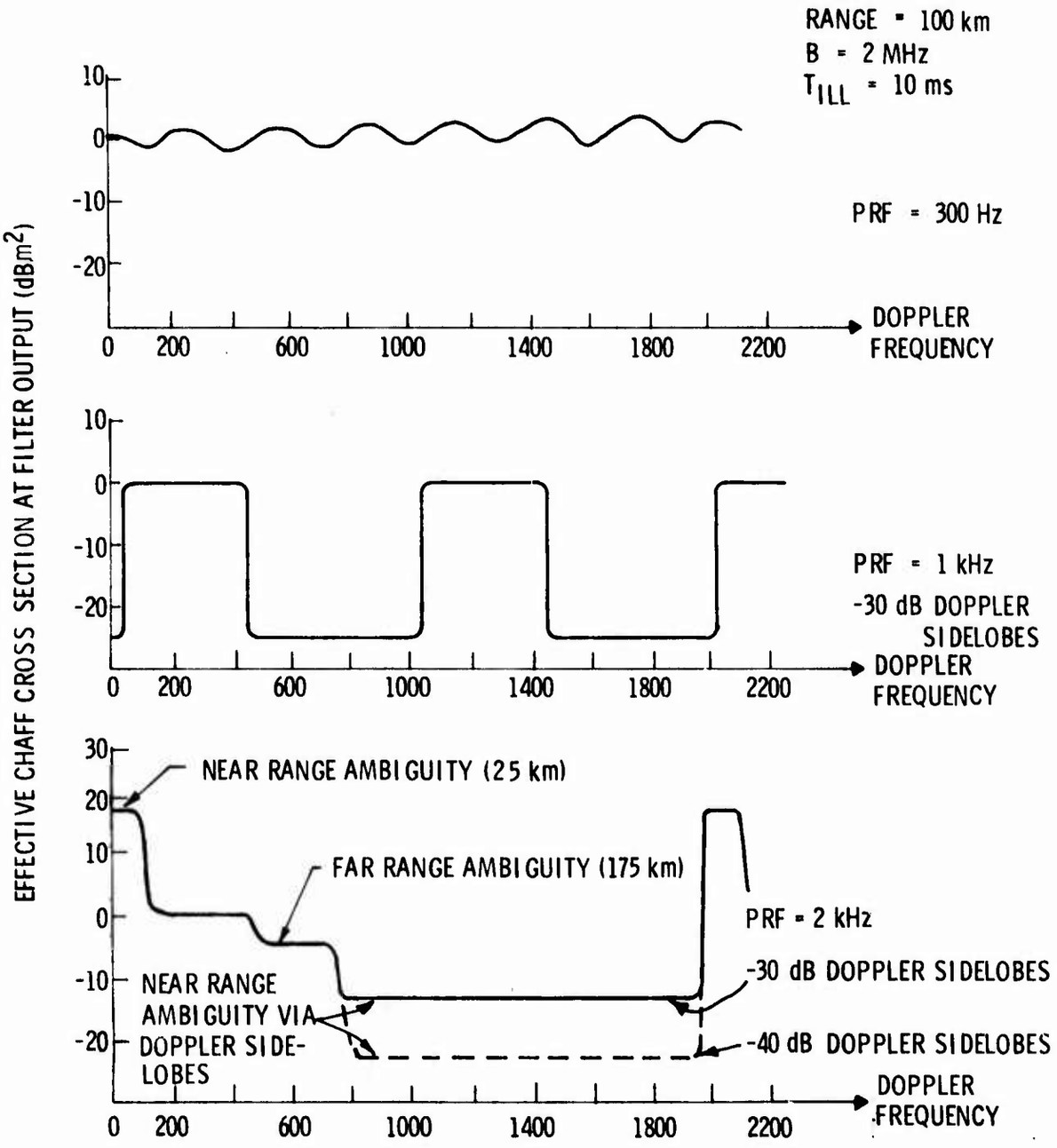

Figure 36. Effect of Pulse Repetition Frequency Upon Doppler Performance for Matched Filter

spread of the interference is 265 Hz, the chaff and weather cause almost uniformly intense interference at all Doppler frequencies. This is caused by the ambiguity response of this waveform. A uniform period waveform has Doppler ambiguities spaced at the PRF and range/time ambiguities spaced at multiples of the pulse repetition interval. The large chaff cross section at all Doppler frequencies is due to the fact that the PRF is 300 Hz, and the spread of the chaff, 265 Hz, almost equals the PRF. Some benefit can be obtained by increasing the PRF. This is seen from the middle curve of Figure 37 where the PRF is increased to 1 kHz. The waveform Doppler ambiguities are spaced at 1 kHz so that there are now regions where the effective chaff cross section is small and targets can be detected. The frequency range where there is appreciable chaff cross section is the frequency range of approximately 70 Hz to 435 Hz and ambiguities thereof. The frequency range is larger than that of the chaff's Doppler range due to the nonzero bandwidth of the matched filter. For the assumed 10-ms illumination time the filter bandwidth is approximately 100 Hz. At the other Doppler frequencies, the effective cross section is approximately $-25\ dBm^2$. This cross section is due to clutter pickup via the Doppler sidelobes of the response. These sidelobes have been assumed to be an average level of -30 dB for this figure.

Further increases in the PRF value do not necessarily give improvements and in fact may cause degraded performance. This is illustrated by the last curve of Figure 37. The PRF has been increased to 2 kHz. Note that previously the PRF of 1 kHz causes a range ambiguity of 150 km. For this value, the range ambiguities occur at ranges where there is no chaff. However, for the 2-kHz PRF, the range ambiguities are spaced at 75 km. Thus, when the range of interest is 100 km, there is a near range ambiguity of importance at 25 km and a far range ambiguity at 175 km. Both of these ambiguities are at ranges where there is chaff. In order to take account of the effects of the range ambiguities, it is necessary to include the two-way fourth-law range effect upon received power. Thus, though the chaff at 25 km is a significantly smaller cross section than the chaff at 100 km, it causes a much larger effect since it is at one-fourth the range. In addition, note that though when using a PRF of 1 kHz, the effective chaff cross section drops from the $0\ dBm^2$ level to the $-25\ dBm^2$ level for Doppler frequencies greater than 450 Hz, this does not occur when the pulse repetition period is 2 kHz. One cause is the far range ambiguity at 175 km. A second cause is a pickup of chaff cross section via the Doppler sidelobes due to the near range ambiguity. Comparing the results from the two PRF's, it is seen that the

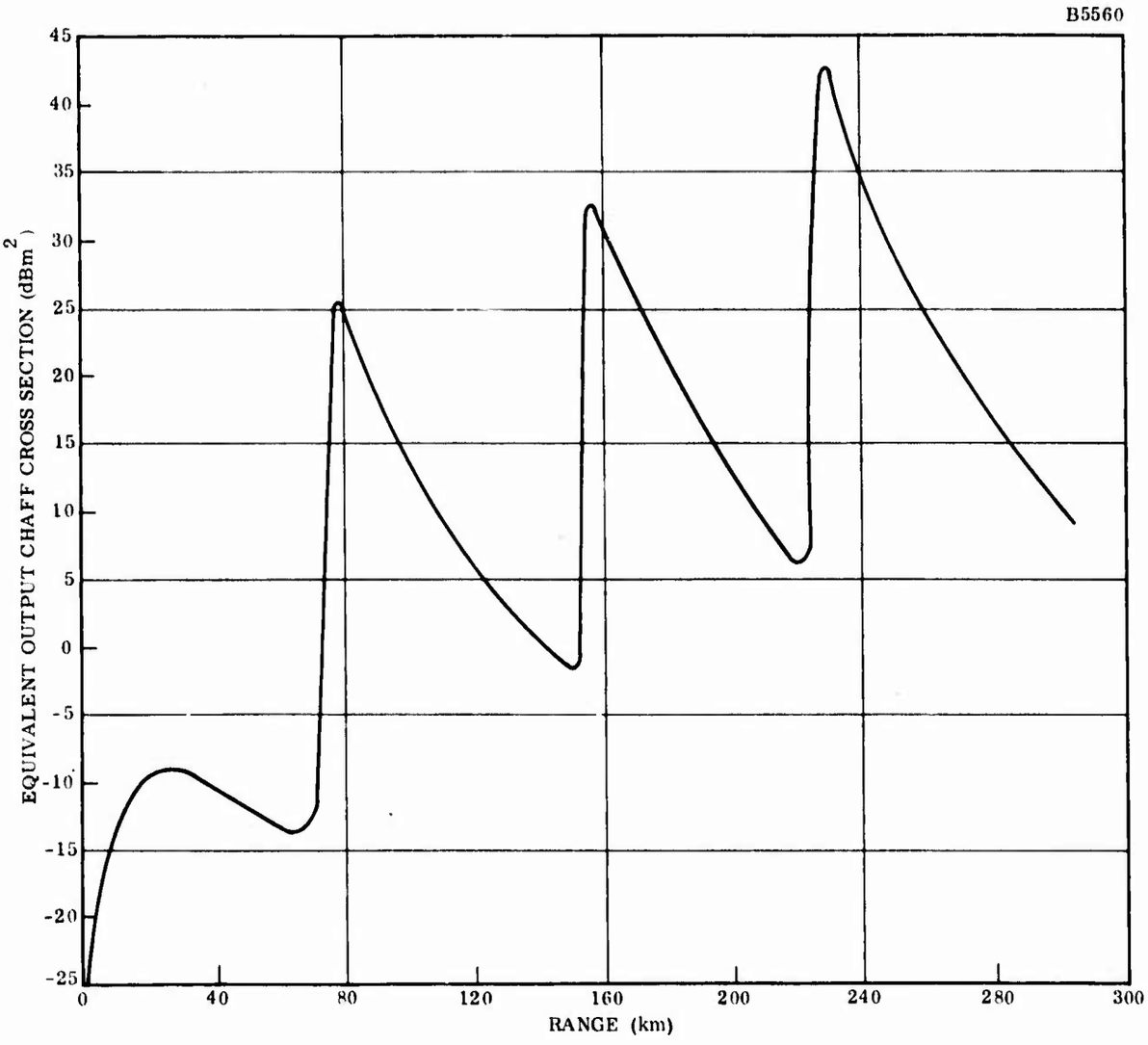

Figure 37. 16-Pulse Waveform Normalized Clutter Power

advantage of the 2 kHz PRF is only at the frequency regions where the 1 kHz PRF suffers due to the Doppler ambiguities. At all other Doppler frequencies the nonrange ambiguous PRF gives better results. However, note that the combination of the two PRF's would give better results than either alone.

The previous material focused upon the effective output clutter cross section as a function of Doppler frequency at a single value of range. The use of range ambiguous waveforms has significant effect upon the effective output clutter cross section vs range. The curve of Figure 37 shows the effective clutter cross section vs range when using a 2-kHz PRF waveform for a single value of Doppler frequency. It is seen that the cross section varies as the expected square of range with an additional sawtooth-like function. The sawtooth-like effect is caused by a near range ambiguity. This effect is important because the previous curves for a fixed range showed a significant dependence upon near range ambiguities. The effect of the near range ambiguities upon the clutter magnitude profile vs Doppler depends upon the particular range of interest. This is illustrated by the curves of Figures 38 and 39. Figure 38 is for a 50-km range and Figure 39 is for a range of 155 km. The first curves of each figure are for PRF's of 300 Hz and 790 Hz. The latter value has an unambiguous range equal to the range extent of the clutter. It is seen that at both ranges and both PRF's the peak clutter cross section is approximately 0 dB. The 300-Hz PRF has some regions of clear Doppler at a 50-km range, but no regions of clear Doppler at 155 km range. The 790-Hz PRF is clear for appreciable percentages of the Doppler extent at both ranges. At the 50-km range, increasing the PRF to 1 kHz increases the percentage of clear Doppler and the maximum clutter cross section is kept at 0 dBm^2. This also happened for the previously discussed 100-km range. Note, however, that for the 155-km range increasing the PRF to 1 kHz gives substantially degraded performance as compared to the 790-Hz PRF. This effect is due to the near range ambiguity. In addition, at the 50-km range, increasing the PRF from 1 kHz to 2 kHz does not substantially increase the percentage of clear Doppler because here also the effect of range ambiguities becomes of significance. Note that with the 2-kHz waveform there are some Doppler regions which are clear, whereas the same Doppler region is cluttered when using the 1-kHz waveform. The reverse is also true. Thus, it is seen that for the middle and short ranges, the use of several highly range-ambiguous PRF's can improve the detectability of targets in chaff or weather clutter. At long ranges, use of a PRF that causes a near range ambiguity is disastrous.

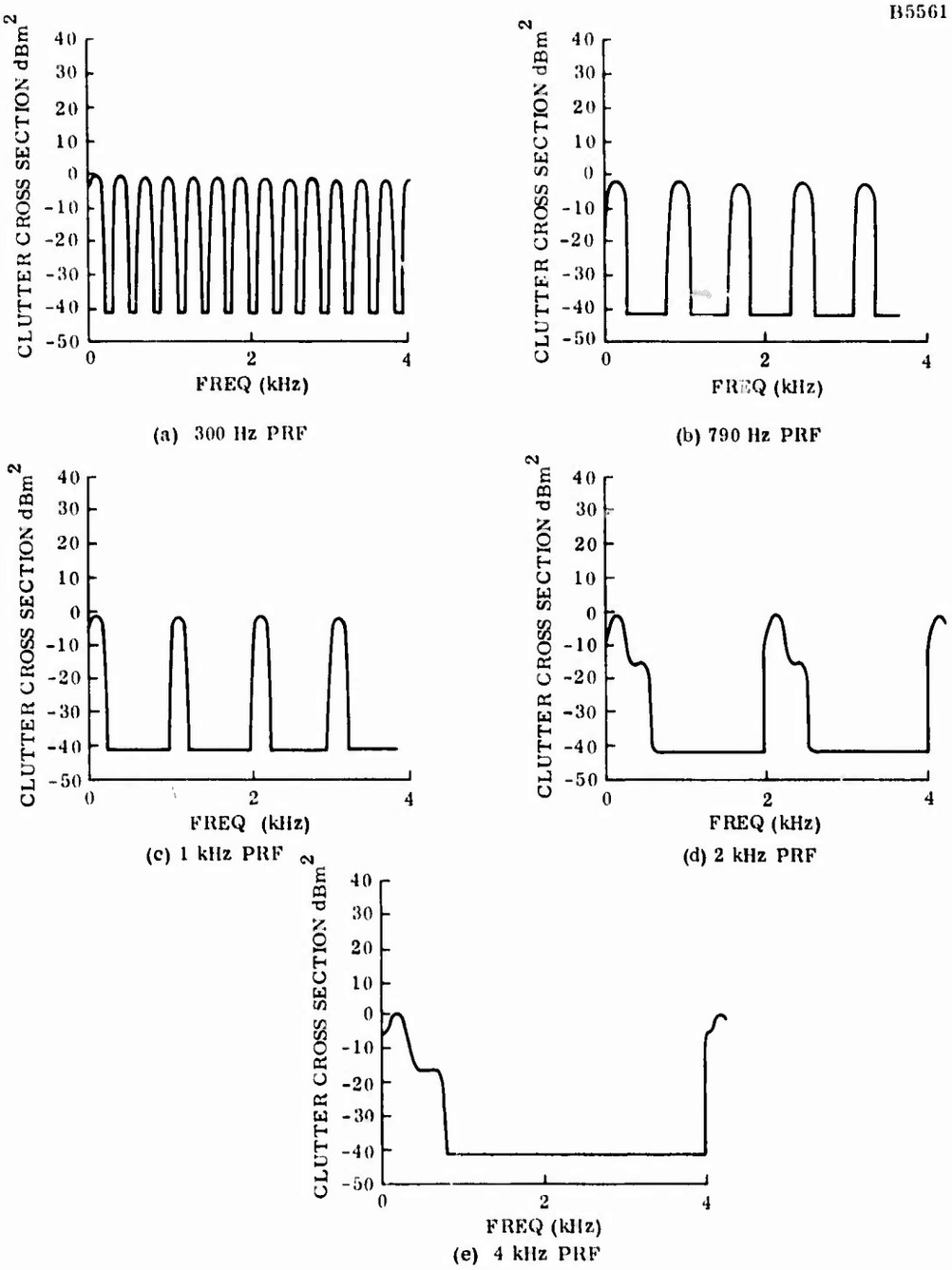

Figure 38. Equivalent Clutter Cross Section vs Target Doppler 50-km Range, 2-MHz Bandwidth, 40-dB Tchebyscheff Weights

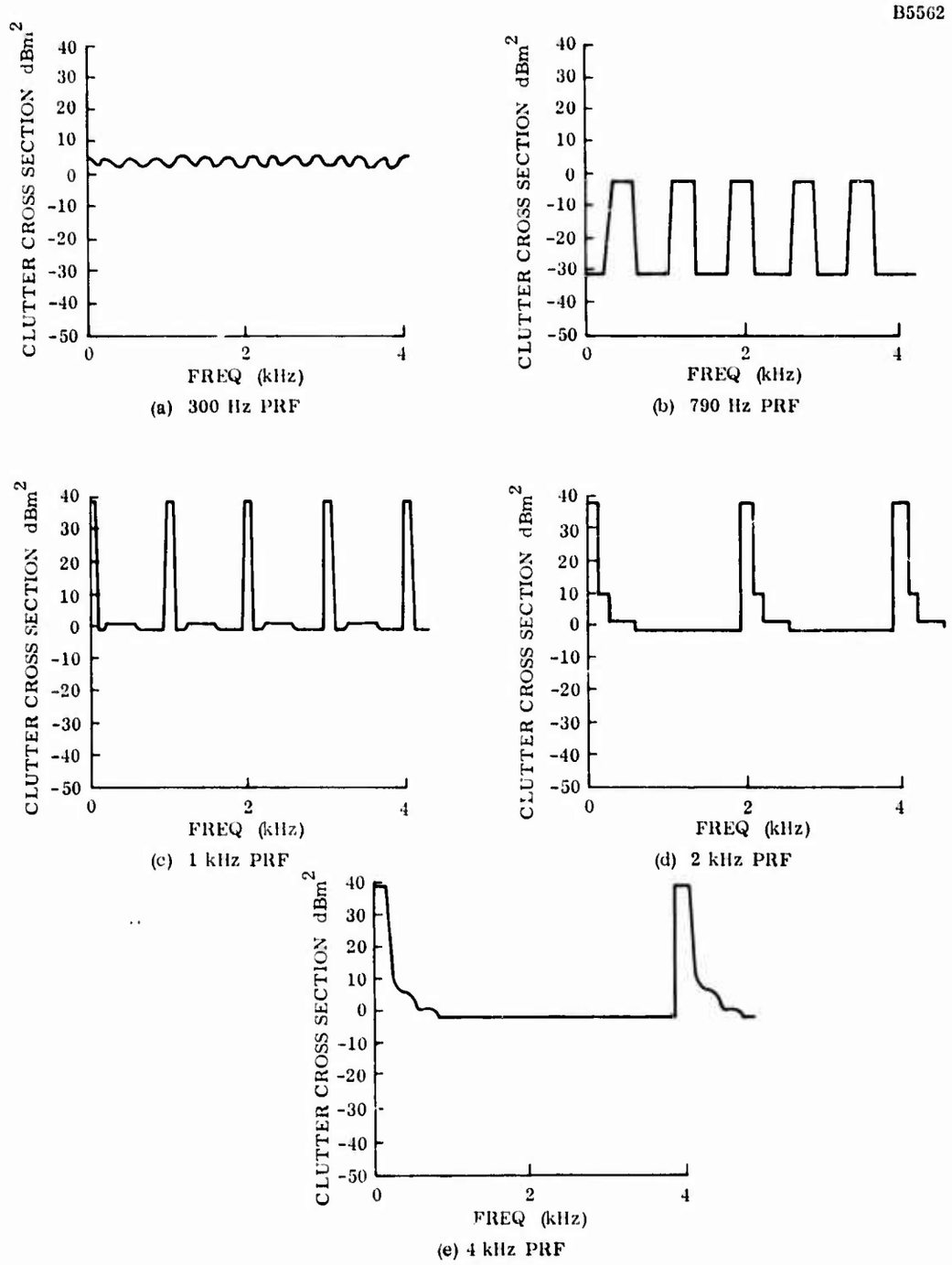

Figure 39. Equivalent Clutter Cross Section vs Target Doppler (2-MHz Pulse Bandwidth, Range = 155 km)

A PRF value whose unambiguous range is at least equal to the range extent of the clutter is required.

It is necessary to resolve the range ambiguity of the target that occurs when using the range ambiguous PRF's. One method of ambiguity resolution is the detection scheme indicated in Figure 40. The technique operates by transmitting two waveforms with different PRF values and comparing the return from each waveform to a threshold. The decision that a target is present is made only in those range cells where a threshold crossing occurs for each waveform. The true target location is indicated by the arrow; the potential ambiguity ranges are indicated by the crosses. A false alarm due to thermal noise occurs if in any particular range cell a threshold crossing occurs on both waveforms due to noise alone. A false alarm due to the combination of thermal noise and a potential ambiguity occurs in those range cells indicated by a cross if for one waveform thermal noise exceeds the threshold while in the other waveform the ambiguity exceeds the threshold. Since the probability of the ambiguity exceeding the threshold is approximately unity, the probability of an ambiguous detection is approximately equal to the square root of the false alarm probability.

As the ambiguity removal requires the transmission of two waveforms, there is an SIR loss as compared to the case of using a single nonambiguous range waveform. Modifications of this coincidence detection technique can be used to decrease the SIR losses. The loss decrease is obtained by increasing the probability of ambiguity; for many circumstances this is a satisfactory tradeoff since for the coincidence detection technique the probability of ambiguity may be much less than is needed. As an example, if the false alarm probability due to thermal noise is 10^{-6} the probability of ambiguity is 10^{-3} and larger values are often satisfactory. An alternate scheme is shown in Figure 41. This technique is a generalization of coincidence detection. In addition to comparing each individual waveform to a threshold, the sum of the two waveforms is formed and the sum is compared to a threshold. Only if all three exceed their respective thresholds is a target declared. This procedure is identical to coincidence detection when the threshold T2 equals 0. Similarly, when the threshold T1 equals 0, the circuit corresponds to noncoherent summing of the two waveforms. The probability of ambiguity is a function of the ratio of the thresholds T1 and T2, the probability of detection, and whether or not the two waveforms are at the same carrier frequency. The graphs of Figure 42 show this for the different carrier frequency case. It is seen that the probability of ambiguity can be either quite high or can be made as low as the square root of the false alarm probability.

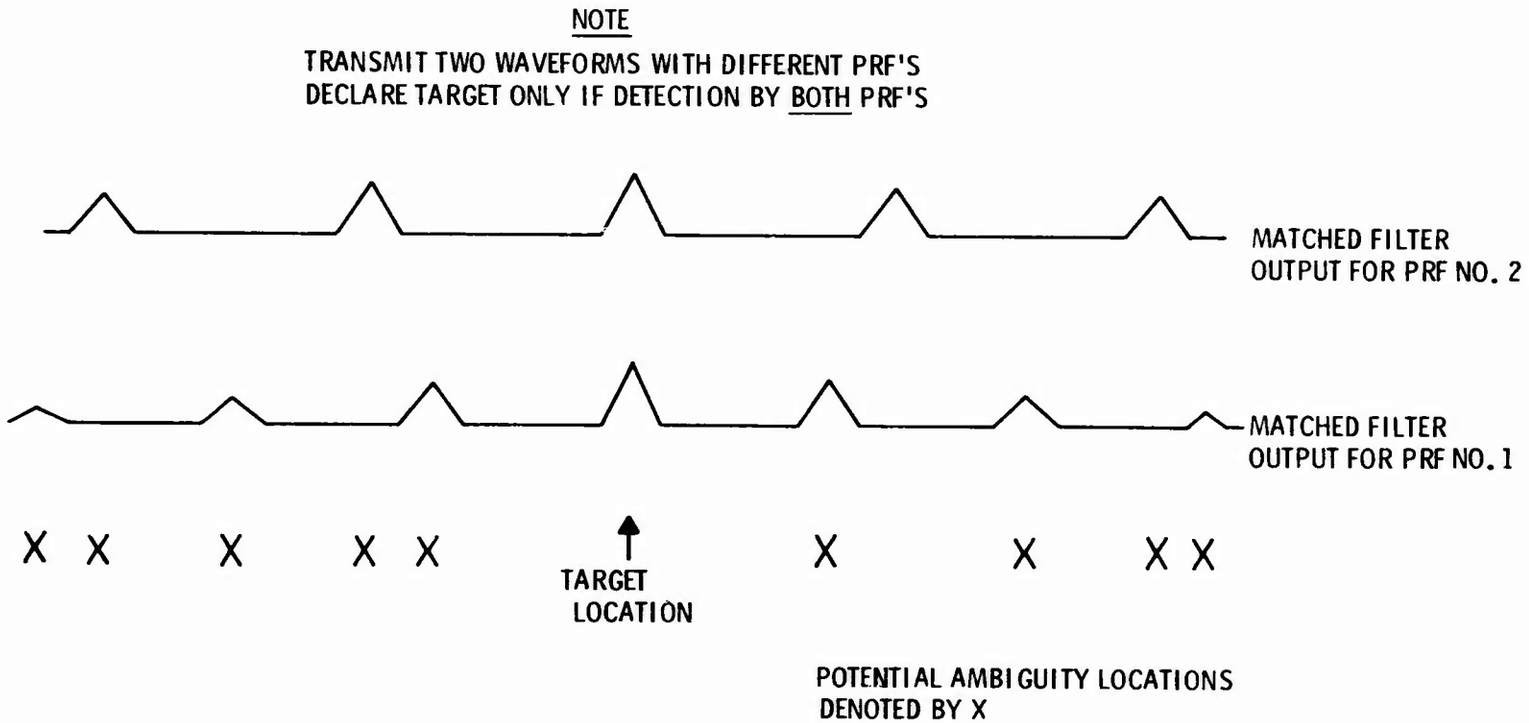

Figure 40. Coincidence Detection for Ambiguity Removal

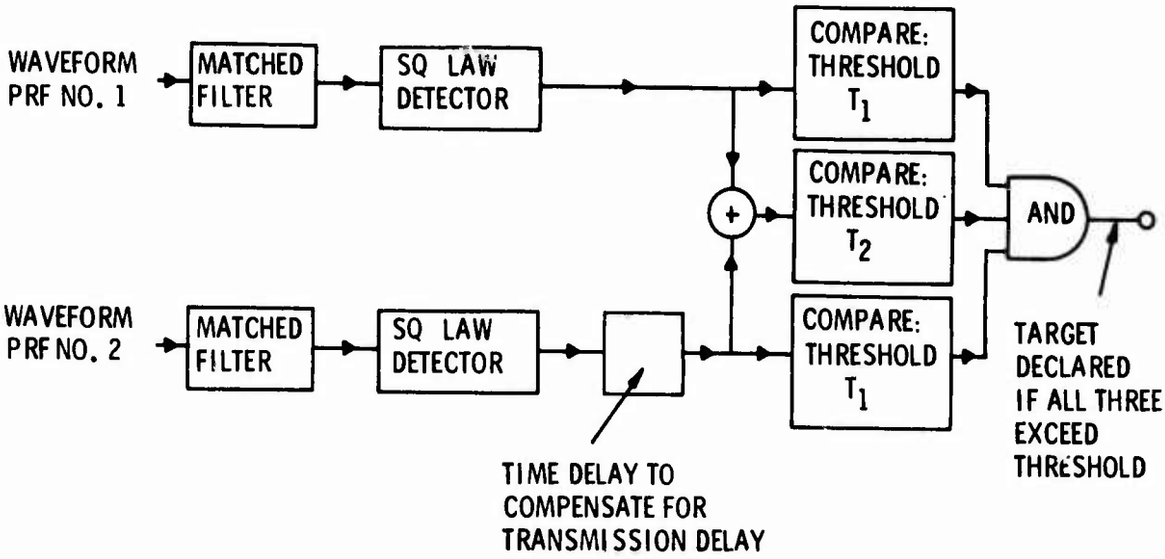

Figure 41. Tradeoff Between Loss and Probability of Ambiguity

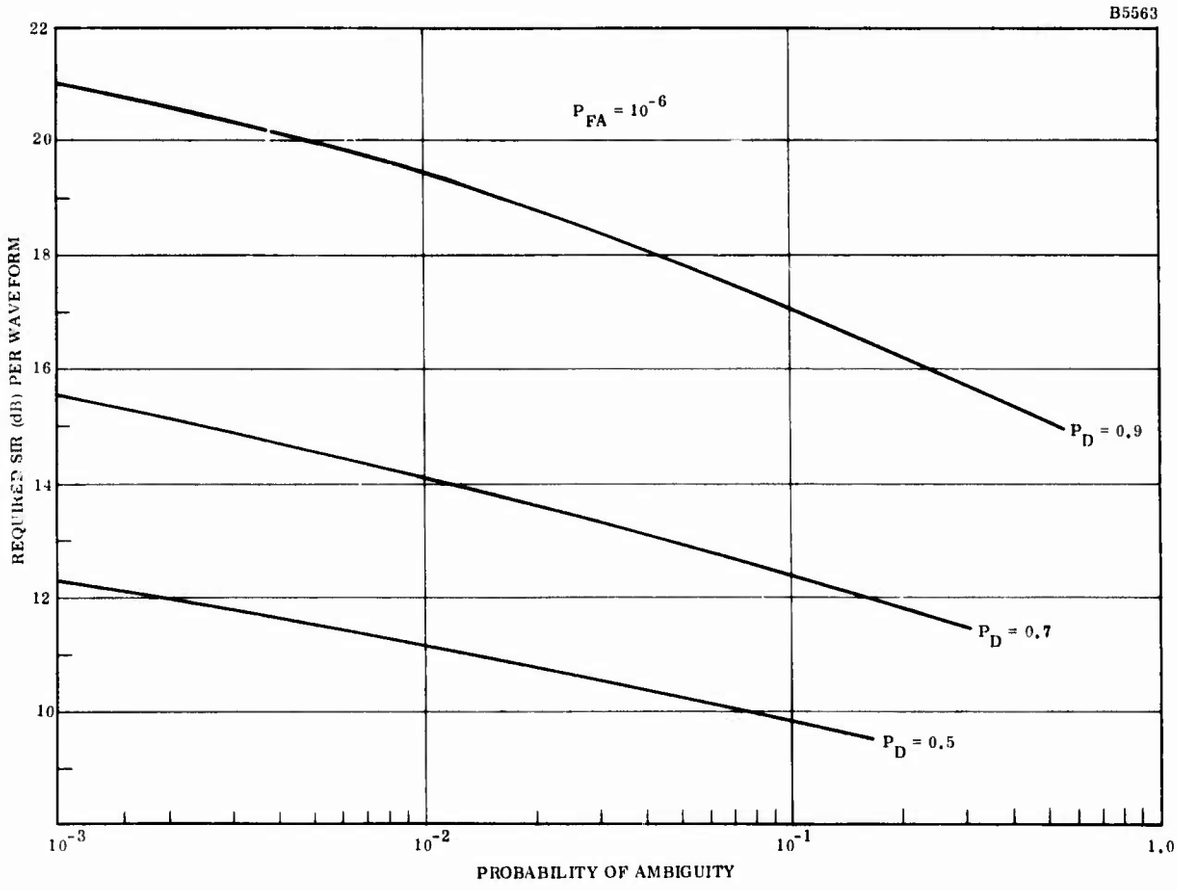

Figure 42. SIR vs Probability of Ambiguity

ENGLISH-METRIC/METRIC-ENGLISH CONVERSION TABLE

mm	=	0.1 cm
cm	=	0.3937 in.
cm	=	0.0328 ft
cm	=	10 mm
cm^2	=	0.1550 $in.^2$
cm^2	=	$1.076 \cdot 10^{-3}$ ft^2
cm^3	=	0.061 $in.^3$
cm^3	=	$3.531 \cdot 10^{-5}$ ft^3
ft	=	30.48 cm
ft	=	0.3048 m
ft^2	=	0.0929 m^2
ft^2	=	929.37 cm^2
ft^2	=	$9.294 \cdot 10^{-3}$ km^2
ft^3	=	0.0283 m^3
in.	=	2.54 cm
$in.^2$	=	6.452 cm^2
$in.^3$	=	16.387 cm^2
μm (micron)	=	0.001 mm
μm	=	10^{-6}m
μm	=	10^{-4} cm
μin.	=	$2.54 \cdot 10^{-5}$mm
kg	=	2.2046 lbs
km	=	3281 ft
km	=	0.6214 mi
km	=	0.55 nmi
km^2	=	$1.076 \cdot 10^7$ ft^2
km^2	=	0.381 mi^2
km/h	=	0.913 ft/s
knot	=	1.152 mi/h
oz	=	28.35 g
oz	=	0.062 lbs
lb	=	453.6 g
lb	=	0.4536 kg
metric ton	=	1.12 tons (U.S.)
m	=	39.37 in.
m	=	3.281 ft
m	=	1.0936 yd
m^2	=	10.76 ft^2
m^2	=	1.196 yd^2
m^3	=	35.32 ft^3
m^3	=	1.430 yd^3
mi	=	1.6093 km
mi	=	5280 ft
mi	=	0.87 nmi
mi	=	1760 yd
mi^2	=	2.59 km^2
mi/h	=	0.87 knots
nmi	=	1.852 km
nmi	=	6076 ft
nmi	=	1.15 mi
yd	=	0.9144 m
yd^2	=	0.836 m^2
yd^3	=	0.7645 m^3
qt	=	0.946 liter
liter	=	1.057 qt
acre	=	43,560 ft^2
acre	=	4046.72 m^2
rad	=	57.2958°
deg	=	0.017 rad
°F	=	9/5(°C) + 32
°C	=	5/9(F° - 32)

MISSION
of
Rome Air Development Center

RADC plans and conducts research, exploratory and advanced development programs in command, control, and communications (C^3) activities, and in the C^3 areas of information sciences and intelligence. The principal technical mission areas are communications, electromagnetic guidance and control, surveillance of ground and aerospace objects, intelligence data collection and handling, information system technology, ionospheric propagation, solid state sciences, microwave physics and electronic reliability, maintainability and compatibility.